

**IMPACTS OF CLIMATE CHANGE AND LAND USE CHANGE**  
**ON THE WATER RESOURCES OF THE**  
**MULA AND MUTHA RIVERS CATCHMENT**  
**UPSTREAM OF PUNE, INDIA**

**INAUGURAL-DISSERTATION**

zur

Erlangung des Doktorgrades

der Mathematisch-Naturwissenschaftlichen Fakultät

der Universität zu Köln

vorgelegt von

**Paul Daniel Wagner**

aus Aachen

Köln, 2013

Berichterstatter: Prof. Dr. Karl Schneider

Prof. Dr. Georg Bareth

Tag der mündlichen Prüfung: 21.01.2013

# Abstract

Water scarcity is one of the most challenging problems the world is facing in the 21<sup>st</sup> century. Population growth and economic development often lead to an increase of water demand, whereas climate change and land use change have an impact on water availability. The assessment of the impacts of climate change and land use change on the water resources is highly relevant as it is a prerequisite for water management adaptation and for the development of suitable mitigation strategies, especially in regions with scarce water resources, high climate sensitivity, and a rapid socio-economic development. This thesis aims at the development of a hydrologic model to analyze the impacts of climate change and land use change on the water balance components in the meso-scale (2036 km<sup>2</sup>) Mula and Mutha Rivers catchment upstream of the city of Pune, India. To this end, the hydrologic model SWAT (Soil and Water Assessment Tool) was modified and adapted to the study area. By combining generally available data, locally available data, field measurements, expert knowledge, and data preprocessing methods in this hydrologic modeling approach, the problem of limited data availability was addressed. A focus was set on the spatial interpolation of sparse rainfall data, as rainfall is one of the most important inputs for hydrologic models. It was found that the applied modeling approach is suitable for data scarce regions. Furthermore, the methodology is transferable to tropical and sub-tropical regions. In particular, the use of a TRMM rainfall pattern as a covariate for spatial rainfall interpolation was very promising. Climate change impacts were analyzed using regional climate model data based on IPCC emission scenario A1B. A new downscaling approach was developed that is based on representing the scenario data by rearranging historically measured data in order to link the coarse resolution regional climate model data to the catchment scale. The hydrologic model was run for the scenario period from 2020 to 2099 using the rearranged weather data. The developed downscaling technique provided a consistent weather input for the scenario period, but was limited by the range of measured temperature values. Hence, climate change impacts at the end of the scenario period were likely to be underestimated. The climate change scenario resulted in higher evapotranspiration, particularly in the first months of the dry season. Thus, water availability was decreased more rapidly and earlier in the dry season. In addition, more frequent dry years led to repeated low water storages in the reservoirs at the end of rainy season. Past land use changes between 1989 and 2009 were identified with the help of three multitemporal land use classifications which were based on multispectral satellite data. Two model runs were performed and compared using the land use

classifications of 1989 and 2009. The main land use changes in the past two decades were an increase of urban area and cropland, while semi-natural land use decreased. Urbanization in the eastern part of the catchment resulted in a shift of cropland towards the west. On the catchment scale the impacts of these land use changes upon the water balance canceled each other out. However, at the sub-basin scale, urbanization led to an increase of the water yield and a decrease of evapotranspiration, whereas the increase of cropland resulted in an increase of evapotranspiration. These changes yielded a change of the intra-annual course of runoff, so that runoff increased in the rainy season due to urbanization, and decreased in the dry season due to increased irrigation water demand. Climate change and land use change pose challenges to the diverse water users inside and outside of the catchment. In particular, the indicated decrease of water availability in the dry season exacerbates the imbalance of water availability and water demand at this time of the year. Overall this thesis substantially enhances the knowledge of global change impacts on the water resources in the study area, which provides a means to mitigate future impacts by adapting water management. Furthermore, the developed and improved methods for hydrologic modeling in data scarce regions are transferable to other study areas and applicable in future research.

# Kurzzusammenfassung

Wasserknappheit stellt eine der größten Herausforderungen des 21. Jahrhunderts dar. Bevölkerungswachstum und wirtschaftliche Entwicklung führen häufig zu steigendem Wasserbedarf, während Klimawandel und Landnutzungsänderungen das Wasserdargebot beeinflussen. Die Untersuchung der Auswirkungen von Klimawandel und Landnutzungsänderungen auf die Wasserressourcen ist insofern hoch relevant, weil sie Voraussetzung für eine Anpassung des Wassermanagements und die Entwicklung geeigneter Mitigationsstrategien ist. Besonders in Regionen mit knappen Wasserressourcen, hoher Klimasensitivität und großer sozioökonomischer Dynamik ist eine solche Untersuchung von großer Bedeutung. Das Ziel dieser Arbeit ist die Entwicklung eines hydrologischen Modells für die Untersuchung von Auswirkungen des Klimawandels und von Landnutzungsänderungen auf die Wasserhaushaltskomponenten des mesoskaligen (2036 km<sup>2</sup>) Einzugsgebiets der Flüsse Mula und Mutha oberhalb der Stadt Pune in Indien. Zu diesem Zweck wurde das hydrologische Modell SWAT (Soil and Water Assessment Tool) modifiziert und an das Untersuchungsgebiet angepasst. Durch die Kombination von allgemein und lokal verfügbaren Daten, Messungen, Expertenwissen und Methoden der Datenaufbereitung wurde dem Problem der eingeschränkten Datenverfügbarkeit in diesem Modellansatz begegnet. Ein Schwerpunkt wurde auf die räumliche Interpolation der wenigen Niederschlagsmessungen gelegt, da der Niederschlag eine der wichtigsten Eingangsgrößen für die hydrologische Modellierung ist. Die Ergebnisse der Arbeit zeigen, dass die verwendete Methode für die hydrologische Modellierung in datenarmen Gebieten geeignet, und überdies auf andere datenarme Gebiete in den Tropen und Subtropen übertragbar ist. Insbesondere war die Verwendung eines TRMM Niederschlagsmusters als Kovariate für die räumliche Interpolation des Niederschlags sehr vielversprechend. Die Auswirkungen des Klimawandels wurden unter Verwendung von Berechnungen eines Regionalen Klimamodells, die auf dem IPCC Emissionsszenario A1B basieren, analysiert. Um die grob aufgelösten Daten des Regionalen Klimamodells auf die Einzugsgebietskala zu übertragen, wurde eine Downscaling-Methode entwickelt, die den Szenarienverlauf durch neu angeordnete Messdaten wiedergibt. Das hydrologische Modell wurde mit diesen neu angeordneten Messdaten für den Szenarienzeitraum von 2020 bis 2099 betrieben. Die entwickelte Downscaling-Methode lieferte ein in sich konsistentes Wetter für den Szenarienzeitraum, wurde aber durch den Wertebereich der gemessenen Temperaturen begrenzt. Deshalb wurden die Auswirkungen des Klimawandels gegen Ende des Szenarienzeitraums wahrscheinlich

unterschätzt. Das Klimawandelszenario führte zu erhöhter Evapotranspiration, besonders in den ersten Monaten der Trockenzeit. Dadurch nahm das verfügbare Wasser in der Trockenzeit schneller und früher ab. Häufigere Trockenjahre führten außerdem mehrfach zu niedrigen Speicherständen in den Stauseen am Ende der Regenzeit. Die Landnutzungsänderungen zwischen 1989 und 2009 wurden mit der Hilfe von drei multitemporalen Landnutzungs-klassifikationen, die auf multispektralen Satellitendaten basieren, erfasst. Zwei Modellläufe für die Klassifikationen aus den Jahren 1989 und 2009 wurden durchgeführt und miteinander verglichen. Die wichtigsten Landnutzungsänderungen der letzten beiden Jahrzehnte sind die Zunahme von Siedlungsflächen und Ackerflächen und die Abnahme naturnaher Landnutzungsflächen. Urbanisierung im östlichen Teil des Einzugsgebiets führte zu einer Verlagerung der Ackerflächen nach Westen. Die Auswirkungen dieser Landnutzungsänderungen auf den Wasserhaushalt des Einzugsgebiets glichen sich gegenseitig aus. In den Teileinzugsgebieten wurde jedoch deutlich, dass die Urbanisierung zu einer Erhöhung der Abflussspende und einer Abnahme der Evapotranspiration führte, während die Zunahme der Ackerfläche in einer Zunahme der Evapotranspiration resultierte. Diese Veränderungen führten zu einer Änderung des Abflussgangs, so dass der Abfluss aus dem Einzugsgebiet in der Regenzeit durch Urbanisierung zunahm und in der Trockenzeit durch den gestiegenen Bewässerungsbedarf abnahm. Klimawandel und Landnutzungsänderungen sind eine Herausforderung für die unterschiedlichen Wassernutzer innerhalb und außerhalb des Einzugsgebiets. Besonders während der Trockenzeit kommt es zu einer Verschärfung des Ungleichgewichts von Wasserverfügbarkeit und Wasserbedarf. Insgesamt erweitert diese Arbeit das Wissen über die Auswirkungen des Globalen Wandels auf die Wasserressourcen im Untersuchungsgebiet deutlich und schafft damit die Voraussetzungen dafür, zukünftige Auswirkungen abzuschwächen, indem das Wassermanagement angepasst wird. Außerdem können die neu- und weiterentwickelten Methoden zur hydrologischen Modellierung in datenarmen Gebieten auf andere Gebiete übertragen werden und in zukünftigen Forschungsprojekten Anwendung finden.

# Acknowledgements

This thesis was supported by a scholarship awarded by the German National Academic Foundation (Studienstiftung des deutschen Volkes). I gratefully acknowledge the financial support and the opportunity to take part in the interesting and very useful seminars that were a part of this scholarship. Furthermore, the complementary funding received from the German Academic Exchange Service (DAAD) and the Geographical Association of Cologne (Gesellschaft für Erdkunde zu Köln) for attending conferences in Korea, Spain, the USA, and India is appreciated very much.

I would like to thank Prof. Dr. Karl Schneider, who supervised this thesis, for introducing me to the truly diverse and fascinating topic of hydrologic modeling, as well as for providing guidance and stimulating suggestions that improved my work. Moreover, I appreciate that he supported this project in many ways, from mutual field measurements in India at the beginning of the project to the financial support for completing this thesis.

Furthermore I would like to thank Prof. Dr. Georg Bareth, who agreed to act as a second referee for this thesis, and Prof. Dr. Susanne Crewell, who consented to take the role of the head of the examination commission.

I am grateful to Prof. Dr. Peter Fiener, who was always open for discussions, willing to bring in his research experience, and from whom I have learned so much, especially with regard to writing papers.

This thesis would not have been possible without the support of many people in India. I truly thank Prof. Dr. Erach Bharucha and Prof. Dr. Shamita Kumar for introducing me to their country and taking interest in this project. Their hospitality and the tremendous support offered by them and by the staff and the students of the Institute of Environment Education & Research at Bharati Vidyapeeth University Pune is highly appreciated. In particular, I would like to thank Ganesh Zende, Prajakta Kelkar, and Lakshmi Kantakumar Neelamsetti for their practical assistance in Pune. Furthermore, I am grateful to Prof. Dr. Vishwas Kale and Prof. Dr. Bhavana Umrikar for valuable discussions at University of Pune, and to all the Indian agencies that provided data for this study as well as to all the people involved for their cooperation.

Moreover, the provision of environmental data by various international agencies is gratefully acknowledged. In this context, I would like to thank Dr. Chris Kidd for sharing data

on TRMM rainfall patterns with me, and Shakeel Asharaf and Prof. Dr. Bodo Ahrens for providing regional climate model projections for this thesis.

I would like to express great thanks to the SWAT community. Throughout this project I have received feedback and useful advice from various SWAT users and developers. In particular, I would like to thank Prof. Dr. Raghavan Srinivasan, Dr. Jeff Arnold, Dr. Phil Gassman, and Dr. Daniel Moriasi for their interest in my work, helpful advice, and encouraging discussions at the annual SWAT conferences.

I am grateful to all of my colleagues in the Hydrogeography and Climatology work group for the good working atmosphere, moral support, and their friendly advice. Particularly, I would like to thank Dr. Tim Reichenau for in-depth discussions on downscaling methods, Dr. Verena Dlugoß for reviewing parts of this thesis, and Wolfgang Korres for exchanging practical tips to complete this work. Moreover, I thank Marius Schmidt, Norman Barth and Florian Wilken for the crucial investment in a shared coffee machine and a comfortable day-to-day working atmosphere in our office.

Special thanks go to Karen Schneider (chapters 2, 3, and 4) and Wayne Dunn (chapters 1, 5, and 6) for proofreading parts of this thesis.

Finally, I would like to thank my family. My parents Rudolf and Ursula Wagner always supported me in many ways and showed great interest in my work. My brother Ulrich was always available for good advice in the academic field. I would also like to express my heartfelt gratitude to Maike Seegel, who supported me in countless ways. I am particularly grateful to her for her encouragement, patience, and understanding.

# Contents

- List of Abbreviations..... i
- 1 Introduction ..... 1
- 2 Hydrological Modeling with SWAT in a monsoon-driven environment:  
Experience from the Western Ghats, India ..... 8
- 3 Comparison and evaluation of spatial interpolation schemes  
for daily rainfall in data scarce regions..... 17
- 4 Assessing climate change impacts on the water resources  
in Pune, India ..... 31
- 5 Assessing past land use change and its impacts on the water resources  
in Pune, India ..... 56
- 6 Summary of Results and Conclusions ..... 88
- References ..... 96



# List of Abbreviations

ASABE	American Society of Agricultural and Biological Engineers
ASTER	Advanced Spaceborne Thermal Emission and Reflection Radiometer
DEM	Digital Elevation Model
ENSO	El Niño Southern Oscillation
ET	Evapotranspiration
ETM+	Enhanced Thematic Mapper Plus
FAO	Food and Agriculture Organization of the United Nations
GIS	Geographic Information System
HRU	Hydrological Response Unit
IAHS	International Association of Hydrological Sciences
IDW	Inverse Distance Weighting
IMD	Indian Meteorological Department
IPCC	Intergovernmental Panel on Climate Change
IRS-P6	Indian Remote Sensing Satellite P6 also known as Resourcesat-1
LAI	Leaf Area Index
LISS-III	Linear Imaging Self-Scanning Sensor III
NDVI	Normalized Difference Vegetation Index
NSE	Nash-Sutcliffe Efficiency
OK	Ordinary Kriging
PBIAS	Percentage Bias
PR	Precipitation Radar
PWP	Permanent Wilting Point
RCM	Regional Climate Model
RIDW	Regression-Inverse Distance Weighting
RK	Regression-Kriging
RMSE	Root Mean Square Error
RSR	Ratio of the RMSE to the Standard Deviation of the Observations
SCS	Soil Conservation Service

SD	Standard Deviation
SRTM	Shuttle Radar Topography Mission
SWAT	Soil and Water Assessment Tool
SWC	Soil Water Content
TH	Thiessen Polygons
TM	Thematic Mapper
TRMM	Tropical Rainfall Measuring Mission
USGS	U.S. Geological Survey
UTM	Universal Transverse Mercator

# 1 Introduction

Water scarcity is one of the most challenging problems the world is facing in the 21<sup>st</sup> century (Simonovic, 2002). Global change affects local and regional water resources. Population growth and economic development often lead to an increase of water demand, whereas climate change and land use change have an impact on water availability. Especially in regions with scarce water resources, high climate sensitivity, and a rapid socio-economic development, a decrease of water availability due to climate or land use change will further exacerbate the imbalance of water supply and demand. Therefore, assessment of the impacts of land use and climate change on the water resources is particularly relevant in these regions, as it is a prerequisite for developing suitable water management adaptation and mitigation strategies.

The fourth assessment report of the Intergovernmental Panel on Climate Change (IPCC) highlights climate change impacts on freshwater resources worldwide and their implications for sustainable development (IPCC, 2007a). Scientific consensus has been achieved about the contribution of anthropogenic greenhouse gas emissions to climate change (IPCC, 2007b; Oreskes, 2004). In order to assess future impacts of climate change, the IPCC developed emission scenarios, following different storylines that represent possible human development in different economic, technical, environmental and social dimensions (Nakićenović et al., 2000). With the help of global coupled atmosphere-ocean general circulation models these emission scenarios are used to derive climate predictions. A multi-model approach indicates an increase of global mean surface temperature and a general intensification of the global hydrological cycle with regionally different impacts on precipitation (IPCC, 2007b). These climate projections are typically available at large spatial scales with coarse spatial resolution, whereas hydrologic impact assessment is particularly relevant on significantly smaller scales, where water management can be adapted. Therefore, downscaling approaches are employed to link the coarse climate model results to meso-scale hydrologic models (Diaz-Nieto and Wilby, 2005; Fowler et al., 2007; Teutschbein and Seibert, 2010).

The consequences of land use changes are a key research question in the 21<sup>st</sup> century (DeFries and Eshleman, 2004). Large proportions of the world's surface have already been changed (Foley et al., 2005). Land use is understood as a general term for land use and land cover. Thus, land use change comprises any transition of land use classes, e.g., conversion of cropland to urban area, as well as changes within classes such as a change of crops or crop rotations. Most rapid land use changes in the recent decades include tropical deforestation, agricultural intensification, and urbanization (Ramankutty et al., 2006), and are expected to accelerate in the coming decades (DeFries and Eshleman, 2004). These land use changes have a large potential to affect water resources (Stonestrom et al., 2009) as land use has a direct influence on the partitioning of precipitation into runoff, evapotranspiration and infiltration (Foley et al., 2005). In a global-scale study, Vörösmarty et al. (2000) suggest that the impacts of land use change due to human development outweigh those of climate change on the water resources in the near future. Foley et al. (2005) give a review of typical land use change impacts on water resources that were reported in regional studies. Generally, runoff increases if natural vegetation decreases (e.g., Costa et al., 2003; Sahin and Hall, 1996) and if built-up area increases (e.g., Arnold and Gibbons, 1996; Wijesekara et al., 2012). Runoff decreases if water demand and, consequently, withdrawal from rivers increase (Foley et al., 2005). Irrigation agriculture accounts for nearly 85% of the worldwide human consumptive water use (Gleick, 2003). Hence, increase of irrigation agriculture has a large impact on water resources, resulting in increased water withdrawal, decreased runoff, and increased evapotranspiration.

In order to assess land use changes with sufficient spatial precision, spatially distributed information is needed. Satellite images provide valuable spatially distributed information for this purpose. The collection of satellite images in international archives offers an unprecedented opportunity to assess past land use changes (DeFries and Eshleman, 2004), as historic satellite images can be used to derive past land use maps (e.g., Miller et al., 2002; Seeber et al., 2010). Using these data as an input to hydrologic models provides a feasible method to analyze the impacts of past land use changes on water resources (e.g., Ghaffari et al., 2010; Im et al., 2009; Miller et al., 2002).

Due to the scientific relevance of global change (comprising land use and climate change), large interdisciplinary research programs, e.g., BRAHMATWINN (Twinning European and South Asian River Basins to enhance capacity and implement adaptive management approaches, 2006-2009), the GFI (Global Freshwater Initiative, 2010-present), GLOWA

(Global Change and the Hydrological Cycle, 2000-2011), KLIWA (Climate change and consequences for water management, 1998-present), RIVERTWIN (A regional model for integrated water management in twinned river basins, 2003-2007), and WaterGAP (Global modeling of water availability, water use, and water quality, 1996-2011) focus on the assessment of its impacts on water resources in individual catchments. To this end, modeling approaches are typically employed.

Many hydrologic models are available for different aspects of water resources management, such as flood forecasting, water supply and demand analysis, and water quality evaluation. A comprehensive review of hydrologic models is available in the literature (e.g., Mulligan, 2004; Singh, 1995). Detailed information on model use, calibration and validation for 25 commonly used hydrologic and water quality models is provided in a recent special issue of *Transaction of the ASABE* (Vol. 55, No. 4), including exemplary case studies for each model (Moriassi et al., 2012). In general, the different modeling approaches vary in conception and complexity from physically based, spatially distributed models (e.g., MIKE SHE; Refsgaard and Storm, 1995; e.g., Im et al., 2009), to more conceptual lumped models (e.g., TOPMODEL; Beven and Kirkby, 1979; e.g., Vincendon et al., 2010). Following Kirchner (2006), physically based models are more suitable to analyze impacts of environmental change on hydrology as the predictive quality of models with (calibrated) empirical components depends on the environmental conditions of the past and may therefore not be suitable if these conditions change. Furthermore, with regard to spatially distributed changes such as land use changes, spatially distributed models are most suitable to represent these changes (Beven, 2001). However, fully distributed physically based models are very data intensive (Singh, 1995) and therefore feasible in catchments where intensive measurements and further high resolution input data are available. Semi-distributed models simplify the representation of space (Mulligan, 2004) and thus balance data requirements and process representations. These models are therefore an alternative for impact studies in regions with limited data availability. For this reason the Soil and Water Assessment Tool (SWAT; Arnold et al., 1998), a semi-distributed catchment model, was used in this thesis.

SWAT was developed in the early 1990s by the Agricultural Research Service of the U.S. Department of Agriculture to study impacts of management on water, sediment, and agricultural chemical yields in ungauged catchments (Gassman et al., 2007). Since that time, it was continuously developed and improved from model versions SWAT94.2, 96.2, 98.1, 99.2, 2000, 2005, 2009, to the very recent version 2012 (Arnold et al., 2012; Gassman et al.,

2007). The model is a comprehensive, semi-distributed, process based catchment model (Arnold et al., 2012). The implemented process representations are simplifications of reality (Gassman et al., 2007) which are constantly improved (Arnold et al., 2012). These simplifications of reality (e.g., hydrologic response units are not spatially identified within a sub-basin) make SWAT a computationally efficient model, which is capable of continuous simulation over long time periods (Gassman et al., 2007). Arnold et al. (2012) highlight SWAT's flexibility in combining upland and channel processes and the simulation of land management as fundamental strengths of the model. A further strength is its well-documented open source code, which allows for adaptation of the model to many different environments or for specific needs, such as e.g., coupling with the groundwater model MODFLOW (Kim et al., 2008; Sophocleous et al., 1999), modifying the nitrogen cycle (Pohlert et al., 2007), adapting the model to forested catchments (Watson et al., 2008), and to an African catchment (Notter et al., 2012). Another factor that contributes to the increasing use of the model is the user support by the model developers through training seminars, online tutorials, and the model website. Moreover, data requirements for an initial setup of the model are moderate, and pre-processing is supported by the ArcSWAT extension for ArcGIS, which allows for the extraction of parameters from GIS layers and prepares the model input files. Recently, freely available data sets (e.g., global weather data, formatted for SWAT, since October 2012; global soil data base, including the soil parameters for SWAT, in preparation) are provided on the model website (<http://swat.tamu.edu>).

SWAT is increasingly used for applications all around the world (Gassman et al., 2007). More than 1100 peer reviewed journal articles have been published, which are related to SWAT (SWAT Literature Database, 2012). It is a suitable model to conduct impact studies, as the impacts of land use change (e.g., Ghaffari et al., 2010; Miller et al., 2002), and climate change (e.g., Jha et al., 2006; Liu et al., 2011) or both (e.g., Mango et al., 2011; Park et al., 2011) on hydrology have been assessed using SWAT in different parts of the world. Furthermore, the model has proven its capability to model water fluxes in regions with limited data availability (Ndomba et al., 2008; Stehr et al., 2008). In India, SWAT is increasingly used for large scale (e.g., Gosain et al., 2006; 2011; Immerzeel and Droogers, 2008; Immerzeel et al., 2008), meso-scale (e.g., Dhar and Mazumdar, 2009; Garg et al., 2012; Kelkar et al., 2008; Kusre et al., 2010) and small scale studies (e.g., Behera and Panda, 2006; Mishra et al., 2007; Pandey et al., 2009; Tripathi et al., 2005). Hence, SWAT is a suitable hydrologic model to assess impacts of climate change and land use change on the water resources in an Indian catchment.

In a worldwide assessment of threats to human water security, Vörösmarty et al. (2010) found that water security is particularly threatened in poorer countries (e.g., in many African countries, and India). Thus research on water resources is particularly relevant in these regions, while data availability is often limited. One approach to cope with the problem of scarce and missing data is to fully exploit the use of worldwide data archives, transferable literature values, and remotely sensed data. The use of remotely sensed data for hydrologic modeling in general (e.g., Houser et al., 1998; Schneider, 2003) and particularly in data scarce environments has previously been shown (e.g., Chaponnière et al., 2008; Immerzeel and Droogers, 2008). Research on a suitable methodology for hydrologic modeling in data scarce regions addresses the problem of hydrological predictions in catchments with missing or scarce measurements, which is a core issue of the decadal initiative (2003-2012) of the International Association of Hydrological Sciences (IAHS) on “Predictions in Ungauged Basins” (Sivapalan et al., 2003). Particularly, with regard to rainfall data, precaution is necessary as this is the major input for hydrologic models (Beven, 2001). Poorer modeling results in some SWAT modeling studies (e.g., Bouraoui et al., 2005; Cao et al., 2006; Conan et al., 2003) are in part attributed to an inadequate representation of spatial rainfall variability (Arnold et al., 2012).

One of the regions where data availability is limited and water resources are scarce is India. India has undergone rapid socio-economic development (CIA World Factbook, 2012; World Bank, 2012) and population growth (United Nations, 2012) in the past decades. Currently, it is the country with the second largest population (1.2 billion in 2010), by 2025 it will be the country with the largest population in the world, and in the year 2050 a population of 1.7 billion is expected (United Nations, 2012). Consequently, the past and future socio-economic development and population growth result in an increase of water demand.

Furthermore, land use and climate change affect the water availability in India. India’s water resources are heavily dependent on seasonally limited rainfall. The largest parts of the country receive rainfall from the southwest monsoon from June to September, whereas the east coast receives larger rainfall amounts in October and November from the northeast trade winds (Gadgil, 2003). The Indian monsoon is related to the El Niño Southern Oscillation (ENSO) phenomenon: El Niño can be attributed to a weakening of the Indian monsoon, whereas La Niña results in above normal monsoon rainfall in India (Kripalani et al., 2003). The Indian monsoon has a high intra-seasonal variation with varying onsets of the monsoon, which has a large impact on agriculture (Gadgil, 2003). Climate change may exacerbate these

impacts (e.g., droughts) directly by increasing temperatures and indirectly by influencing the ENSO phenomenon (e.g., weaker monsoon seasons due to more frequent El Niño conditions; Timmermann et al., 1999).

Main land use changes in India include urbanization (Chauhan and Nayak, 2005), increase of agricultural area (Jayakumar and Arockiasamy, 2003; Sharma et al., 2007), and deforestation (Jha et al., 2000; Sharma et al., 2007). As noted above all of these land use changes affect the water resources. While urbanization and deforestation typically result in an increase of runoff, increase or intensification of agriculture leads to an increase of water demand and water withdrawal (Foley et al., 2005). Thus, both climate change and land use change have the potential to further decrease water availability in India. Increase of water demand and decrease of water availability will consequently result in an exacerbation of water scarcity. It is therefore highly relevant to investigate impacts of climate change and land use change on the water resources in India. The catchment of the Mula and Mutha Rivers upstream of the city of Pune has many of the outlined characteristics of India. It experiences rapid socio-economic development, population growth, and seasonally limited rainfall between June and September. Although it is relatively water rich, as it receives large rainfall amounts in some parts, the water resources are under pressure from water users inside and outside of the catchment.

Against this background, the impacts of climate change and land use change on a meso-scale (2036 km<sup>2</sup>) catchment in a monsoon-driven environment are analyzed in this thesis. The scope of this thesis is to analyze land use and climate change impacts separately, although it is understood that climate change and land use change are linked through the hydrologic cycle (Stonestrom et al., 2009) and that the combined impact may thus result in more severe impacts on water resources. A climate scenario is employed to assess climate change impacts, whereas past land use changes are examined and used to assess the impacts of land use changes on water resources. Employing observed land use changes gives confidence in the relevance of the analyzed changes. The response to climate scenario and observed land use changes allow for drawing general conclusions on how climate change and land use change affect hydrology in the study area.

Hence, the main research questions of this thesis are:

- How can generally available data from satellite observations and GIS databases be used in conjunction with sparse local measurements to provide a suitable input for spatially distributed hydrologic modeling?

- How does climate change affect the water resources in the study area?
- How does land use change affect the water resources in the study area?

In order to address these questions the following objectives are defined and addressed in the subsequent chapters:

- 1) Evaluation and adaptation of the Soil and Water Assessment Tool for an application in a monsoon-driven, data scarce environment (chapter 2).
- 2) Evaluation of different interpolation methods for spatial interpolation of rainfall in a data scarce environment (chapter 3).
- 3) Downscaling of a climate scenario and analysis of its impact on the water resources in the study area (chapter 4).
- 4) Analysis of the land use changes in the past 20 years and their impact on the water resources in the study area (chapter 5).



## 2 Hydrological Modeling with SWAT in a monsoon-driven environment: Experience from the Western Ghats, India

Journal article (published)

Authors: Wagner, P.D., Kumar, S., Fiener, P., Schneider, K.

Journal: Transactions of the ASABE

Volume (Issue): 54 (5)

Date of publication: September/October 2011

Reprinted with permission from:

Wagner, P.D., Kumar, S., Fiener, P., Schneider, K., 2011. Hydrological modeling with SWAT in a monsoon-driven environment: Experience from the Western Ghats, India. Transactions of the ASABE 54(5): 1783-1790. St. Joseph, Mich.: ASABE.

# HYDROLOGICAL MODELING WITH SWAT IN A MONSOON-DRIVEN ENVIRONMENT: EXPERIENCE FROM THE WESTERN GHATS, INDIA



P. D. Wagner, S. Kumar, P. Fiener, K. Schneider

**ABSTRACT.** Monsoon regions are characterized by a pronounced seasonality of rainfall. Model-based analysis of water resources in such an environment has to take account of the specific natural conditions and the associated water management. Especially, plant phenology, which is predominately water driven, and water management, which aims at reducing water shortage, are of primary importance. The aim of this study is to utilize the Soil and Water Assessment Tool (SWAT) in a monsoon-driven region in the Indian Western Ghats by using mainly generally available input data and to evaluate the model performance under these conditions. The test site analyzed in this study is the meso-scale catchment of the Mula and Mutha Rivers (2036 km<sup>2</sup>) upstream of the city of Pune, India. Most input data were derived from remote sensing products or from international archives. Forest growth in SWAT was modified to account for the seasonal limitation of water availability. Moreover, a dam management scheme was derived by combining general dam management rules with reservoir storage capacity and estimated monthly outflow rates from river discharge. With these model adaptations, SWAT produced reasonable results when compared to mean daily discharge measured in three of four subcatchments during the rainy season (Nash-Sutcliffe efficiencies 0.58, 0.63, and 0.68). The weakest performance was found at the gauge downstream of four dams, where the simple dam management scheme failed to match the combined management effects of the four dams on river discharge (Nash-Sutcliffe efficiency 0.10). Water yield was underestimated by the model, especially in the smallest (headwater) subcatchment (99 km<sup>2</sup>). Due to the absence of rain gauges in these headwater areas, the extrapolation errors of rainfall estimates based on measurements at lower elevations are expected to be large. Moreover, there is some indication that evapotranspiration might be underestimated. Nevertheless, it can be concluded that using generally available data in SWAT model studies of monsoon-driven catchments provides reasonable results, if key characteristics of monsoon regions are accounted for and processes are parameterized accordingly.

**Keywords.** Data-scarce environment, India, Monsoon, SWAT, Water management.

Monsoon regions are characterized by a pronounced seasonality of water and energy fluxes. This seasonality has a strong impact upon the environment. The varying water availability governs the phenological development of natural and agricultural vegetation (Goldsworthy and Fisher, 1984) and is a major motivation for the construction of large reservoirs

to secure year-round water supply (Jain et al., 2007). Seasonal disparity of the natural water supply is often met by an increasing water demand due to rapid population growth and industrial development as well as changes in land use patterns and land management procedures (Pangare et al., 2006). Under such conditions, hydrologic models are essential tools for a sustainable current and future water resources management (Ajami et al., 2008).

A huge number of hydrologic models is available for different aspects of water resources management, such as flood forecasting, water supply and demand analysis, and water quality evaluation. These modeling approaches vary in conception and complexity from physically based (e.g., MIKE SHE; Refsgaard and Storm, 1995; Im et al., 2009) to more conceptual models (e.g., TOPMODEL; Beven and Kirkby, 1979; Vincendon et al., 2010). In monsoon regions, model application is often restricted by limited data availability or outdated data due to the rapid socio-economic development. Therefore, modeling approaches that balance data requirements and process representations are essential for water resources analysis and management in these regions. Among others, the Soil and Water Assessment Tool (SWAT; Arnold et al., 1998) has proven its capability to model water fluxes in regions with limited data availability (Ndomba et al., 2008;

---

Submitted for review in October 2010 as manuscript number SW 8885; approved for publication as a Technical Note by the Soil & Water Division of ASABE in May 2011.

The authors are **Paul Daniel Wagner**, ASABE Member, Doctoral Student, Hydrogeography and Climatology Research Group, Institute of Geography, University of Cologne, Germany; **Shamita Kumar**, Associate Professor and Vice-Principal, Institute of Environment Education and Research, Bharati Vidyapeeth University, Pune, India; **Peter Fiener**, Professor, Indo-German Centre of Sustainability, Indian Institute of Technology Madras, Chennai, India, and Hydrogeography and Climatology Research Group, Institute of Geography, University of Cologne, Germany; and **Karl Schneider**, Professor and Chair, Hydrogeography and Climatology Research Group, Institute of Geography, University of Cologne, Germany. **Corresponding author:** Karl Schneider, Hydrogeography and Climatology Research Group, Institute of Geography, University of Cologne, D-50923 Cologne, Germany; phone: +49-221-470-4331; fax: +49-221-470-5124; e-mail: karl.schneider@uni-koeln.de.

Stehr et al., 2008) and has already been utilized in larger-scale studies in India (Dhar and Mazumdar, 2009; Gosain et al., 2006; Immerzeel and Droogers, 2008; Immerzeel et al., 2008). Hence, SWAT is a suitable tool for hydrological modeling of a meso-scale catchment in the Indian Western Ghats.

The main objective of this study is to utilize SWAT in a monsoon-driven meso-scale catchment by using mainly generally available input data and evaluate the model's potential for water resources management under these conditions. Successful implementation of this methodological approach provides a transferable method for the assessment of water resources in a monsoon-driven, data-scarce environment.

## MATERIALS AND METHODS

### STUDY AREA

The Western Ghats catchment of the Mula and Mutha Rivers (2036 km<sup>2</sup>, fig. 1) is a sub-basin and source area of the Krishna River, which drains towards the east and into the Bay of Bengal. It has a tropical wet and dry climate characterized by seasonal monsoon rainfall from June to October and low annual temperature variation, with an annual mean of 25°C at the catchment outlet in Pune (18.53° N, 73.85° E). There is a pronounced west (approximately 3500 mm) to east (750 mm) decline of annual precipitation in the catchment (Gadgil, 2002; Gunnell, 1997); likewise, the relief declines from 1300 m on the top ridges in the Western Ghats to 550 m at Pune.

About two-thirds of the study area consists of grassland, shrubland and (semi-evergreen) deciduous forest (table 1). The agricultural areas are characterized by small fields (<1 ha). Typically, two crops per year are harvested. A rainfed crop is grown from June to October, and an irrigated crop is cultivated after the end of the monsoon season (November to March). In a few locations, where irrigation water supply is sufficient, a third crop is grown in April and May.

Water resources are highly managed by maintenance of six large dams in the catchment, which serve various purposes, such as power generation, irrigation, and municipal water supply for the city of Pune. Within the catchment, four gauged subcatchments that are defined by the locations of the gauges (G1, G2, G3, and G4) are used for model validation (table 1).

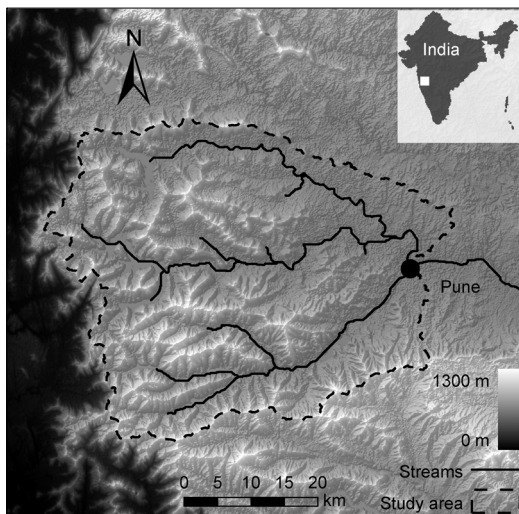


Figure 1. Location and elevation of the Mula-Mutha catchment.

Table 1. Main characteristics of the Mula-Mutha catchment and of four subcatchments, defined by gauge locations G1 to G4.

Catchment	Mula-Mutha	G1	G2	G3	G4
Area (km <sup>2</sup> )	2036	498	331	680	99
Mean elevation (m)	676	634	694	729	803
Mean slope (%)	17	12	21	22	26
Forest (%)	20.6	10.5	34.2	31.3	45.1
Shrubland (%)	26.6	19.8	30.1	34.1	33.5
Grassland (%)	22.8	31.0	17.5	17.1	15.9
Cropland (%)	11.2	17.3	4.4	4.6	3.2
Water (%)	5.8	5.5	12.6	6.6	1.6
Urban (%)	13.0	16.0	1.3	6.2	0.7

### DIGITAL ELEVATION MODEL

A suitable digital elevation model (DEM) is an essential prerequisite for hydrological model studies. We used a DEM based on ASTER (Advanced Spaceborne Thermal Emission and Reflection Radiometer) satellite data with a spatial resolution of 30 m (fig. 1). Four readily processed DEMs, calculated from stereo images of the near-infrared band, were acquired from the U.S. Geological Survey (USGS, 2009). To cover the entire study area, these four ASTER DEMs were merged. However, water surfaces are poorly represented in DEMs derived from optical satellite data. To determine water surfaces, a Landsat 7 ETM+ scene was used, and the water levels were derived from the ASTER elevations of the reservoir banks.

Compared to the 90 m × 90 m SRTM DEM (Jarvis et al., 2008), the ASTER DEM has a mean offset in elevation of 13.6 m. After correcting for this offset, the mean absolute error, which indicates the mean deviation from the SRTM DEM, is 8.8 m and the root mean square error is 15.3 m. The most pronounced differences can be observed in the mountain ranges, which typically result from the different spatial resolutions. The major advantage of the higher spatial resolution is a more accurate representation of slopes and the possibility to derive a more detailed stream network. Visual comparison to the drainage maps acquired from the Groundwater Department of Pune confirms the accuracy of the calculated stream network.

### SOIL MAP

The spatial distribution of the soils was derived from the *Digital Soil Map of the World* (FAO, 2003). Major parts (92.5%) of the study area consist of a sandy clay loam (Hh11-2bc, Haplic Phaeozem). Minor parts (7.5%) are covered by a clay (Vc43-3ab, Chromic Vertisol). The two-layer soil parameterization used for modeling (table 2) was partly taken from a macro-scale modeling study of the region by Immerzeel et al. (2008).

### WEATHER DATA

Daily weather data (temperature, precipitation, humidity, solar radiation, and wind speed) from the Indian Meteorological Department (IMD) weather station in Pune (ID 430630, 18.533° N, 73.85° E, 559 m) were used as model input. In addition, three daily rainfall measurement stations that are maintained during the monsoon season by Tahasil (subdistrict administrative division) offices supplemented the record of precipitation in the catchment. Weather data is incorporated into the model at the SWAT sub-basin level. Due to the strong elevation gradient and the resulting east-to-west rainfall gradient (Gadgil, 2002; Gunnell, 1997), the SWAT stan-

**Table 2. Parameterization for the two soils in the catchment adapted from Immerzeel et al. (2008); bulk density and organic carbon content taken from FAO (2003).**

FAO Soil Code	Layer	Depth (cm)	Clay (%)	Silt (%)	Sand (%)	Sat. Hydraulic Conductivity (mm h <sup>-1</sup> )	Available Water Capacity (mm mm <sup>-1</sup> )	Bulk Density (g cm <sup>-3</sup> )	Organic Carbon Content (%)
Hh11-2bc	Topsoil	0-30	28.0	26.2	45.8	0.17	0.22	1.27	1.81
	Subsoil	30-137	28.3	23.1	48.6	0.14	0.07	1.35	0.70
Vc43-3ab	Topsoil	0-30	51.7	23.7	24.6	0.11	0.05	1.65	0.76
	Subsoil	30-143	54.6	22.9	22.5	0.16	0.01	1.75	0.46

standard method of using the nearest measurement station to represent precipitation in the sub-basin is not a suitable approach in the Mula-Mutha catchment. Therefore, a virtual weather station was generated in the center of each of the 27 sub-basins generated by SWAT. The precipitation for these virtual stations was estimated from the measurements of the four weather stations using an approach by Mauser and Bach (2009) that is based upon combining a regression technique with an inverse distance interpolation scheme. Firstly, a linear regression of elevation and mean daily measured rainfall amount was calculated ( $R^2 = 0.8$ ,  $p = 0.10$ ). Secondly, the regression equation and the mean elevation of the respective sub-basin were used to estimate the mean daily rainfall amounts for each sub-basin. Thirdly, the residual of daily rainfall (daily rainfall - mean daily rainfall) was calculated for every wet day and every measurement station. These residuals were interpolated to the center of each sub-basin using an inverse distance weighting scheme. Finally, by adding the interpolated residuals to the mean daily rainfall values calculated from the regression equation, a complete precipitation record was produced for every sub-basin.

To account for temperature differences in the catchment, temperature values were adjusted for every sub-basin using adiabatic temperature gradients of 0.98°C per 100 m on a dry day (no precipitation) and 0.44°C per 100 m on a wet day (Weischet, 1995). Using the sub-basin specific temperature records and the specific humidity measured at the weather station in Pune, relative humidity was calculated for each sub-basin. Solar radiation and wind speed data are only available in Pune and were therefore used for the whole catchment. In the two sub-basins that include a weather station or a rain gauge, the measurements from these stations were used as model input instead of the interpolated sub-basin specific data.

#### LAND USE MAP

A land use map (fig. 2) was derived from a satellite image taken on 30 November 2009 by the Linear Imaging Self-Scanning Sensor III (LISS-III) on the Indian satellite IRS-P6. LISS-III is a medium-resolution (23.5 m) multi-spectral sensor with two bands in the visible region, one band in the near-infrared region, and one band in the shortwave infrared region. All four of these bands were used for the classification. A stratified knowledge-based classification approach, using a maximum likelihood classifier, was applied as follows: thresholds of elevation (<800 m) and slope (<10%) were set for agricultural land use. In the study area, agriculture depends on the proximity to rivers and is therefore located in the valleys, which typically meet the 800 m elevation criterion. Pixels classified as agriculture in areas exceeding these thresholds were assumed to be grassland.

Finally, a majority analysis was applied on a moving 3 × 3 raster window to remove misclassified, spatially singular

pixels within areas covered by one homogeneous class. Ground truth mapped at three test sites between 20 September and 9 October 2009 was used for calibration and validation. The time gap between ground truth and satellite imagery resulted from the need for a cloud-free image. This time lag has an influence on the classification of agricultural classes, as rice fields and some sugarcane fields had been harvested in between. Hence, the good quality of the classification (overall accuracy of 79%) decreases when rice and sugarcane are distinguished from other agricultural land use types (overall accuracy of 65%). The user's accuracy, which expresses the quality of the land use classification from the user's perspective (Story and Congalton, 1986), ranges from low accuracy for mixed cropland (27%), bare soil (41%), shrubland (45%) and grassland (69%) to high accuracy for forest (79%), rice (86%), urban (89%), and sugarcane (92%). Evidence of the quality of the land use classification is also derived from comparison with the most recent (cropping year 2007-2008) agricultural statistics available from the Department of Agriculture in Pune.

The land use classification indicates the dominance of semi-natural vegetation (table 1) in the catchment, with forest covering the higher elevations in the west, and grassland and shrubland dominating the lower elevations (fig. 2). Agricultural land mainly located in proximity to rivers and dams accounts for only 10.6% of the catchment (4.7% rice, 0.7% sugarcane, and 5.3% mixed cropland). The eastern part of the catchment is dominated by the city of Pune and its surrounding settlements (1.9% high-density and 11.1% medium-density urban area).

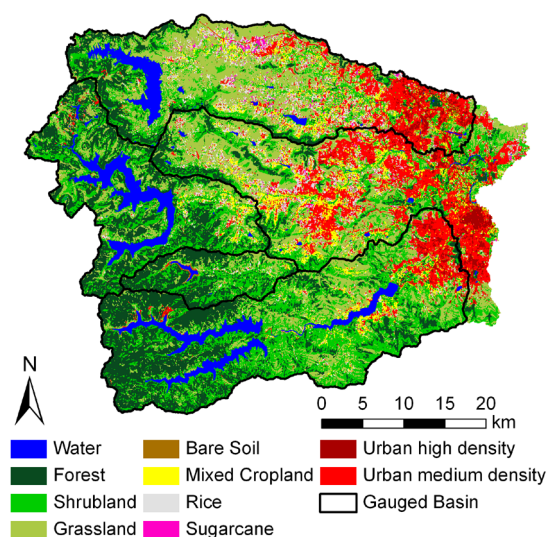


**Figure 2. Land use map of the study area derived from LISS-III satellite data.**

**Table 3. Model setup for the vegetation land use classes.**

Land Use	SWAT Land Use Code (Neitsch et al., 2010)	Management Details
Forest	FRSD	Original forest modified for the final model run
Grassland	BERM	Two growth cycles in rainy season, one in dry season
Shrubland	BERM, FRSD	Combination of 70% grassland and 30% forest
Bare soil	BERM, AGRL	Combination of 50% grassland and 50% mixed cropland
Mixed cropland	AGRR, AGRL	50% per class, grown as Kharif and Rabi crop, including auto irrigation and fertilization
Rice	RICE, SWHT	Rice as Kharif crop, wheat as Rabi crop, including auto irrigation and fertilization
Sugarcane	SUGC	18-month period of growth, including auto irrigation and fertilization

### MODEL SETUP

The catchment was divided into 27 sub-basins, which were defined by stream confluences and reservoir outlets. These sub-basins were subdivided into 922 hydrological response units (HRUs), representing homogenous slope (0% to 5%, 5% to 10%, 10% to 15%, and above 15%), soil, and land use classes. Surface runoff is generated using the SCS curve number method (Mockus, 1972). For channel routing according to a kinematic wave approach, a default value for Manning's roughness coefficient of  $0.014 \text{ s m}^{-1/3}$  was used. Potential evapotranspiration was calculated using the Penman-Monteith equation (Monteith, 1965). The chosen model plant types and management of the vegetation land use classes are given in table 3. Shrubland was modeled as a mixture of forest and grassland to account for the percentage of trees. Two of the general crop classes in SWAT (AGRL, AGRR; Neitsch et al., 2010) contribute equally to the modeling of mixed cropland. The bare soil class was split between agriculture and grassland, as some fields were harvested and bare when the satellite image was taken. For the rice fields, the typical crop rotation of growing rice in the Kharif season (June to October) and wheat in the Rabi season (November to March) was implemented. This rotation was the only crop rotation pattern that was clearly observable from the field surveys. A growing period of 18 month was realized for the modeling of sugarcane. Heat units to bring a plant to maturity were calculated and adjusted to the growing periods of the local crops. For all crops, auto-irrigation was initialized. The irrigation procedure is based on plant water demand, triggering irrigation when plant growth falls below 95% of potential plant growth (Neitsch et al., 2010). In sub-basins with reservoirs, water for irrigation is taken from the reservoirs. In the other sub-basins, irrigation water is supplied by the rivers. A fraction of two-thirds of river discharge is allowed to be used for irrigation purposes, which is in agreement with the percentage of surface water used for irrigation in Pune Division (districts of Pune, Sangli, Satara, Solapur, and Kolhapur; Bhagwat, 2006). Apart from rivers and reservoirs, wells are also used as water sources for irrigation in the study area (Bhagwat, 2006). A model run performed without any water limitation did not indicate remarkable differences in the growth of irrigated crops. Hence, we assume that the implemented irrigation management supplies a sufficient amount of water. On an annual average, this irrigation setup resulted in a supply of 764 mm to sugarcane, 292 mm to the rotation of rice and wheat, and 275 mm to mixed cropland. For auto-fertilization, elemental nitrogen was used. The model (SWAT 2009) was run for eight years from 2000 to 2007. Only seven years (2001-2007) of the simulation period were analyzed, allowing for a one-year model spin-up phase.

### ADAPTATION OF FOREST GROWTH

The SWAT model provides a land use and crop database with plant parameters for the respective land use type. Basically, three types of forests are supported: deciduous, coniferous, and mixed forests. The forest in the Western Ghats consists of deciduous trees. The annual growth cycle starts with the beginning of the monsoon in June and ends in the dry season, when leaves are dropped due to water and temperature stress. Most forests can be classified as tropical semi-evergreen forests, whereas evergreen forests are very limited in extent (Dikshit, 2002). Plant growth of deciduous trees in SWAT incorporates a dormancy period. The phenology model in SWAT predicts dormancy as a function of latitude and day length (Neitsch et al., 2005). The shortest day of the year triggers the beginning of tree dormancy in the model. However, in our region, dormancy is related to water and temperature stress. The methodology used by SWAT, which was developed for regions of the temperate zone, is not suitable for monsoon-driven or tropical climates. Consequentially, we modified this SWAT subroutine by shifting the dormancy period to the dry season, starting at the beginning of April and lasting until mid-May. Additionally, the maximum LAI for deciduous forests was modified ( $BLAI = 6$ ) based on the LISS-III satellite image and using a relationship of normalized differenced vegetation index (NDVI) and LAI observed by Madugundu et al. (2008). Due to the unusually wet November in 2009, the LAI derived for 30 November is a suitable estimate for maximum LAI. Heat units were calculated (4500 heat units to maturity) to allow for a maximum of ten months of growth. Throughout this period, forest growth is primarily driven by water availability (fig. 3). The course of the annual LAI development of the modified forest growth model from mid-May to the end of March agrees significantly better with the phenology of the mainly semi-evergreen forests in the region (Dikshit, 2002) than the original model does.

### DAM MANAGEMENT

The hydrology in the Mula-Mutha catchment is largely affected by six large dams (fig. 4), which are maintained to mitigate the effects of the pronounced seasonality in rainfall. Hence, it is essential for any successful model application to implement dam management. However, the available information regarding the dams is limited to maximum target storage and remotely sensed surface area. Maximum target storage for the reservoirs was made available by the Government of Maharashtra (2010), and the surface area of the reservoirs, corresponding to maximum target storage, was derived from satellite data (LISS-III image, 30 November 2009), which is assumed to be a valid estimate due to the wet November in 2009. On this basis, a simple dam management scheme was developed.

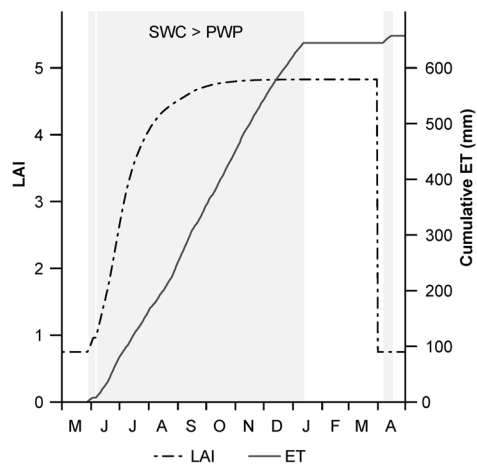


**Figure 3.** Modified forest growth allows for soil water limited evapotranspiration (ET): total (green and brown) leaf area index (LAI), cumulative evapotranspiration (ET), and periods (gray shaded) when soil water content (SWC) is above permanent wilting point (PWP) of an exemplary forest HRU from May 2001 to April 2002.

The dam management in SWAT is controlled by monthly target storage and monthly minimum and maximum flow rates that were estimated from discharge observations at the river gauges. From June to October, the target storage is equal to the maximum target storage of the dam (table 4). From November on, the target storage is decreased every month, so that the water is released from the dams at a linear rate that is limited by the dry season maximum flow rate (table 4). This setup secures the water supply until a potentially late onset of monsoon in mid-July. A constant minimum flow rate during monsoon season was specified (table 4). If the mean annual amount of precipitation occurs, then the minimum flow rate allows the dam to fill up to the maximum target storage. When the target storage is reached, additional water is stored in flood storage. No flood storage information was available; therefore, flood storage was assumed to account for 10% of the maximum target storage. The flood storage is decreased at a dam-specific constant maximum flow rate. Table 4 presents the derived parameterization for each reservoir. Dam storage information, which is supplied online by the Government of Maharashtra (2010) and is updated on a daily basis, was logged for the rainy season of 2010 and provides evidence for the adequacy of the assumed dam management.

#### RIVER GAUGING STATIONS

The Government of India implemented a Hydrological Information System within the World Bank supported Hydrology Project, through which the river discharge data were provided by the Water Resources Department of Nashik. In the catchment, four river gauging stations are available that define four gauged subcatchments (table 1). All gauges are located downstream of a managed reservoir (fig. 4); consequently, no record of unmanaged river discharge is available. The runoff record only provides data for the monsoon seasons of the years 2001 to 2007. Some data gaps are also observable in the rainy season. On average, 70 to 100 daily measurements per year were available at gauges G1, G2, and G4. The record for gauge G3 consists of only 127 measured values for the entire observation period.

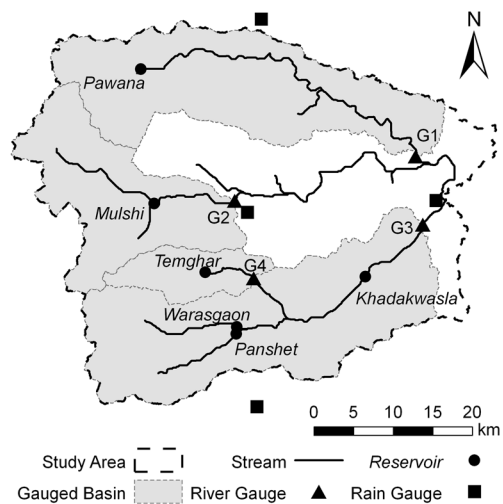


**Figure 4.** Location of river gauges, reservoirs, and rain gauges in the Mula-Mutha catchment.

**Table 4.** Reservoir characteristics acquired from the Government of Maharashtra (2010) and derived from LISS-III satellite data; dam outflow rates estimated by combining general management rules with river discharge observations at downstream gauges.

Dam	Maximum	Surface	Dry Season	Rainy Season
	Target		Maximum	Minimum
	Storage	Area	Outflow	Outflow
	( $10^6 \text{ m}^3$ )	( $\text{km}^2$ )	( $\text{m}^3 \text{ s}^{-1}$ )	( $\text{m}^3 \text{ s}^{-1}$ )
Pawana	241	23.5	8	2
Mulshi	523	40.0	15	6
Khadakwasla	56	10.0	31.5	2
Panshet	298	13.7	12	2
Warasgaon	362	19.2	15	3
Temghar	70	1.6	2.5	2.2

#### MODEL CALIBRATION AND VALIDATION

Although the SWAT model does not require much calibration (Gosain et al., 2005; Gosain et al., 2006), the model was not calibrated with ground-based measurements in this study. Site-specific model calibration often results in significant improvements of the model output. However, achieving good agreement between model results and independent measurements, such as river runoff, through model calibration does not imply that the underlying processes and parameterization are correctly described. Thus, our study does not primarily aim at achieving the best match between model and measurements through model calibration, but rather at analyzing processes and setting model parameters based on process understanding and regional knowledge, in order to learn from discrepancies between models and observations and thereby gain a better understanding of the system. It is assumed that proper process understanding and model parameterization build a solid and transferable basis to apply models in data-scarce regions or under conditions of environmental change resulting from land use or climate change or from alternative management decisions (Kirchner, 2006).

The model was validated with respect to simulated discharge and water balance. To evaluate the capability of the model to reproduce measured discharge at the four subcatchment gauges, a set of commonly used goodness-of-fit indicators was calculated: the coefficient of determination ( $R^2$ ), the Nash-Sutcliffe efficiency (NSE; Nash and Sutcliffe, 1970), and the ratio of root mean square error and standard

deviation of the observations (RSR; Moriasi et al., 2007). Direct validation of the simulated water balance is only possible for the periods for which measured data are available. Hence, water yield can only be validated in monsoon time. Additionally, supplementary information from regional studies regarding runoff coefficient and evapotranspiration (ET) was used to evaluate the simulated water balance.

## RESULTS AND DISCUSSION

### RIVER DISCHARGE

Comparing modeled and measured discharge for the four gauged subcatchments indicates a reasonable performance of the model (table 5). Except for gauge G3, where the smallest number of validation values (127 days) is available, more than 60% of the variability in discharge is explained by the model, and the NSE (0.58 to 0.68) and RSR (0.57 to 0.65) values suggest satisfactory to good performance. Exemplary hydrographs for the years 2003 and 2005 (lowest and highest discharge rates) at gauge G1 (best model performance, table 5) show the capability of the model to simulate runoff dynamics accurately (fig. 5).

The importance of an appropriate dam management is indicated by the substantially lower goodness-of-fit indicators

in a simulation without dams (table 5). The most notable increase in model performance was achieved at G2, which is located downstream of the largest reservoir (Mulshi dam) in the catchment. Although the model performance at G3 was improved by implementation of dam management, it is still unsatisfactory. This might result from its position downstream of four dams (Khadakwasla, Panshet, Warasgaon, and Temghar), which are operated by the same agency that potentially applies more complex, interrelated management rules for these dams. Two gauges (G1 and G4) show satisfactory results even without implementation of dam management rules. Hence, it can be concluded that management of these dams is less important for river discharge at these gauges. In the case of G4, this is probably due to the smaller size of the upstream Temghar dam (table 4), while at G1 the longer distance between gauge and dam (49.4 km, fig. 4) mitigates the impact of the Pawana dam on river discharge. The satisfactory model performance at these two gauges, where the impact of dam management is less important, shows that natural hydrology was generally modeled with acceptable accuracy.

Although effects should be smallest at gauge G1, the implementation of dam management helps to simulate runoff peaks more accurately, as shown in figure 4 for the peaks on 30 June, 3 July, and 26 July 2005. Model results without dam management clearly overestimated discharge peaks, whereas the implemented dam management reproduced the dampening effect of the reservoir. Nevertheless, it should be noted that the relatively simple, knowledge-based management scheme does not allow for more complex dam operations; for example, the higher observed discharge between the peaks on 26 July and 2 August 2005 was not matched by the simulation.

**Table 5. Model performance at the river gauges based on daily discharge during rainy season; results without incorporation of dam management are given in parentheses.**

Gauge	R <sup>2</sup>	NSE	RSR	No. of Validation Values	Validation Period
G1	0.71 (0.70)	0.68 (0.55)	0.57 (0.67)	655	2001-2007
G2	0.63 (0.51)	0.63 (-0.17)	0.61 (1.08)	586	2001-2007
G3	0.34 (0.33)	0.10 (-0.38)	0.94 (1.17)	127	2002, 2004-2007
G4	0.70 (0.60)	0.58 (0.53)	0.65 (0.69)	689	2001-2006

### WATER BALANCE

For long-term water resources management, changes in the catchment water balance are of special interest and possibly more important than discharge rates during the monsoon season. However, a direct validation of simulated long-term water balance components (ET = 679 mm,  $Q$  = 1172 mm, and  $P$  = 1860 mm) calculated for the period from 2001 to 2007

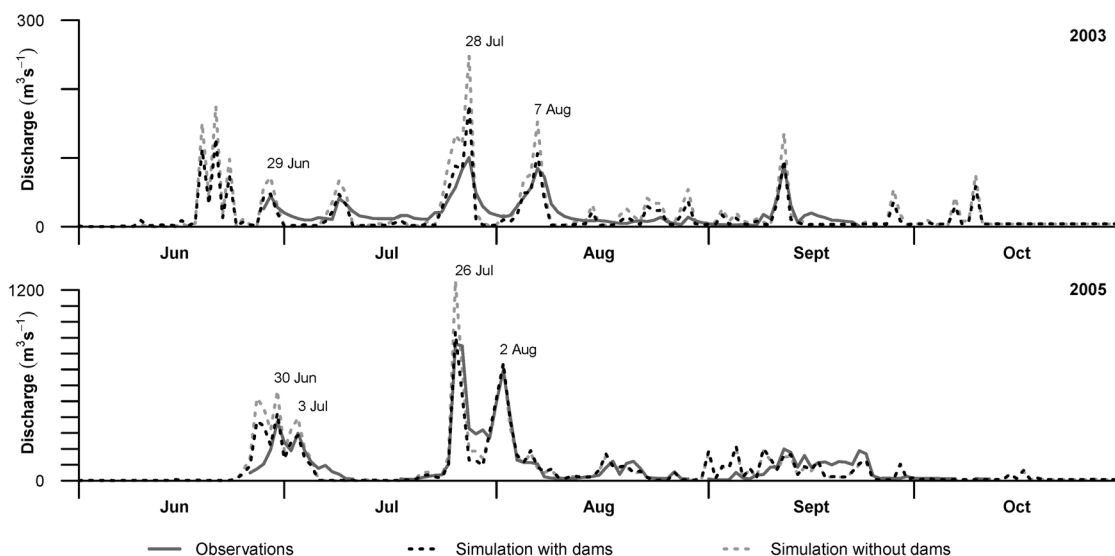


**Figure 5. Observed and modeled discharge at gauge G1 with and without dam management for low-flow (2003) and high-flow (2005) years.**

is not possible, as measured ET data are missing,  $Q$  is only available during the monsoon season, and measurements of  $P$  are spatially limited to four rain gauges. Comparison of the modeled runoff coefficient ( $Q/P$ ) of the Mula-Mutha catchment (0.63) to a comparable catchment in the Western Ghats region (upper Krishna: 0.68; Biggs et al., 2007) gives some confidence in the modeled water balance. The available average water yield measured during the monsoon periods from 2001 to 2007 are 878 mm for the catchment upstream of G1, 796 mm for G2, 1006 mm for G3, and 2432 mm for G4. Due to some data gaps, these cumulative values underestimate the total monsoon discharge by approximately 10% to 25%, as estimated from the ratio of the modeled amount of discharge during validation to the entire monsoon period. For those periods for which measurements are available, the model underestimated water yields by 12.8%, 11.1%, 9.5%, and 44.7% at gauges G1, G2, G3, and G4, respectively. This underestimation may have resulted from one or more of the following reasons: (1) modeled ET is too large; (2) during monsoon season, water is stored and hence baseflow is underestimated by the model; or (3) precipitation is underestimated, especially in the headwater subcatchments.

The mean annual ET (2001-2007) in the catchment is 679 mm. Implementation of the modified forest phenology model increased forest ET by 18.6%, which corresponds to an increase of 5.3% at the catchment scale. Figure 3 shows that this increase is mainly due to ET in the dry months from November to January, as the modified model allows for ET until soil water content is decreased to the wilting point. As irrigation is only applied on 11.2% of the catchment area and only a small areal percentage is irrigated in the summer months (sugarcane 0.7%), irrigation does not have a major impact on ET (13.2% on the catchment scale). Despite the increase of forest ET, especially in the dry season, overall ET seemed to be low compared to the results of other studies that include the Mula-Mutha catchment (Immerzeel and Droogers, 2008; Immerzeel et al., 2008). In the region of our study, Immerzeel and Droogers (2008) calculated ET values between 500 and 700 mm for the period from October 2004 to May 2005. For the same period, ET amounts to 370 mm in our model. Although the comparison of a short period of time with macro-scale studies that are based on coarser land use maps is questionable, it may be concluded that ET during the dry season tends to be underestimated by the model; therefore, it seems highly unlikely that the low water yield results from an overestimation of ET.

The second potential reason for the underestimation of water yield during the monsoon season might be an overestimation of modeled groundwater recharge and storage. However, as declining simulated hydrographs do not show a prolonged baseflow effect (e.g., 29 June, 28 July, and 7 August 2003; fig. 5), groundwater storage seems to have an unimportant effect on modeled water yield.

Underestimation of precipitation is the most likely error source for the underestimation of water yield, especially in the case of headwater subcatchments. In G4 (fig. 4, table 1), where measured water yield (2432 mm) is almost as large as modeled annual precipitation (2606 mm), the precipitation interpolation seems to fail. This failure probably originates from the small number of input rainfall stations (four) that do not sufficiently represent horizontal and vertical characteristics of rainfall in the catchment (e.g., the highest station is 694 m, whereas mean elevation of G4 is 803 m). Hence, the

applied dependency between elevation and precipitation is extrapolated and more uncertain for high altitudes. Additionally, spatial distribution of rainfall may also be influenced by factors other than elevation, e.g., by the dominant southwest wind direction during monsoon. This underlines the importance of appropriate precipitation data. To improve precipitation input, additional data from the region may be used to derive large-scale dependencies that are also applicable in the Mula-Mutha catchment. Remote sensing products such as those from the Tropical Rainfall Measuring Mission (TRMM) may be used to reduce errors in the spatial distribution of rainfall. However, coarse spatial resolution or incomplete timely resolution of the available TRMM products does not allow for a direct integration of the data into the model. Nevertheless, development and application of a more sophisticated rainfall interpolation scheme using auxiliary variables (Verworn and Haberlandt, 2011) like wind direction or TRMM rainfall patterns could improve our model results.

## SUMMARY AND CONCLUSIONS

In this study, the SWAT model was used to simulate river discharge and water balance in the catchment of the Mula and Mutha Rivers. The catchment hydrology is dominated by a pronounced seasonality of rainfall due to the yearly monsoon, which governs vegetation growth and leads to strong management of water resources (e.g., irrigation measures and management of large reservoirs). Despite the limited availability of model input data, which were mainly derived from remote sensing and other freely available data sources, it was possible to reproduce the measured discharge accurately in three of four subcatchments by applying an expert-based model parameterization. A relatively simple dam management scheme was derived from reservoir volumes, remote sensing, and local expert knowledge. In addition, the forest growth model in SWAT was modified to take into account water-limited plant growth during the dry season. However, modeled evapotranspiration during the dry season was small compared to results from macro-scale modeling studies. Moreover, precipitation input was especially underestimated in headwater catchments, and therefore water yield was underestimated, too. The determination of spatial patterns and amounts of precipitation remains a source of error that must be addressed in further studies.

In general, the quality of the model output, which was achieved by using mainly freely available and at times very coarse input data, is very promising. The methodology can be transferred to other monsoon-driven, data-scarce environments and may be adopted for predictions in ungauged catchments.

## ACKNOWLEDGEMENTS

We gratefully acknowledge support by a grant from the German National Academic Foundation. We would like to thank IMD Pune, Water Resources Department Nashik, Khadakwasla Irrigation Division Pune, Groundwater Department Pune, Department of Agriculture Pune, and NRSC Hyderabad for supplying environmental data and for their good cooperation and discussions. Moreover, we acknowledge supply of ASTER data by the USGS Land Processes Distributed Active Archive Center. Special thanks go to the students from the Institute of Environment Education and Research at

Bharati Vidyapeeth University in Pune for assistance with the field measurements. The authors thank the editors and the three anonymous reviewers for their helpful comments on the manuscript.

## REFERENCES

- Ajami, N. K., G. M. Hornberger, and D. L. Sunding. 2008. Sustainable water resource management under hydrological uncertainty. *Water Resources Res.* 44(11): W11406.
- Arnold, J. G., R. Srinivasan, R. S. Muttiah, and J. R. Williams. 1998. Large-area hydrologic modeling and assessment: Part 1. Model development. *J. American Water Resources Assoc.* 34(1): 73-89.
- Beven, K. J., and M. J. Kirkby. 1979. A physically based, variable contributing area model of basin hydrology. *Hydrol. Sci. Bull.* 24(1): 43-69.
- Bhagwat, S. B. 2006. Economic issues in the management of water resources in the drought prone Pune district of Maharashtra state, India. ACWADAM Tech. Report ACWA 2006-H1. Pune, India: Advanced Center for Water Resources Development and Management.
- Biggs, T. W., A. Gaur, C. A. Scott, P. Thenkabail, G. R. Parthasaradhi, M. K. Gumma, S. Acharya, and H. Turrall. 2007. Closing of the Krishna basin: Irrigation, streamflow depletion, and macroscale hydrology. Research Report 111. Colombo, Sri Lanka: International Water Management Institute.
- Dhar, S., and A. Mazumdar. 2009. Hydrological modelling of the Kangsabati River under changed climate scenario: Case study in India. *Hydrol. Proc.* 23(16): 2394-2406.
- Dikshit, K. R. 2002. Forests of Maharashtra. In *Geography of Maharashtra*, 120-133. J. Diddee, S. R. Jog, V. S. Kale, and V. S. Datye, eds. Jaipur, India: Rawat Publications.
- FAO. 2003. *Digital Soil Map of the World and Derived Soil Properties*. Rome, Italy: United Nations FAO.
- Gadgil, A. 2002. Rainfall characteristics of Maharashtra. In *Geography of Maharashtra*, 89-102. J. Diddee, S. R. Jog, V. S. Kale, and V. S. Datye, eds. Jaipur, India: Rawat Publications.
- Goldsworthy, P. R., and N. M. Fisher, eds. 1984. *The Physiology of Tropical Field Crops*. Chichester, N.Y.: John Wiley.
- Gosain, A. K., S. Rao, R. Srinivasan, and N. G. Reddy. 2005. Return-flow assessment for irrigation command in the Palleru River basin using SWAT model. *Hydrol. Proc.* 19(3): 673-682.
- Gosain, A. K., S. Rao, and D. Basuray. 2006. Climate change impact assessment on hydrology of Indian river basins. *Current Sci.* 90(3): 346-353.
- Government of Maharashtra. 2010. Bhima basin flood control cell. Pune, India: Government of Maharashtra, Water Resources Department. Available at: [www.punefloodcontrol.com](http://www.punefloodcontrol.com). Accessed 15 October 2010.
- Gunnell, Y. 1997. Relief and climate in south Asia: The influence of the Western Ghats on the current climate pattern of peninsular India. *Intl. J. Climatol.* 17(11): 1169-1182.
- Im, S., H. Kim, C. Kim, and C. Jang. 2009. Assessing the impacts of land use changes on watershed hydrology using MIKE SHE. *Environ. Geol.* 57(1): 231-239.
- Immerzeel, W. W., and P. Droogers. 2008. Calibration of a distributed hydrological model based on satellite evapotranspiration. *J. Hydrol.* 349(3-4): 411-424.
- Immerzeel, W. W., A. Gaur, and S. J. Zwart. 2008. Integrating remote sensing and a process-based hydrological model to evaluate water use and productivity in a south Indian catchment. *Agric. Water Mgmt.* 95(1): 11-24.
- Jain, S. K., P. K. Agarwal, and V. P. Singh. 2007. *Hydrology and Water Resources of India*. Dordrecht, The Netherlands: Springer.
- Jarvis, A., H. I. Reuter, A. Nelson, and E. Guevara. 2008. Hole-filled seamless SRTM data V4. Cali, Colombia: International Center for Tropical Agriculture (CIAT). Available at: <http://srtm.csi.cgiar.org>. Accessed 3 November 2008.
- Kirchner, J. W. 2006. Getting the right answers for the right reasons: Linking measurements, analyses, and models to advance the science of hydrology. *Water Resources Res.* 42(3): W03S04.
- Madugundu, R., V. Nizalapur, and C. S. Jha. 2008. Estimation of LAI and above-ground biomass in deciduous forests: Western Ghats of Karnataka, India. *Intl. J. Applied Earth Obs. and Geoinfo.* 10(2): 211-219.
- Mauser, W., and H. Bach. 2009. PROMET: Large-scale distributed hydrological modelling to study the impact of climate change on the water flows of mountain watersheds. *J. Hydrol.* 376(3-4): 362-377.
- Mockus, V. 1972. Estimation of direct runoff from storm rainfall. In *SCS National Engineering Handbook*, Section 4: Hydrology, 10.1-10.24. Washington, D.C.: USDA.
- Monteith, J. L. 1965. Evaporation and the environment. In *The State and Movement of Water in Living Organisms: 19th Symposia of the Society for Experimental Biology*, 205-234. G. E. Fogg, ed. London, U.K.: Cambridge University Press.
- Moriasi, D. N., J. G. Arnold, M. W. Van Liew, R. L. Bingner, R. D. Harmel, and T. L. Veith. 2007. Model evaluation guidelines for systematic quantification of accuracy in watershed simulations. *Trans. ASABE* 50(3): 885-900.
- Nash, J. E., and J. V. Sutcliffe. 1970. River flow forecasting through conceptual models: Part I. A discussion of principles. *J. Hydrol.* 10(3): 282-290.
- Ndomba, P., F. Mtalo, and A. Killingtveit. 2008. SWAT model application in a data scarce tropical complex catchment in Tanzania. *Physics and Chem. of the Earth* 33(8-13): 626-632.
- Neitsch, S. L., J. G. Arnold, J. R. Kiniry, and J. R. Williams. 2005. *Soil and Water Assessment Tool: Theoretical Documentation, Version 2005*. Temple, Tex.: USDA-ARS Grassland, Soil and Water Research Laboratory.
- Neitsch, S. L., J. G. Arnold, J. R. Kiniry, R. Srinivasan, and J. R. Williams. 2010. *Soil and Water Assessment Tool: Input/Output File Documentation, Version 2009*. Temple, Tex.: USDA-ARS Grassland, Soil and Water Research Laboratory.
- Pangare, G., V. Pangare, and B. Das. 2006. *Springs of Life: India's Water Resources*. New Delhi, India: Academic Foundation.
- Refsgaard, J. C., and B. Storm. 1995. MIKE SHE. In *Computer Models of Watershed Hydrology*, 809-846. V. P. Singh ed. Highlands Ranch, Colo.: Water Resources Publications.
- Stehr, A., P. Debels, F. Romero, and H. Alcayaga. 2008. Hydrological modelling with SWAT under conditions of limited data availability: Evaluation of results from a Chilean case study. *Hydrol. Sci. J.* 53(3): 588-601.
- Story, M., and R. G. Congalton. 1986. Accuracy assessment: A user's perspective. *Photogram. Eng. and Remote Sensing* 52(3): 397-399.
- USGS. 2009. AST14DEM: On-demand digital elevation model. Sioux Falls, S.D.: U.S. Geological Survey, Land Processes Distributed Active Archive Center. Available at: <http://lpdaac.usgs.gov>. Accessed 4 June 2009.
- Verworn, A., and U. Haberlandt. 2011. Spatial interpolation of hourly rainfall: Effect of additional information, variogram inference, and storm properties. *Hydrol. and Earth System Sci.* 15(2): 569-584.
- Vincendon, B., V. Ducrocq, G.-M. Saulnier, L. Bouilloud, K. Chancibault, F. Habets, and J. Noilhan. 2010. Benefit of coupling the ISBA land surface model with a TOPMODEL hydrological model version dedicated to Mediterranean flash-floods. *J. Hydrol.* 394(1-2): 256-266.
- Weischet, W. 1995. *Einführung in die Allgemeine Klimatologie*. 6th ed. Stuttgart, Germany: Teubner.



### 3 Comparison and evaluation of spatial interpolation schemes for daily rainfall in data scarce regions

Journal article (published)

Authors: Wagner, P.D., Fiener, P., Wilken, F., Kumar, S., Schneider, K.

Journal: Journal of Hydrology

Volumes: 464-465

Date of publication: 25 September 2012

Reprinted with permission from Elsevier from:

Wagner, P.D., Fiener, P., Wilken, F., Kumar, S., Schneider, K., 2012.

Comparison and evaluation of spatial interpolation schemes for daily rainfall in data scarce regions. Journal of Hydrology 464-465: 388-400.



## Comparison and evaluation of spatial interpolation schemes for daily rainfall in data scarce regions

Paul D. Wagner<sup>a</sup>, Peter Fiener<sup>a,b</sup>, Florian Wilken<sup>a</sup>, Shamita Kumar<sup>c</sup>, Karl Schneider<sup>a,\*</sup>

<sup>a</sup>Hydrogeography and Climatology Research Group, Institute of Geography, University of Cologne, D-50923 Köln, Germany

<sup>b</sup>Indo-German Centre of Sustainability, Indian Institute of Technology Madras, Chennai 600 036, India

<sup>c</sup>Institute of Environment Education & Research, Bharati Vidyapeeth University, Pune 411 043, India

### ARTICLE INFO

#### Article history:

Received 28 February 2012

Received in revised form 26 June 2012

Accepted 16 July 2012

Available online 24 July 2012

This manuscript was handled by Andras Bardossy, Editor-in-Chief, with the assistance of Uwe Haberlandt, Associate Editor

#### Keywords:

Rainfall  
Interpolation  
Kriging  
SWAT  
TRMM  
India

### SUMMARY

Accurate rainfall data are of prime importance for many environmental applications. To provide spatially distributed rainfall data, point measurements are interpolated. However, in low density measurement networks, the use of different interpolation methods may result in large differences and hence in deviations from the actual spatial distribution of rainfall. Our study aims at analyzing different rainfall interpolation schemes with regard to their suitability to produce spatial rainfall estimates in a monsoon dominated region with scarce rainfall measurements. The study was carried out in the meso-scale catchment of the Mula and the Mutha Rivers (2036 km<sup>2</sup>) upstream of the city of Pune, India. Rainfall data from 16 rain gauges were spatially interpolated using seven different methods, including Thiessen polygons, statistical, and geostatistical approaches. The two most suitable covariates for rainfall interpolation were identified as (i) distance in wind direction from the main orographic barrier and as (ii) a 0.05° pattern of mean annual rainfall derived from satellite data acquired by the Tropical Rainfall Measuring Mission (TRMM). Consequently, these two covariates were used in the regression-based interpolation approaches. The quality of the different methods was assessed using a two step validation approach: (i) Cross-validation was used to evaluate the capability to reproduce measured data. (ii) Spatially integrated interpolation performance was assessed by using a hydrologic model to calculate runoff and compare modeled to measured runoff. By this assessment, the regression-based methods showed the best performance. We found that the choice of the covariate had a significant impact on precipitation and runoff amounts, as well as on the temporal course of runoff events. Our results show, that the decision on the suitable interpolation scheme should not only be based on the comparison with point measurements, but should also take the representativeness of the given measurement network as well as of the interpolated spatial rainfall distribution into account. The successful application of regression-based interpolation methods using a high resolution TRMM pattern as covariate is very promising as it is transferable to other data scarce regions.

© 2012 Elsevier B.V. All rights reserved.

### 1. Introduction

Accurate precipitation data are of prime importance for many environmental studies, especially if related to water resources. At small scales, the use of measurements from individual rain gauges might be appropriate. However at larger scales, it is required to draw special attention to the appropriate representation of the spatial precipitation patterns, which are usually interpolated from point measurements (Chaubey et al., 1999; Tabios and Salas, 1985; Zhang and Srinivasan, 2009). A wide range of interpolation methods is available, ranging from simple techniques such as Thiessen polygons (Thiessen, 1911) or inverse distance weighting schemes

(Di Piazza et al., 2011; Teegavarapu et al., 2009) to more complex and computationally intensive approaches such as geostatistical kriging (Buytaert et al., 2006; Zhang and Srinivasan, 2009). The more complex approaches often use additional information from static (e.g., elevation) or dynamic (e.g., rainfall radar) covariates that are available as spatially distributed data sets.

In many regions of the world, precipitation measurements are scarce and interpolation is not only more important, but also more difficult (Croke et al., 2011). Since spatial patterns are often more heterogeneous and pronounced at short time scales, an appropriate interpolation scheme is particularly important at short time scales such as daily or hourly precipitation. These short time steps are usually required for distributed hydrologic modeling studies, and model accuracy critically depends on these input data (Beven, 2001). Nevertheless in data scarce regions, the use of simple

\* Corresponding author. Tel.: +49 221 470 4331; fax: +49 221 470 5124.

E-mail address: [karl.schneider@uni-koeln.de](mailto:karl.schneider@uni-koeln.de) (K. Schneider).

approaches is very common (e.g., Croke et al., 2011; Ndomba et al., 2008; Stehr et al., 2008). Especially with regard to daily values, the application of more complex interpolation schemes is relatively rare (e.g., Buytaert et al., 2006), although these may lead to substantial improvements in hydrologic model performance (Stehr et al., 2008). In general, complex methods are more commonly used, when data availability is sufficient (Hattermann et al., 2005; Ly et al., 2011; Zhang and Srinivasan, 2009) or with coarser time resolution (e.g., annual data, Basistha et al., 2008).

In case of coarse measurement networks, interpolation schemes that include additional information from covariates are most promising as they may (partly) compensate for the low network density. Particularly for precipitation, covariates can substantially improve the representation of spatial patterns (Verworn and Haberlandt, 2011). Suitable and applicable covariates should be available at a higher spatial resolution and be inexpensive to measure in comparison to the interpolated variable (Burrough and McDonnell, 1998). A further requisite of a covariate is that it should – to some extent – explain the interpolated variable. This characteristic is typically given by a process that links the covariate to the variable and is proven by a regression analysis based on the available data. Traditionally, elevation or other parameters extracted from digital elevation models (DEMs) are used for rainfall interpolation (Buytaert et al., 2006; Goovaerts, 2000; Kurtzman et al., 2009; Lloyd, 2005; Verworn and Haberlandt, 2011). Satellite products, especially from radar remote sensing, are increasingly used as covariates, since they provide spatially detailed information of rainfall distribution (Velasco-Forero et al., 2009; Verworn and Haberlandt, 2011; Schiemann et al., 2011). Furthermore, interpolation methods that use remotely sensed observations can easily be transferred to different regions, whereas other covariates (e.g., elevation; Lloyd, 2005) are often suitable only for a specific region or time of the year, depending on local climatic conditions. The spatially detailed information provided by satellite data is even more valuable in the context of data scarce regions.

Another difficulty associated with applying interpolation schemes in data scarce regions is the accuracy assessment. Usually interpolation results are evaluated applying cross-validation techniques (Hattermann et al., 2005; Lloyd, 2005). Unfortunately, the accuracy of this validation method depends on the number and the location of the gauges within the study area, which should be representative of the distribution of rainfall in space. These criteria are hardly met in case of a limited number of measurements, as rain gauges are often found close to settlements to reduce maintenance efforts. Additional more robust validation is often difficult to achieve and is mostly of a qualitative nature, e.g., comparison and analysis of interpolated rainfall patterns (Carrera-Hernández and Gaskin, 2007; Lloyd, 2005; Velasco-Forero et al., 2009). However, a qualitative, manual assessment of interpolation techniques is not feasible, if interpolation is carried out for a time series (e.g., on a daily time step). Furthermore, spatially integrated assessment of interpolation accuracy would be highly favorable. Zhang and Srinivasan (2009) include areal mean precipitation amounts into the comparison of different interpolation methods. This approach can be enhanced by the application of a hydrologic model. Such a modeling approach not only provides temporally and spatially integrating information in the sense of a water balance study, it also provides a spatially integrating and temporally explicit perspective through the analysis of the modeled hydrograph. Thus, results of different precipitation interpolation schemes may be used as inputs to hydrologic models to analyze their effect upon modeled runoff. The approach of using a hydrologic model to assess the performance of different interpolation schemes has previously been used in several studies (e.g. Cole and Moore, 2008; Gourley and Vieux, 2005; Heistermann and Kneis, 2011; Hwang et al., 2012). This method is especially relevant in catchments that are

dominated by heavy rainfall events, producing mostly direct runoff and resulting in highly dynamic hydrographs, which allow for a simple evaluation of the rainfall inputs.

Particularly in mountainous areas, spatial patterns are consistently affected by topography and wind direction (Barros and Lettenmaier, 1993; Barry, 1992). This is the case in the Western Ghats, India, where topography and monsoon winds result in spatially highly variable rainfall, which is largely determined by orographic lift and foehn effects. In a previous study carried out in the meso-scale catchment of the Mula and the Mutha Rivers upstream of the city of Pune, India, precipitation input was identified as a major source of error for runoff modeling (Wagner et al., 2011).

The main objective of this paper is to analyze different rainfall interpolation schemes with regard to their suitability to produce spatial rainfall estimates on a daily time step in a monsoon dominated region with scarce precipitation measurements. A special focus is set on the identification of an appropriate and transferable covariate and on the validation of the interpolation schemes using hydrologic modeling results and measured runoff.

## 2. Materials and methods

### 2.1. Study area

The meso-scale catchment of the Mula and the Mutha Rivers (2036 km<sup>2</sup>) is located in the Western Ghats upstream of the city of Pune (18.53°N, 73.85°E; Fig. 1). It is a sub-basin and source area of the Krishna River, which drains towards the east and into the Bay of Bengal. Its elevation ranges from 550 m in Pune up to 1300 m a.s.l. on the top ridges in the Western Ghats. The catchment has a tropical wet and dry climate, which is characterized

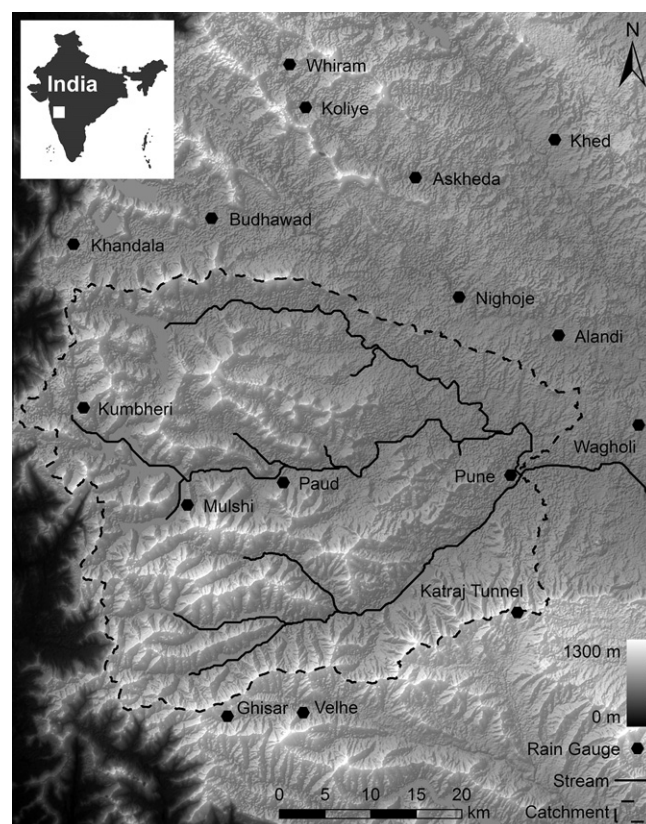


Fig. 1. Topography of the study area with the Mula–Mutha catchment and the available rain gauges.

by seasonal rainfall from June to October and low annual temperature variations with an annual mean of 25 °C at the catchment outlet in Pune. Annual rainfall amounts decrease from approximately 3500 mm in the western to 750 mm in the eastern part of the catchment (Gadgil, 2002; Gunnell, 1997). Land use is dominated by semi-natural vegetation, with forests (20.6%) mainly on the higher elevations in the west, whereas shrubland (26.6%) and grassland (22.8%) occupy lower elevations. Agriculture comprises only 10.6% of the catchment and is mainly located in proximity to rivers and to six large dams (5.8% of the catchment is covered by water). Agriculture is dominated by small fields (<1 ha) with rain-fed agriculture during the monsoon season and irrigation during the dry season. Typically two crops per year are harvested. Urban area (13%) is mainly found in the eastern part of the catchment, where the city of Pune and its surrounding settlements are situated (Wagner et al., 2011).

## 2.2. Precipitation data

Daily measurements of precipitation at 16 gauges within or close to the catchment (Fig. 1) were provided by the Water Resources Department Nashik and the Indian Meteorological Department (IMD) Pune. Measurements are carried out with a Symon's rain gauge, which is the Indian standard gauge (Jain et al., 2007). It measures rainfall at a height of 30 cm above ground level. The surface area of the gauge is 200 cm<sup>2</sup>. The gauge is typically installed on a concrete foundation block (60 × 60 × 60 cm) embedded in the ground. A fence (5.5 × 5.5 m) secures a minimum distance to possibly measurement interfering objects like bushes. Furthermore, such gauges should not be unduly exposed to wind (Jain et al., 2007). Twenty-four hour rainfall sums are given for each day at 8:30 a.m. Indian Standard Time. Ten of these gauges are operated manually, whereas six are self-recording gauges. Five of the latter only recorded data during the monsoon season. To provide accurate daily precipitation data, the following processing steps were applied: (i) quality control, (ii) filling of data gaps, (iii) correction of systematic measurement errors, and (iv) analysis of three different interpolation schemes.

### 2.2.1. Quality control, gap filling, and error correction

Daily precipitation measurements were available to this study from all 16 rain gauges. The data was tested for consistency using double mass curves (Searcy et al., 1960). Due to the higher amounts of rainfall and larger number of rain days in the upper catchment, gauges within the western part and gauges within the eastern part were tested separately. The 73.7°E longitude was used to divide the data set into gauges recording more (west) or less (east) than 1500 mm mean annual rainfall. For both parts of the catchment, one reliable rain gauge with a continuous data set was chosen as reference. The gauge in Pune, which is maintained by the IMD, is possibly one of the most reliable gauges in the catchment, because its record covers the entire period from 1988 to 2008 and had only one missing value. Due to its central location in the east, it was chosen as the reference gauge for the eastern part of the catchment. For the western part, the central gauge in Paud was used, as its record shows no missing value from 1988 to 2008. The cumulative sums of each of the other stations were compared to their respective reference station on a daily basis. If the double mass curves showed inconsistencies (e.g., steps or a change in slope), the data were checked and questionable data were marked as missing values (e.g., in some cases missing values are given as 0 mm in the original data sheet). Apart from questionable values some shifts in time were detected. Since inconsistent double mass curves on a daily time step could also result from other effects such as local thunderstorms, data were only corrected, if there was clear evidence from other gauges (e.g., a time

shift was only corrected, if comparisons with all neighboring gauges indicated the shift).

Thereafter, the missing values were filled using a regression-based gap filling approach. The available data at the gauge with data gaps was summed up for each year. Corresponding annual precipitation sums were calculated for every gauge using the same dates. On this basis, a linear regression was carried out to establish a relationship between the station with the incomplete data and each of the other stations. The slope of the regression was used as a factor to estimate missing data at the incomplete station from each of the other gauges. To identify the most suitable gauge to fill the incomplete station, 120 randomly chosen precipitation days (4 months) were estimated from each of the other rain gauges. Subsequently the root mean square error (RMSE) was calculated to evaluate the performance of each gauge. This procedure was repeated 10 times, providing a mean RMSE to identify the most suitable gauge. Filling was not applied, if measurements for a whole year were missing. Thus, the derived precipitation data set consists of 10 gauges with complete daily records from 1988 to 2008 and six gauges with gaps that comprised one or more years.

Finally, to account for the systematic undercatch of precipitation measurements due to wind loss, wetting loss, and evaporation a correction method developed by Richter (1995) was applied. This method that had been developed for the German measurement network was chosen, since a specific method for India was not available. It estimates precipitation errors based on precipitation type and wind exposition (shielding) of the rain gauge. To account for the precipitation character and rain gauge setup in the catchment, we chose the coefficients for German summer rain and light shielding (Richter, 1995). Depending on the rain gauge location, the correction adds between 2.9% (106 mm mean annual rainfall) and 7.4% (40 mm mean annual rainfall) to the measured rainfall amounts.

## 2.3. Interpolation schemes

Seven different interpolation schemes (Table 1) that use data from the Mula–Mutha catchment and its surroundings (Fig. 1) were applied and compared. These interpolation schemes were carried out on a 1 km<sup>2</sup> grid. Inputs for the hydrologic model were derived from this grid by averaging the gridded rainfall values for each sub-basin used in the model. Two sets of interpolation schemes were tested: (i) univariate methods and (ii) regression-based methods, which incorporate additional information from covariates.

### 2.3.1. Univariate interpolation methods

As a reference, Thiessen polygons (Thiessen, 1911) were used. Each grid point was assigned the value of the nearest rain gauge. This simple approach balances the contributions of the nearest gauges within each sub-basin and is therefore superior to simply using

**Table 1**  
Spatial interpolation schemes for daily rainfall interpolation.

Method	Interpolation scheme	Covariate	Abbreviation
1	Thiessen polygons	–	TH
2	Inverse distance weighting	–	IDW
3	Ordinary kriging	–	OK
4a	Regression–inverse distance weighting	(a) X-coordinate	RIDW <sub>X</sub>
4b		(b) TRMM pattern	RIDW <sub>TRMM</sub>
5a	Regression–kriging	(a) X-coordinate	RK <sub>X</sub>
5b		(b) TRMM pattern	RK <sub>TRMM</sub>

the nearest rain gauge, which is the standard method implemented in the ArcSWAT model setup interface (Winchell et al., 2010).

Inverse distance weighting (IDW) is a widely used and easy to implement interpolation method. The influence of the measured point data  $z(x_i)$  is weighted according to the distance  $d_{0i}$  from the sampled point  $x_i$  to the estimated point  $x_0$ . Based on the optimal cross-validation performance the exponent of one was chosen, providing better estimates in this study than the frequently used standard exponent of two (Heistermann and Kneis, 2011; Shepard, 1968). The weights  $\lambda_i$  can hence be calculated as

$$\lambda_i = \frac{d_{0i}^{-1}}{\sum_{j=1}^n d_{0j}^{-1}} \quad (1)$$

In our case we used a localized IDW approach that only takes the values of the  $n$  gauges within a 30 km distance into account. Thus the value at the interpolated location is estimated as

$$\hat{z}(x_0) = \sum_{i=1}^n \lambda_i \cdot z(x_i), \quad \text{where} \quad \sum_{i=1}^n \lambda_i = 1. \quad (2)$$

Thirdly, an ordinary kriging scheme (OK) was evaluated. Analogous to the IDW scheme, weights are calculated for every sampled point, but in contrast to IDW, the weights  $\lambda_0(i)$  are optimized based on the information that is inherent in the measured data. The weights are obtained by solving the system

$$\begin{aligned} \sum_{i=1}^n \lambda_0(i) \gamma(x_i, x_j) + \phi &= \gamma(x_j, x_0) \text{ for all } j \\ \sum_{i=1}^n \lambda_0(i) &= 1, \end{aligned} \quad (3)$$

where  $\gamma(x_i, x_j)$  represents the value of the semivariogram function for the distance between the points  $x_i$  and  $x_j$ ,  $\gamma(x_j, x_0)$  is the value for the distance between  $x_j$  and the estimated location  $x_0$ , and  $\phi$  is the Lagrange parameter. The semivariogram function is derived by fitting a semivariogram model to the empirical semivariogram, which can be calculated for all distances  $h$  by solving

$$\hat{\gamma}(h) = \frac{1}{2n} \sum_{i=1}^n (z(x_i) - z(x_i + h))^2. \quad (4)$$

Point estimates are calculated by using the optimized weights  $\lambda_0(i)$  instead of the IDW weights  $\lambda_i$  in formula (2). Further theoretical details on geostatistics are available in the literature (e.g., Wackernagel, 2003; Webster and Oliver, 2007).

Geostatistical methods are commonly used for spatial interpolation of rainfall (Goovaerts, 2000; Zhang and Srinivasan, 2009). However, to detect spatial autocorrelation, at least 100 measurement locations (ideally 150) are required to supply a sufficient number of data pairs, which is evidently needed to derive an accurate empirical semivariogram (Webster and Oliver, 2007). Furthermore, variogram analysis and fitting of variogram models is very important and should be carried out manually, as it requires considerable judgment and skill (Burrough and McDonnell, 1998). To meet these requirements, pooled semivariograms (Fiener and Auerswald, 2009; Schuurmans et al., 2007; Voltz and Webster, 1990) for each month were used. These pooled semivariograms were calculated from mean daily precipitation values for every month in every year. The monthly values of the individual years were treated as spatially independent measurements, resulting in 312 data sets per month (21 years \* 16 stations – 24 years missing at different stations) that give 1938 point pairs for every semivariogram, which were grouped into 14 lag classes. A Matern semivariogram model was fitted to these empirical semivariograms (Fig. 2). This model is recommended for interpolation of spatial data (Stein, 1999) and includes as special case the Gaussian model, which Ly et al. (2011) recommend for rainfall interpolation. On this basis,

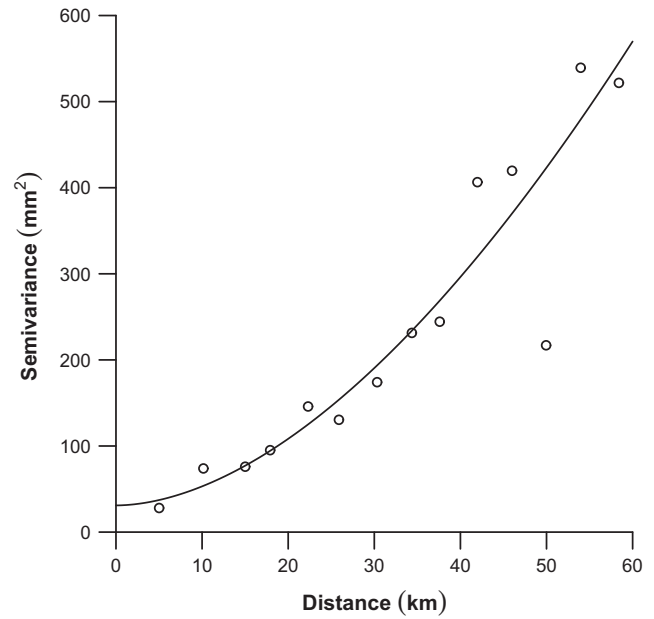


Fig. 2. Semivariogram and fitted Matern model for pooled July rainfall data (1988–2008).

a local kriging approach was applied taking only stations within a 30 km distance into account. Due to the small number of rain days in dry season months, variograms of mean monthly rainfall are not useful for interpolation of the rare rainfall events in this period. Therefore, kriging was only applied from June to September, whereas IDW was used in the remaining months. All interpolations and geostatistical analyses were carried out using the statistical software GNU R, version 2.13.0 (R Development Core Team, 2011) and the add-on package gstat (Pebesma, 2004).

2.3.2. Covariates for rainfall interpolation

The use of covariates can substantially improve interpolation results. In principal, a spatially distributed variable is utilized to estimate rainfall amounts. To identify appropriate, easily available and spatially distributed covariates, a linear regression between mean annual rainfall and the value of the covariates at the rain gauges was carried out. Four covariates were taken into account: (i) elevation, (ii) distance from the main orographic barrier in main wind direction, (iii) X-coordinate, (iv) a pattern of mean annual rainfall derived from satellite data acquired by the Tropical Rainfall Measuring Mission (TRMM).

Elevation is commonly used as a covariate for precipitation (e.g., Buytaert et al., 2006; Goovaerts, 2000; Kurtzman et al., 2009; Lloyd, 2005; Verworn and Haberlandt, 2011), but in our case there was no significant correlation between rainfall and elevation data (Table 2). The distance in the main south-west (SW) wind direction from the main orographic barrier in the region, the Western Ghats escarpment, provides a high coefficient of determination. The escarpment marks the sharp decline from the Western Ghats

Table 2  
Capability of different covariates to represent mean annual rainfall data, as indicated by the coefficient of determination ( $R^2$ ) and the  $p$ -value.

Covariate	$R^2$	Significance
Elevation	0.07	$p = 0.32$
Distance from the Western Ghats escarpment in main wind direction (SW)	0.84	$p < 0.001$
X-coordinate	0.92	$p < 0.001$
TRMM pattern	0.83	$p < 0.001$

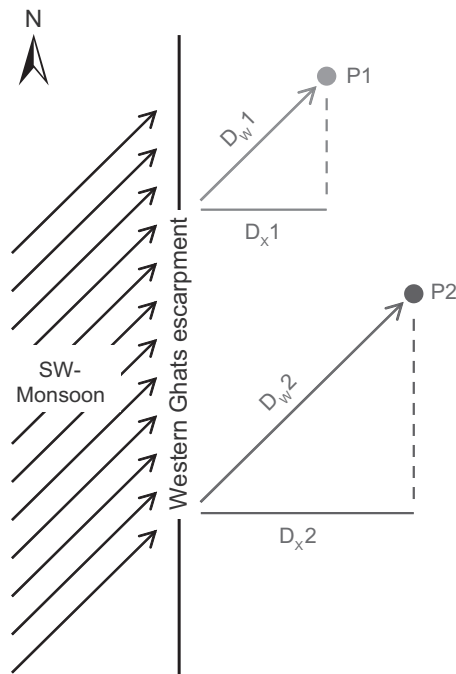


**Fig. 3.** Proportionality of the distance in main wind direction ( $D_w$ ) and the distance in east–west direction ( $D_x$ ) from the Western Ghats escarpment for any location  $P$  in the catchment.

mountain range to the coastal plain, which also constitutes the western boundary of the catchment (Fig. 1). Due to the general north–south direction of the Western Ghats escarpment, the distance from the escarpment (in east–west direction) is proportional to the distance in wind direction from the escarpment (Fig. 3) for any location in the catchment and all western wind directions. Thus, this east–west-distance, which can be expressed by the UTM  $X$ -coordinate, represents the downwind fetch and consequently, the west to east decline of precipitation starting from the escarpment. Since the  $X$ -coordinate is valid for all western wind directions, it is superior to the distance from the escarpment in SW wind direction. This becomes obvious in the higher coefficient of determination (Table 2). An additional advantage of this covariate is its simplicity of calculation. However, spatial transferability of this covariate to different regions is obviously limited.

A pattern of mean annual rainfall was derived from the Precipitation Radar (PR) instrument of the Tropical Rainfall Measuring Mission (TRMM). The TRMM product 2A25 provides a near-surface rainfall rate estimated from the precipitation radar at a 4.3 km resolution. All available observations between 1998 and 2008 were used and remapped to  $0.05^\circ$  resolution by the Earth System Science Interdisciplinary Center, University of Maryland and NASA/Goddard Space Flight Center. The PR system is stable and accurate enough to allow for quantitative radar reflectivity (Kummerow et al., 2000). Due to the orbital period of the TRMM satellite, the number of observations has an effect on uncertainty of the derived annual rainfall pattern. However, Kidd and McGregor (2007) demonstrated the use of seasonal rainfall patterns acquired from a shorter period (8 years) of PR observations in a study on Hawaii. In our study area, the TRMM product clearly underestimates precipitation by 17–61% (RMSE = 1044 mm) when compared to the measured mean annual precipitation sums. However, the correlation of the pattern with the measured data is high ( $R^2 = 0.83$ ; Table 2). It can therefore be concluded that although the amounts are not valid without further calibration using regional measurements, the spatial pattern is a valid covariate for precipitation interpolation. For

further analysis, the two most promising covariates ( $X$ -coordinate and TRMM pattern) were chosen to be used for interpolation.

### 2.3.3. Regression-based interpolation methods

Two regression-based methods, a statistical and a geostatistical method, were tested using the two covariates, one at a time (Table 1). For both methods, a regression equation for the covariate was used to estimate rainfall amounts. This regression equation between rainfall and the covariate was calculated for every wet day using the mean precipitation value of a period of 3 days before and after the interpolation day. A wet day was defined when at least one gauge recorded precipitation on this day. The significance of the regression was tested for every day at the 10% significance level. In case of the  $X$ -coordinate, we additionally tested if the correlation was negative, because only negative correlation expressed a decline of rainfall from west to east. If these criteria were met (Fig. 4), the regression was used to estimate the mean precipitation for every grid point. In addition, daily residuals for every rain gauge

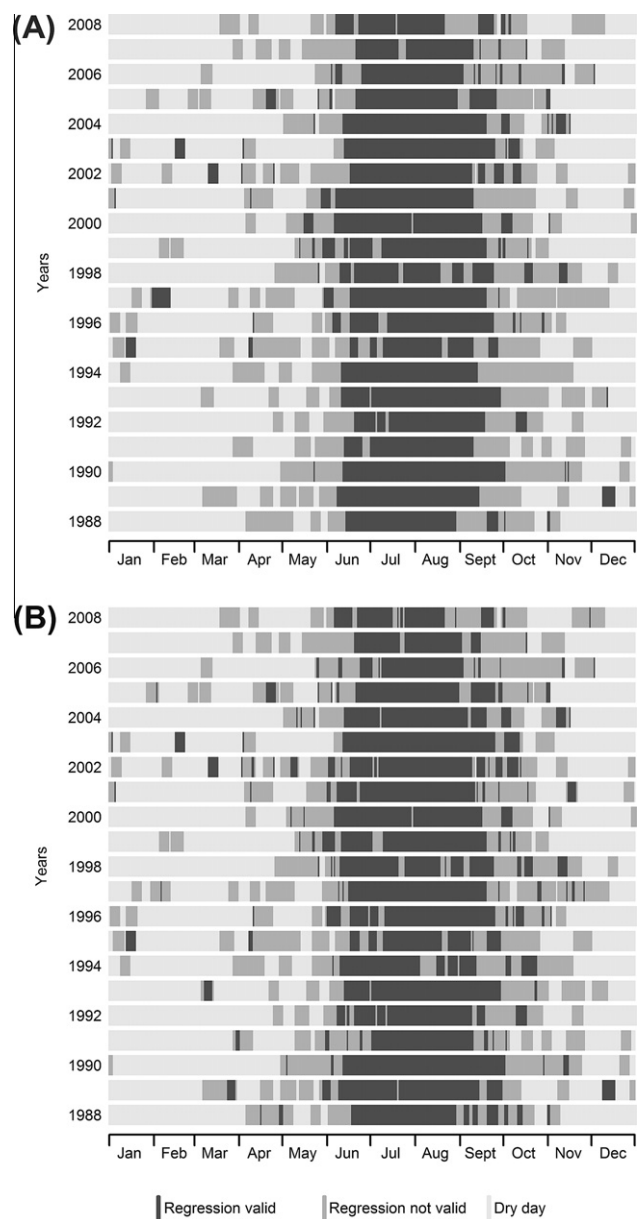


**Fig. 4.** Validity of the regression approach for (A) covariate  $X$ -coordinate ( $p < 0.1$  and correlation coefficient  $r < 0$ ) and (B) covariate TRMM pattern ( $p < 0.1$ ) for every day from 1988 to 2008.

were calculated by subtracting the regression rainfall from the measured rainfall. It is worth noting that the TRMM pattern can be used more frequently (4% more days) than the X-coordinate, if the described criteria are applied. Typically the criteria were met within the rainy season, whereas in the dry season, the local convective rainfall events led to a non-significant relationship with the covariates (Fig. 4). If the criteria were not met, a local IDW approach using the gauges within a 30 km distance was applied. In case of a valid regression, values at every grid point were calculated by adding the explained variance, which is given by the regression, to the unexplained variance, which is expressed by the interpolated residuals. Negative estimates were set to 0 mm rainfall. Either an IDW or a kriging scheme was used to interpolate the residuals. The IDW method can be referred to as regression-inverse distance weighting approach (RIDW) and has previously been applied using elevation as a covariate (e.g., Mauser and Bach, 2009). A local IDW approach using the gauges within a 30 km distance and an optimized exponent of one was used to interpolate the residuals.

As an alternative to the IDW interpolation scheme, a pooled ordinary kriging approach was applied to the residuals. A mean monthly residual was calculated from the daily residuals for every month in every year. These values were pooled to derive residual variograms for every month. A Matern semivariogram model was fitted to these empirical variograms. On the basis of the fitted semivariogram, a local (30 km distance) ordinary kriging approach was applied. Valid variograms were only derived for the rainy season, so that IDW (30 km distance, exponent = 1) was used for interpolation in dry season. Finally, by adding the interpolated residuals to the mean daily rainfall values, calculated from the regression equation, a rainfall estimate was derived for every grid point.

This linear regression-kriging (subsequently referred to as RK) results in the same predictions given the same input parameters as kriging with external drift (Hengl et al., 2007). Both methods allow for incorporation of an external variable that is linearly correlated to the predicted variable (Webster and Oliver, 2007). RK separates regression calculation and residual interpolation and is therefore more flexible, allowing in this case, the combination of day specific regression equations with kriging based on a monthly pooled residual semivariogram.

#### 2.4. Hydrologic model

In this study, the Soil and Water Assessment Tool (SWAT; Arnold et al., 1998) was used to assess the impact of different rainfall interpolation methods on runoff. The SWAT model has proven its capability to model water fluxes also in regions with limited data availability (Ndomba et al., 2008; Stehr et al., 2008). In a preceding study, it was adapted to the Mula–Mutha catchment (Wagner et al., 2011). Thus in the following, we will only present a brief summary of data inputs and model parameterization.

A digital elevation model (DEM) with a spatial resolution of 30 m was derived from ASTER satellite data. This DEM was corrected using a regression with elevation data from topographic maps. The spatial distribution of soils was taken from the digital Soil Map of the World (FAO, 2003). Soil parameterization was partly adapted from a modeling study of the region by Immerzeel et al. (2008), and partly taken from the FAO (2003) database. The land use map was derived from a satellite image taken by LISS-III on the Indian satellite IRS-P6 (Wagner et al., 2011). Crop rotations as well as irrigation schemes were set up for arable land (rice 4.7%, sugarcane 0.7%, mixed cropland 5.3% of the catchment area) to account for the two main cropping seasons in the region. Additionally, the forest growth module was modified to represent the local conditions. For the six major dams in the catchment, a management scheme was developed, which is based on general man-

agement rules allowing for water storage in the rainy season and water release in the dry season (Wagner et al., 2011). At the Mulshi and Khadakwasla dams, water is abstracted for energy, irrigation, and water supply purposes. This is incorporated into the model based on a monthly abstraction rate, which is estimated using downstream river gauge measurements. If dams are filled up to 95% of the storage capacity, the abstraction rate is increased to allow for an efficient use of the available water.

Temperature, humidity, solar radiation, and wind speed data were only available at the IMD weather station in Pune (ID 430630, 18.53°N, 73.85°E, 559 m.a.s.l.). Missing temperature values ( $n = 9$  days) were filled using the value of similar days in terms of rain, minimum or maximum temperature, and solar radiation in the same month. Missing humidity ( $n = 6$ ) and missing wind speed values ( $n = 10$ ) were filled linearly, by averaging the values of the previous and the following day. On 1269 days, solar radiation values were missing. However, for most of these days some hourly values were available. These were used to fill the hourly data gaps with the hourly observations from a day in the same month with a similar course of solar radiation. The majority of daily missing values ( $n = 1101$ ) were filled with the help of this procedure. The remaining 168 missing values were filled using the value of a similar day in terms of rain, temperature, and humidity in the same month.

To account for temperature differences within the catchment, temperature values were adjusted for every sub-basin using adiabatic temperature gradients (0.98 °C/100 m on a dry day, 0.44 °C/100 m on a wet day; Weischet, 1995). The two humidity measurements per day in Pune (8:30 am and 5:30 pm) were linearly interpolated to obtain an hourly course of humidity. Mean daily humidity was derived from this hourly course. Relative humidity was calculated for every sub-basin using the sub-basin specific temperature values and the daily specific humidity values measured in Pune. Solar radiation and wind speed from Pune are used for the whole catchment.

Daily discharge data for model validation was only available during rainy seasons between 2001 and 2007. The runoff measurements were quality checked. Values were removed, if the runoff record showed exactly the same value for 3 days in a row. Furthermore, a questionable peak runoff value was found for gauge G1 on 29 and 30 July 2006. For both days, about the same extreme runoff was recorded. This runoff value could not be explained by the measured precipitation. Eliminating the runoff record on 30 July and shifting the runoff measurements 1 day backward between 31 July and 19 September led to a removal of the observed systematic lag between modeled and measured runoff peaks.

The catchment model bases its calculations on 25 sub-basins, which are subdivided into 882 hydrological response units (HRUs). It was run for 21 years from 1988 to 2008, but only 20 years were used for analysis allowing for a 1 year model spin-up phase. To not implicitly correct errors in precipitation measurements with model parameters that were derived from a specific model calibration procedure, we chose default model parameters or we selected the parameters based upon the literature for the given site conditions (e.g. soil parameterization). The values and sources of the parameters that are usually used for calibration in SWAT are provided in the appendix (Table A1). This parameterization procedure has been successfully applied in other studies, where SWAT input parameters were estimated without calibration from readily available GIS databases (e.g., Fontaine et al., 2002; Srinivasan et al., 2010; Zhang et al., 2008). Under similar (Indian) conditions, SWAT showed generally good performances without much calibration (Gosain et al. (2005) only adjusted the low flow (groundwater) component of river runoff). A preceding model application using the same methodology but a different rainfall input was already relatively successful in the study area (Nash-Sutcliffe efficiencies of

0.68 (G1) and 0.58 (G4) at the river gauges that are less affected by dam management; Wagner et al., 2011). Hence, the model was not calibrated with measured runoff data since the focus is set on obvious differences between measured and modeled hydrographs resulting from different rainfall inputs. Four model runs were performed using the different precipitation inputs derived from the regression-based interpolation methods with the X-coordinate ( $RIDW_X$ ,  $RK_X$ ) and the TRMM pattern ( $RIDW_{TRMM}$ ,  $RK_{TRMM}$ ) as covariate.

## 2.5. Validation

The interpolation schemes were validated in two steps:

(i) A cross-validation was carried out by estimating the daily time series for the entire period from 1988 to 2008 at one gauge by using all other rain gauges. To evaluate the goodness-of-fit, we calculated root mean square error (RMSE), Nash–Sutcliffe efficiency (NSE; Nash and Sutcliffe, 1970), and percentage bias (PBIAS; Moriasi et al., 2007). The NSE is defined as

$$NSE = 1 - \frac{\sum_{i=1}^n (O_i - M_i)^2}{\sum_{i=1}^n (O_i - \bar{O})^2}, \quad (5)$$

and PBIAS is computed in the following way:

$$PBIAS = 100 \cdot \frac{\sum_{i=1}^n (O_i - M_i)}{\sum_{i=1}^n O_i}, \quad (6)$$

where  $O_i$  is the  $i$ th observation,  $M_i$  is the  $i$ th predicted value,  $\bar{O}$  is the mean of the observed values, and  $n$  is the total number of observations.

Performances of the different interpolation schemes were ranked for each gauge and hence a mean ranking of each approach was derived by averaging the ranking for all individual gauges. Thus, the best interpolation methods were identified.

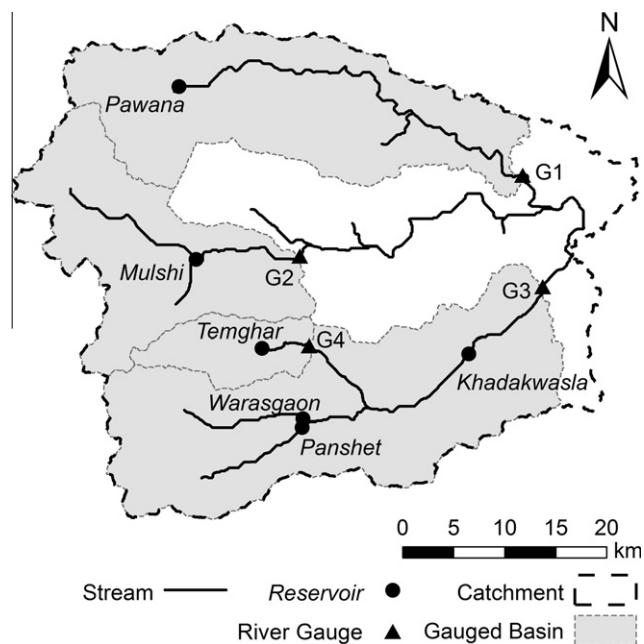


Fig. 5. Location of river gauges and reservoirs in the Mula–Mutha catchment.

(ii) For many environmental applications (such as hydrologic modeling studies) closing the mass balance is of critical importance and reproducing meaningful spatial patterns of rainfall is more important than reproducing point measurements accurately. Therefore, the best approaches identified by cross-validation were compared at the sub-catchment level to assess spatially integrated differences in rainfall and runoff. SWAT was used to evaluate the effects of the different interpolation inputs on the water balance and on runoff dynamics. This validation technique allows for an assessment of the spatially integrated effects of rainfall. It is focused on the two sub-catchments (G1 and G4; Fig. 5) that are less affected by dam management.

## 3. Results

In general, the interpolation schemes that used covariates outperformed the univariate methods. This is indicated by RMSE, NSE, and PBIAS for the different interpolation schemes and the rankings based on cross-validation using these goodness-of-fit indicators (Table 3). Among the regression-based methods, regression-kriging (RK) and regression-inverse distance weighting (RIDW) showed a similar performance. Comparing the covariates, the use of the X-coordinate led to slightly better results than the use of the TRMM pattern as a covariate.

This ranking is also reflected by the performance at the individual gauges as indicated by the NSE (Fig. 6). Except for one station, Thiessen polygons (TH) show the weakest performance, including negative values for three stations. Thiessen polygons typically show reasonable performance for gauges, where the nearby gauge is representative for the estimated gauge (e.g., Kumbheri and Mulshi). If this is not the case, Thiessen polygons do not perform as well as the other methods (e.g., Paud). Ordinary pooled kriging (OK) and IDW perform quite similar with varying performances from gauge to gauge, but significantly better than the Thiessen polygons and slightly worse than the schemes that use covariates. These four regression-based methods often perform similarly. The mean RMSE (Table 3) usually reflects the ranking at the gauges. However, performance varies from one gauge to another. The worst interpolation performance was found at the most eastern gauge Wagholi. As TH and OK show a negative NSE here, it can be concluded that the nearest gauges are not representative for this gauge. The regression-based approaches perform better at this site as they do not rely as much on neighboring gauges, but use information from the covariate. Depending on the chosen goodness-of-fit indicator, the performance of IDW (RMSE; Table 3) and OK (PBIAS; Table 3) is sometimes slightly better than the least best regression-based interpolation method. However taking all indicators into consideration, the regression-based methods show a better performance than the univariate approaches. RK and RIDW can be rated similarly good, as it depends on the rain gauge (Fig. 6) and on the chosen indicator (Table 3) as to which regression-based interpolation method performs best.

For further analysis, the focus is set on the regression-based methods using the two different covariates. Based upon the cross-validation, the incorporation of the X-coordinate led to the best interpolation results (Table 3). However, the TRMM data provide spatial patterns that reflect the mean annual distribution of precipitation and incorporate more spatial detail (e.g., orographic rainfall at mountain ridges) than the X-coordinate that expresses the general decrease of rainfall with distance from the Western Ghats escarpment.

Despite the small differences of the cross-validation results obtained with the two covariates shown in Table 3, the integrative effect of the chosen covariate is quite obvious at the catchment scale (Table 4), when comparing modeled and measured runoff for two

**Table 3**

Cross-validation performance and ranking of different interpolation schemes based on root mean square error (RMSE), Nash–Sutcliffe efficiency (NSE), and percentage bias (PBIAS).

Interpolation scheme	Range RMSE (mm)	Mean RMSE (mm)	Rank of mean RMSE	Range NSE	Median NSE	Mean rank of NSE	Rank of mean rank of NSE	Range absolute PBIAS (%)	Mean absolute PBIAS (%)	Rank of mean absolute PBIAS
Thiessen polygons	6.7–20.1	12.3	7	−0.49–0.68	0.26	6.9	7	15.4–41.9	28.0	7
IDW	5.5–19.2	10.1	4	−0.16–0.73	0.57	4.1	5	5.1–53.7	24.0	6
OK	5.6–19.4	10.2	6	−0.17–0.71	0.56	4.3	6	5.6–41.6	19.3	4
RIDW <sub>X</sub>	5.4–18.1	9.7	1	0.02–0.75	0.60	1.7	1	1.5–41.6	14.8	2
RIDW <sub>TRMM</sub>	5.6–18.3	10.0	3	−0.04–0.73	0.58	3.0	3	2.0–69.1	19.8	5
RK <sub>X</sub>	5.4–18.1	9.8	2	0.01–0.75	0.60	1.9	2	2.0–42.7	14.7	1
RK <sub>TRMM</sub>	5.6–18.4	10.1	5	−0.04–0.72	0.58	3.6	4	1.3–60.0	18.0	3

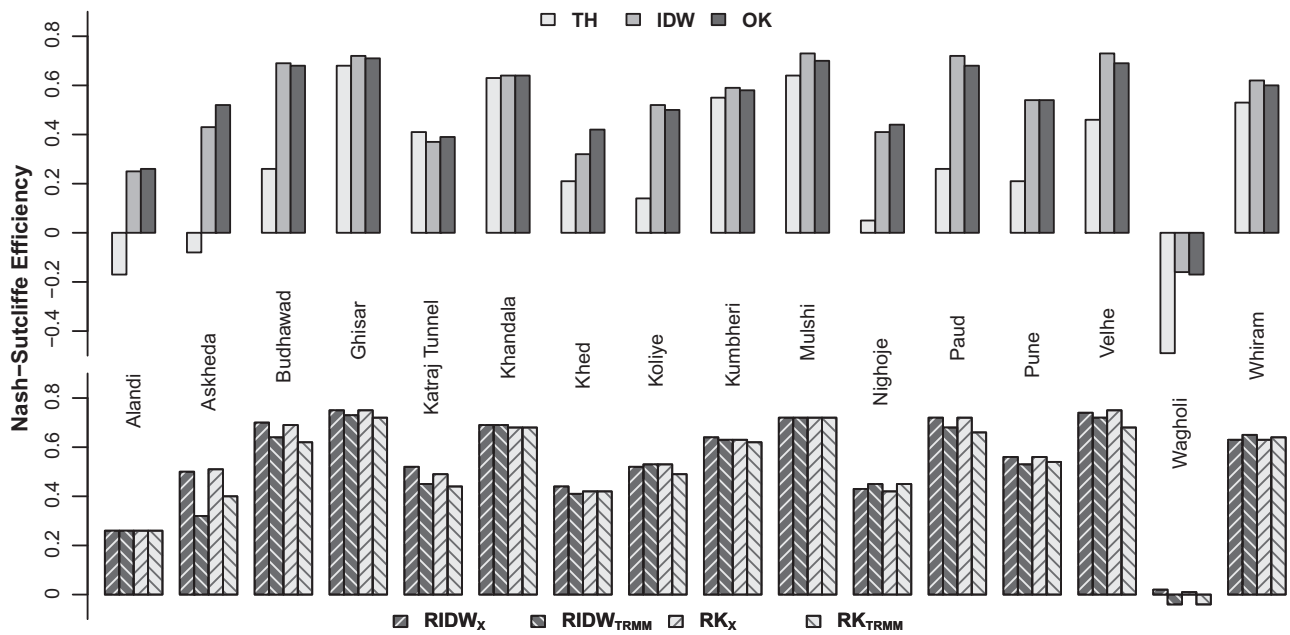


**Fig. 6.** Interpolation performance at the rain gauges as indicated by the Nash–Sutcliffe efficiency (NSE): Univariate methods above and regression-based methods below.

**Table 4**

Model performance as indicated by Nash–Sutcliffe efficiency (NSE) and percentage bias (PBIAS) in two sub-catchments using differently interpolated rainfall inputs.

Catchment	G1		G4	
	NSE	PBIAS	NSE	PBIAS
RIDW <sub>X</sub>	0.59	−29.5	0.61	42.9
RIDW <sub>TRMM</sub>	0.73	7.6	0.65	25.6
RK <sub>X</sub>	0.61	−28.5	0.62	40.4
RK <sub>TRMM</sub>	0.68	4.0	0.67	24.4

different sub-catchments (G1 and G4). The performance of the interpolation methods was evaluated using the available daily discharge data during rainy seasons between 2001 and 2007 (Wagner et al., 2011). This evaluation was restricted to sub-catchments G1 and G4, since the measured runoff at gauge G2 and G3 strongly depends upon the management of the upstream dams. Highest NSE and lowest PBIAS values were found when using TRMM data as covariate (Table 4), because TRMM based interpolation led to less precipitation in catchment G1 and to more precipitation in G4 compared to the results using the X-coordinate (Table 5). The more favorable NSE and PBIAS indicate that interpolation methods using

remotely sensed patterns provide better results with respect to modeled runoff.

The TRMM based methods produce 8.8% and 9.0% (RIDW: 196 mm, RK: 199 mm) higher mean annual precipitation at the catchment scale when compared to the results obtained by using the X-coordinate. For the Mula–Mutha catchment the higher

**Table 5**

Modeled water balance components for the Mula–Mutha catchment and two sub-catchments based on different interpolation schemes.

Sub-catchment	Interpolation scheme	Precipitation (mm)	Runoff (mm)	Evapotranspiration (mm)
Mula–Mutha	RIDW <sub>X</sub>	2215	1421	731
	RIDW <sub>TRMM</sub>	2410	1573	734
	RK <sub>X</sub>	2221	1427	731
	RK <sub>TRMM</sub>	2420	1585	734
G1	RIDW <sub>X</sub>	2312	1631	776
	RIDW <sub>TRMM</sub>	1934	1261	767
	RK <sub>X</sub>	2308	1625	776
	RK <sub>TRMM</sub>	1972	1297	766
G4	RIDW <sub>X</sub>	2630	1972	629
	RIDW <sub>TRMM</sub>	3046	2386	635
	RK <sub>X</sub>	2680	2021	630
	RK <sub>TRMM</sub>	3065	2405	635

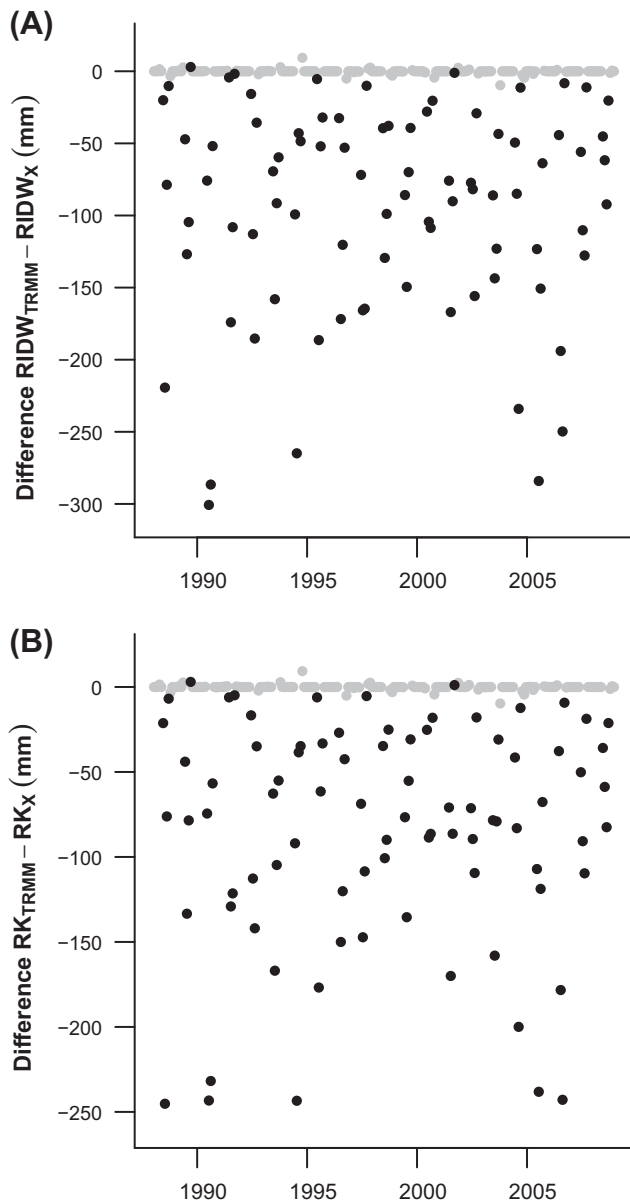


**Fig. 7.** Differences in monthly rainfall for sub-catchment G1 using different covariates for interpolation: (A) Regression-inverse distance weighting (RIDW) and (B) regression-kriging (RK). Rainy and dry season are shown as black and gray dots, respectively.

rainfall amounts lead to 10.7% and 11.1% (RIDW: 152 mm, RK: 158 mm) higher runoff and only slightly higher evapotranspiration. As has to be expected, the effects of using different covariates are even more pronounced at the sub-catchment scale (Table 5).

In the following paragraphs a more detailed analysis with focus on shorter time scales is presented for sub-catchment G1. Differences between the interpolation methods are more pronounced at shorter time scales. Monthly rainfall differences between  $RIDW_{TRMM}$  and  $RIDW_X$  in G1 range from +3 mm and from -245 mm to +3 mm for the RK methods (Fig. 7). These monthly differences in sub-catchment G1 generally showed maximum values (>150 mm) in July and August. The resulting differences in runoff dynamics are exemplarily analyzed for monsoon season 2006. This season was chosen since the summed monthly differences for July and August 2006 (RIDW: 444 mm, RK: 421 mm) are largest within the validation period. The course of the hydrograph of the RIDW and RK methods for

the same covariate is nearly identical during this period ( $X$ -coordinate: 0.999 NSE, 0.03% PBIAS; TRMM pattern: 0.987 NSE, -1.09% PBIAS). Thus, the visual analysis shown in Fig. 8 is restricted to comparing the two RK methods. Generally, the higher rainfall amounts of  $RK_X$  lead to higher runoff peaks in the respective hydrographs (e.g., 12 and 23 July; Fig. 8). The peaks mostly occur at the same time for both model runs, but may also differ by 1 day (e.g., 15/16 August; Fig. 8). The primarily small differences in June and July add up, so that full storage capacity of the upstream dam is reached at different dates. Hence, once the full storage capacity of the dam is reached, the dampening effect of the dam with respect to runoff peaks ceases to exist. If the full storage capacity is reached at different dates in the models, pronounced differences in runoff may follow (e.g., higher runoff amounts from 30 July to 2 August; Fig. 8). This indicates that different interpolation schemes can make an important difference for runoff dynamics.

Comparing the modeled hydrographs to the measured runoff showed more favorable results using the  $RK_{TRMM}$  interpolation (Fig. 8). Particularly during the high flow period between mid July and mid August, the course of the measured runoff is well reproduced by the  $RK_{TRMM}$  model. In the early monsoon season before full storage capacity of the dam is reached, both model runs show peaks on 30 June and 6 July that are not represented in the observations. On these dates, the western rain gauges show high amounts of rainfall whereas the eastern gauges show little amounts. Possibly the western gauges were given too much influence in the interpolation on these days. On the other hand, the dampening effect of the dam might be too low in the model. Once the dam is filled, the dampening effect of the dam with respect to the hydrograph is negligible. Hence, the following period is most reliable for comparison of modeled and measured runoff. The poor match in the late monsoon period after mid August may result from dam management impacts that were not represented by the assumed dam management in the model. In contrast to  $RK_{TRMM}$ , the  $RK_X$  interpolation fails to match the dates of the measured peaks in runoff (e.g., peaks on 6, 10, and 16 August; Fig. 8). The modeled peaks occur either 1 day too early or 1 day too late compared to the measured runoff. Furthermore, the integral between measured and modeled hydrograph shows a large overestimation of runoff by the  $RK_X$  driven model. This result is underlined by PBIAS, which indicates an overestimation of 28.5% for the whole validation period for  $RK_X$ . Similarly PBIAS for  $RK_{TRMM}$  shows only a small underestimation of 4.0%, which matches well with the generally small integral between measured and  $RK_{TRMM}$  modeled runoff in monsoon season 2006. The comparison of runoff dynamics supports the finding that the TRMM pattern is the more suitable covariate to reproduce runoff dynamics.

#### 4. Discussion

The improvement of the interpolation results by using additional information from a covariate (Verworn and Haberlandt, 2011) is very clear in this study, as the regression-based methods outperformed the univariate methods (Table 3 and Fig. 6). This is in agreement with other findings, where external drift kriging (being a modified form of regression kriging) was found to be one of the best interpolation schemes (Goovaerts, 2000; Zhang and Srinivasan, 2009). Pooled semivariograms for rainfall interpolation were previously used only on an event basis (Fiener and Auerswald, 2009; Schuurmans et al., 2007). Our results show that this method can successfully be transferred to monthly pooling, which makes kriging applicable in situations of scarce data availability. However, the superiority of geostatistical methods was not as obvious as in other studies (Buytaert et al., 2006; Goovaerts,

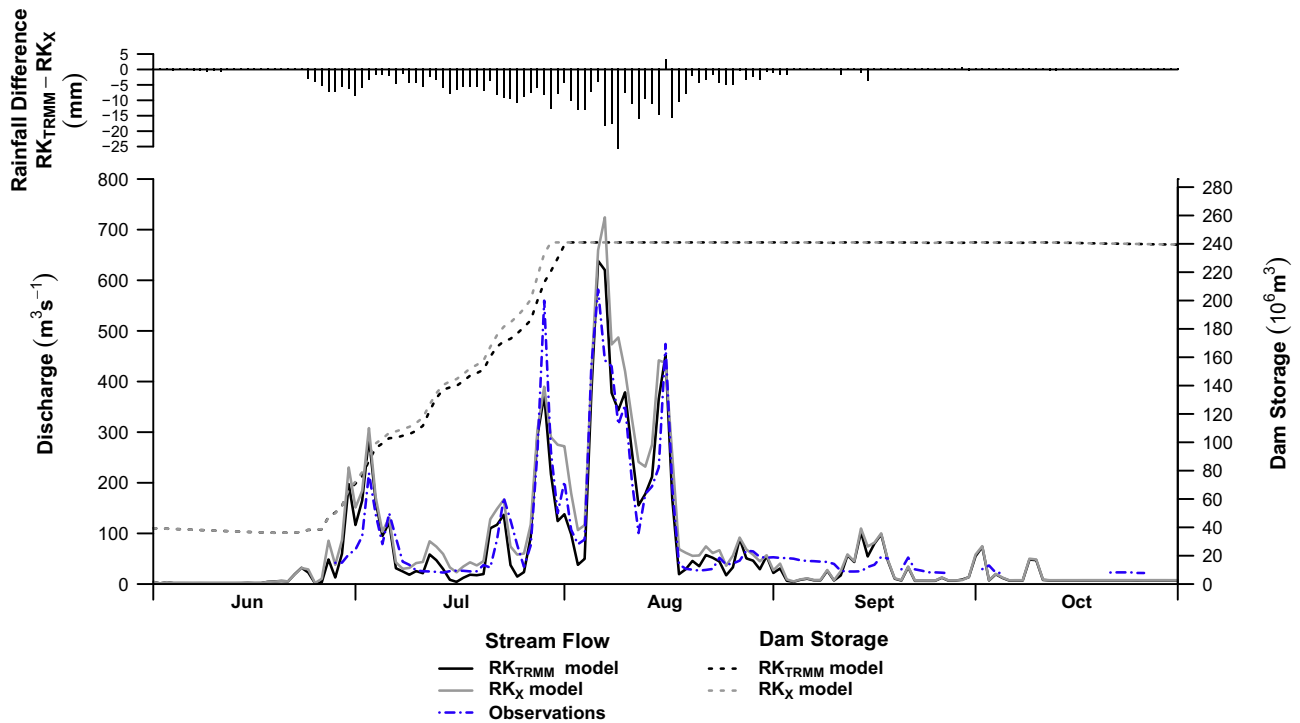


**Fig. 8.** Modeled and measured runoff at gauge G1, the storage volume of the upstream Pawana dam, and rainfall differences in sub-catchment G1 for regression-kriging rainfall interpolation with covariates TRMM pattern and X-coordinate during the 2006 rainy season.

2000; Ly et al., 2011). Two reasons may contribute to this result: (i) In case of the univariate methods the autocorrelation decreases almost linearly with increasing distance (Fig. 2). Thus IDW with an exponent of one is very similar to the applied OK approach. (ii) In case of the regression-based methods the main part of the rainfall estimate is determined by the covariate, giving less influence to the interpolation of the residuals. A major advantage of the IDW method is that it can be used at any time step. Whereas kriging requires a sufficient amount of data to produce a reliable semivariogram, which in our case was achieved by using pooled variograms for every month.

DEM parameters such as elevation are commonly used for rainfall interpolation (Buytaert et al., 2006; Goovaerts, 2000; Lloyd, 2005; Verworn and Haberlandt, 2011). However, a relation between rainfall and elevation could not be found here. If high elevation rainfall measurements are missing or large scale processes dominate the small scale orographic rainfall effects, a relation may not be derived from the data. This is often the case, especially in data scarce regions. In this study, one reason for a missing relation between rainfall and elevation is that the elevation difference of the highest (Katraj Tunnel, 895 m) and the lowest gauge (Pune, 559 m) is not proportionally reflected in the rainfall difference of these gauges. Thus, the mean annual rainfall difference (187 mm) represented by these gauges is small in comparison to the differences in mean annual rainfall, which range up to 3160 mm in the study area. The dominating effect on rainfall distribution is not elevation but distance in wind direction from the Western Ghats escarpment (Table 2), which is expressed by the X-coordinate. As the escarpment is the main orographic barrier, the study area lies in the rain shadow of the escarpment. Hence, the potential amount of rainfall at higher mountain ranges to the east of the escarpment (Fig. 1) is limited by the amount of rain that occurred at the escarpment and other westward barriers. The combination of the dominating south-west monsoon and the north-south exposition of the Western Ghats escarpment clearly leads to the west to east de-

cline of rainfall and consequently no rainfall dependence on elevation can be detected in the study area.

An alternative to DEM parameters are satellite measurements of rainfall patterns. For this reason satellite data is increasingly used for rainfall interpolation (Velasco-Forero et al., 2009; Verworn and Haberlandt, 2011; Schiemann et al., 2011). The results show that the annual rainfall pattern that was derived from TRMM precipitation radar is a useful covariate. Within the geographic range of 38°S to 38°N TRMM provides a spatial precipitation pattern, which is an alternative to empirical covariates. Its spatial detail (0.05° grid) makes it superior to empirical covariates such as the X-coordinate, which might show a higher correlation with the data, but fail to provide a spatially accurate estimate. Compared to the X-coordinate, the TRMM pattern shows a larger spatial variability, which results in some areas in more and in other areas in less rainfall. However, the TRMM based methods provide in any case a better closure of the water balance, as the spatially integrated comparison with measured data shows.

Cross-validation is a widely used and useful technique for the evaluation of interpolation results (Hattermann et al., 2005; Lloyd, 2005). However, with a limited number of values, results are subject to bias that originates from the distribution of the gauges. If this distribution is not representative of the spatial distribution of rainfall, bias is introduced (Heistermann and Kneis, 2011). Particularly in low density measurement networks, interpolation may lead to a large bias, unless these networks were designed with regard to interpolation needs (Cheng et al., 2008). In our study, cross-validation indicated only small differences between  $RK_{TRMM}$  and  $RK_X$  (RMSE of 10.1 mm and 9.8 mm, Table 3), whereas the spatially integrated assessment showed pronounced differences in the catchment's mean annual rainfall (2420 mm and 2221 mm, Table 5), in monthly rainfall on the sub-catchment scale (Fig. 7), and in runoff dynamics (Fig. 8). While the cross-validation result indicated that  $RK_X$  and  $RIDW_X$  are the best interpolation technique, the spatially integrated assessment using the SWAT model showed

that  $RK_{TRMM}$  and  $RIDW_{TRMM}$  are the better interpolation schemes. One reason for this might be the relatively small number of 16 rain gauges. Cross-validation indicated that the interpolation schemes perform similarly at the rain gauge locations. The differences that are exposed by comparing the model based spatially integrated results are due to the different spatial detail provided by the two covariates. The TRMM pattern with its  $0.05^\circ$  resolution was able to reproduce local rainfall effects (e.g., due to topography) better as compared to using the  $X$ -coordinate as covariate. It can be assumed that a denser rain gauge network (covering also mountain ridges) that better reflects local rainfall effects would probably lead to a decrease of the cross-validation performance of  $RK_X$  and  $RIDW_X$ . In data scarce regions with a high spatial variability in rainfall (such as mountainous areas), cross-validation results should be interpreted with care and should be backed up with a spatially integrated assessment of interpolation quality.

The spatially integrative effect of different interpolation methods can be assessed with hydrologic models, as they spatially integrate precipitation to produce runoff. Hydrographs allow for an evaluation of the interpolated rainfall integrating space and time. However, the approach critically relies on the quality of the model, which needs to accurately represent the catchment's hydrologic response (Heistermann and Kneis, 2011), and on the quality of the measured runoff data. The model should not require much calibration, as calibration might compensate for possibly wrong rainfall input (Heistermann and Kneis, 2011; Strauch et al., 2012). The SWAT model parameters were selected based upon literature values (e.g., soil parameters after Immerzeel et al., 2008), or regional knowledge (e.g., definition of dam management, forest phenology). Otherwise default values were used. The model was not calibrated to observed rainfall–runoff events. Thus, we are confident that the obtained results are not compromised by compensatory effects arising from model calibration. Particularly in consolidated rock catchments such as the Mula–Mutha catchment with its fast system response to precipitation inputs, differences in model response can thus be attributed to the spatial patterns and accuracy of the applied interpolation schemes.

The application of this approach has so far been limited to modeling studies (e.g., Cole and Moore, 2008; Gourley and Vieux, 2005; Heistermann and Kneis, 2011; Hwang et al., 2012). However, the presented results show that it is a suitable method to evaluate interpolation performance. Model based spatial assessment of interpolation accuracy enhances commonly used validation methods and provides reliable results that are particularly valuable in data-scarce regions.

## 5. Conclusions

In this study, seven interpolation schemes were carried out to provide rainfall data on a daily time step using 16 rain gauges. The different methods were evaluated using a two step validation approach incorporating cross-validation as well as spatially integrated assessment of interpolation performance with the help of a hydrologic model.

Our analysis indicates that precipitation interpolation approaches using appropriate covariates perform best. The two regression-based methods ( $RIDW$  and  $RK$ ) performed similarly well. Since  $RIDW$  is less complex than  $RK$ , it might be favorable if a quick and straight forward interpolation method is required. Even though its use for interpolation might become more evident in other studies, the additional information that is provided by semivariograms is valuable for analyzing the spatial distribution of rainfall. Monthly pooling is a feasible method to assess autocorrelation of rainfall in data-scarce regions and hence can be used for geostatistical interpolation schemes.

Best interpolation results were obtained using (i) the  $X$ -coordinate that represents the distance from the Western Ghats escarpment as climatic dominant structure and (ii) the spatial pattern of annual rainfall derived from remotely sensed TRMM precipitation radar. Although the differences in interpolation performance judged by cross-validation were small, relatively large differences in catchment rainfall were recognized for the two best performing interpolation schemes. These differences were even more pronounced focusing on a smaller spatial (sub-catchment) and a smaller time (monthly) scale. A spatially integrated analysis based on rainfall–runoff modeling and its comparison with measured discharge helped to identify the TRMM pattern as a more suitable covariate. Regardless of the sub-catchment, modeled runoff based on the interpolation methods that used the TRMM pattern matched the measured runoff best, because TRMM based interpolation produced more rainfall in one sub-catchment and less rainfall in the other sub-catchment when compared to the interpolation methods that used the  $X$ -coordinate. The comparatively high spatial resolution of the TRMM pattern provides an accurate estimate of the spatial rainfall distribution, which is particularly important, when interpolated rainfall is used for spatially distributed analysis, such as spatially distributed modeling. Superior to most empirical covariates, the TRMM pattern allows for a transfer of the methodology to other study areas within the geographic range of  $38^\circ S$  to  $38^\circ N$  covered by TRMM. Moreover, it is a valuable alternative to the commonly used covariate elevation, especially in regions where a rainfall dependence on elevation is not present or cannot be derived from measurements.

Furthermore, the results indicate that cross-validation is not sufficient to identify the most suitable precipitation interpolation method in data scarce regions, and that spatially integrated evaluation is needed to assess the accuracy of interpolated spatial rainfall distributions. In this context, hydrologic models are useful tools as they allow for evaluations that are based on runoff, which temporally and spatially integrates rainfall.

In general, our results indicate the high potential of pooled kriging in combination with TRMM data as a covariate ( $RK_{TRMM}$ ) to derive appropriate daily inputs for hydrologic models in data scarce tropical to sub-tropical regions. Moreover, our study underlines the importance of more sophisticated multi-step validation of interpolations schemes, especially if applied in data scarce regions where cross-validation techniques alone may not be sufficient.

## Acknowledgements

We gratefully acknowledge support by a grant from the German National Academic Foundation. We would like to thank Chris Kidd for providing the TRMM rainfall pattern, which was processed by the Earth System Science Interdisciplinary Center, University of Maryland and NASA/Goddard Space Flight Center. We are grateful to IMD Pune, Water Resources Department Nashik, Khadakwasla Irrigation Division Pune, Groundwater Department Pune, Department of Agriculture Pune, and NRSC Hyderabad for supplying environmental data, good cooperation and discussions. Moreover, we acknowledge supply of ASTER data by the USGS Land Processes Distributed Active Archive Center. Special thanks go to Karen Schneider for proof reading the manuscript and to the students from the Institute of Environment Education & Research at Bharati Vidyapeeth University Pune for assistance with the field measurements. The authors thank the editor and the two anonymous reviewers for their helpful comments.

## Appendix A

See Table A1.

**Table A1**  
Applied SWAT model parameterization of potential calibration parameters.

Parameter name	Description	Value	Source
CN2	Initial SCS runoff curve number for soil moisture condition II	Depends on soil and land use	Estimated by the model (Neitsch et al., 2010)
SOL_AWC	Available water capacity of the soil layer	Depends on the soil, values given in Wagner et al. (2011)	Immerzeel et al. (2008)
SOL_K	Saturated hydraulic conductivity of the soil layer	Depends on the soil, values given in Wagner et al. (2011)	Immerzeel et al. (2008)
CANMX	Maximum canopy storage	0	Default model parameter value
EPCO	Plant uptake compensation factor	1	Default model parameter value
ESCO	Soil evaporation compensation coefficient	0.95	Default model parameter value
CH_N	Manning's roughness coefficient for channel flow	0.014 s m <sup>-1/3</sup>	Default model parameter value
SURLAG	Surface runoff lag coefficient	4	Default model parameter value
GWQMN	Threshold depth of water in the shallow aquifer required for return flow to occur	0 mm	Default model parameter value
GW_DELAY	Groundwater delay time	31 d	Default model parameter value
GW_REVAP	Groundwater "revap" coefficient	0.02	Default model parameter value
ALPHA_BF	Baseflow alpha factor	0.048 d	Default model parameter value
REVAPMN	Threshold depth of water in the shallow aquifer for "revap" or percolation to the deep aquifer to occur	1 mm	Default model parameter value

## References

- Arnold, J.G., Srinivasan, R., Muttiah, R.S., Williams, J.R., 1998. Large area hydrologic modeling and assessment – Part 1: Model development. *J. Am. Water Resour. Assoc.* 34, 73–89.
- Barros, A.P., Lettenmaier, D.P., 1993. Dynamic modeling of the spatial distribution of precipitation in remote mountainous areas. *Mon. Weather Rev.* 121, 1195–1214.
- Barry, R.G., 1992. Mountain climatology and past and potential future climatic changes in mountain regions. *Mt. Res. Dev.* 12 (1), 71–86.
- Basistha, A., Arya, D.S., Goel, N.K., 2008. Spatial distribution of rainfall in Indian Himalayas—a case study of Uttarakhand Region. *Water Resour. Manage.* 22, 1325–1346.
- Beven, K.J., 2001. *Rainfall–runoff Modelling: The Primer*. John Wiley & Sons Ltd., Chichester.
- Burrough, P.A., McDonnell, R.A., 1998. *Principles of Geographical Information Systems*. Oxford University Press, Oxford.
- Buytaert, W., Celleri, R., Willems, P., De Bièvre, B., Wyseure, G., 2006. Spatial and temporal rainfall variability in mountainous areas: a case study from the south Ecuadorian Andes. *J. Hydrol.* 329, 413–421.
- Carrera-Hernández, J.J., Gaskin, S.J., 2007. Spatio temporal analysis of daily precipitation and temperature in the Basin of Mexico. *J. Hydrol.* 336, 231–249.
- Chaubey, I., Haan, C.T., Salisbury, J.M., Grunwald, S., 1999. Quantifying model output uncertainty due to the spatial variability of rainfall. *J. Am. Water Resour. Assoc.* 35 (5), 1113–1123.
- Cheng, K.-S., Lin, Y.-C., Liou, J.-J., 2008. Rain-gauge network evaluation and augmentation using geostatistics. *Hydrol. Process.* 22, 2554–2564.
- Cole, S.J., Moore, R.J., 2008. Hydrological modeling using raingauge- and radar-based estimators of areal rainfall. *J. Hydrol.* 358, 159–181.
- Croke, B.F.W., Islam, A., Ghosh, J., Khan, M.A., 2011. Evaluation of approaches for estimation of rainfall and the unit hydrograph. *Hydrol. Res.* 42 (5), 372–385.
- Di Piazza, A., Lo Conti, F., Noto, L.V., Viola, F., La Loggia, G., 2011. Comparative analysis of different techniques for spatial interpolation of rainfall data to create a serially complete monthly time series of precipitation for Sicily, Italy. *Int. J. Appl. Earth Obs. Geoinf.* 13, 396–408.
- Fiener, P., Auerswald, K., 2009. Spatial variability of rainfall on a sub-kilometre scale. *Earth Surf. Process. Landforms* 34, 848–859.
- Fontaine, T.A., Cruickshank, T.S., Arnold, J.G., Hotchkiss, R.H., 2002. Development of a snowfall–snowmelt routine for mountainous terrain for the soil water assessment tool (SWAT). *J. Hydrol.* 262, 209–223.
- Food and Agriculture Organization of the United Nations (FAO), 2003. *Digital Soil Map of the World and Derived Soil Properties*, FAO, Rome.
- Gadgil, A., 2002. Rainfall characteristics of Maharashtra. In: Diddee, J., Jog, S.R., Kale, V.S., Datye, V.S. (Eds.), *Geography of Maharashtra*. Rawat Publications, Jaipur, pp. 89–102.
- Goovaerts, P., 2000. Geostatistical approaches for incorporating elevation into the spatial interpolation of rainfall. *J. Hydrol.* 228, 113–129.
- Gosain, A.K., Rao, S., Srinivasan, R., Reddy, N.G., 2005. Return-flow assessment for irrigation command in the Palleru river basin using SWAT model. *Hydrol. Process.* 19, 673–682.
- Gourley, J.J., Vieux, B.E., 2005. A method for evaluating the accuracy of quantitative precipitation estimates from a hydrologic modeling perspective. *J. Hydrometeorol.* 6 (2), 115–133.
- Gunnell, Y., 1997. Relief and climate in South Asia: the influence of the Western Ghats on the current climate pattern of peninsular India. *Int. J. Climatol.* 17, 1169–1182.
- Hattermann, F., Krysanova, V., Wechsung, F., Wattenbach, M., 2005. Runoff simulations on the macroscale with the ecohydrological model SWIM in the Elbe catchment – validation and uncertainty analysis. *Hydrol. Process.* 19, 693–714.
- Heistermann, M., Kneis, D., 2011. Benchmarking quantitative precipitation estimation by conceptual rainfall–runoff modeling. *Water Resour. Res.* 47, W06514.
- Hengl, T., Heuvelink, G.B.M., Rossiter, D.G., 2007. About regression–kriging: from equations to case studies. *Comput. Geosci.* 33, 1301–1315.
- Hwang, Y., Clark, M., Rajagopalan, B., Leavesley, G., 2012. Spatial interpolation schemes of daily precipitation for hydrologic modeling. *Stoch. Environ. Res. Risk Assess.* 26, 295–320.
- Immerzeel, W.W., Gaur, A., Zwart, S.J., 2008. Integrating remote sensing and a process-based hydrological model to evaluate water use and productivity in a south Indian catchment. *Agric. Water Manage.* 95, 11–24.
- Jain, S.K., Agarwal, P.K., Singh, V.P., 2007. *Hydrology and Water Resources of India*. Springer, Dordrecht.
- Kidd, C., McGregor, G., 2007. Observation and characterisation of rainfall over Hawaii and surrounding region from the Tropical Rainfall Measuring Mission. *Int. J. Climatol.* 27 (4), 541–553.
- Kummerow, C., Simpson, J., Thiele, O., Barnes, W., Chang, A.T.C., Stocker, E., Adler, R.F., Hou, A., Kaker, R., Wentz, F., Ashcroft, P., Kozu, T., Hong, Y., Okamoto, K., Iguchi, T., Kuroiwa, H., Im, E., Haddad, Z., Huffman, G., Ferrier, B., Olson, W.S., Zipser, E., Smith, E.A., Wilhelm, T.T., North, G., Krishnamurti, T., Nakamura, K., 2000. The status of the tropical rainfall measuring mission (TRMM) after two years in orbit. *J. Appl. Meteorol.* 39, 1965–1982.
- Kurtzman, D., Navon, S., Morin, E., 2009. Improving interpolation of daily precipitation for hydrologic modelling: spatial patterns of preferred interpolators. *Hydrol. Process.* 23, 3281–3291.
- Lloyd, C.D., 2005. Assessing the effect of integrating elevation data into the estimation of monthly precipitation in Great Britain. *J. Hydrol.* 308, 128–150.
- Ly, S., Charles, C., Degré, A., 2011. Geostatistical interpolation of daily rainfall at catchment scale: the use of several variogram models in the Ourthe and Ambleve catchments, Belgium. *Hydrol. Earth Syst. Sci.* 15, 2259–2274.
- Mausner, W., Bach, H., 2009. PROMET – large scale distributed hydrological modelling to study the impact of climate change on the water flows of mountain watersheds. *J. Hydrol.* 376, 362–377.
- Moriasi, D.N., Arnold, J.G., Van Liew, M.W., Bingner, R.L., Harmel, R.D., Veith, T.L., 2007. Model evaluation guidelines for systematic quantification of accuracy in watershed simulations. *Trans. ASABE* 50 (3), 885–900.

- Nash, J.E., Sutcliffe, J.V., 1970. River flow forecasting through conceptual models part I – a discussion of principles. *J. Hydrol.* 10, 282–290.
- Ndomba, P., Mtalo, F., Killingtveit, A., 2008. SWAT model application in a data scarce tropical complex catchment in Tanzania. *Phys. Chem. Earth* 33, 626–632.
- Neitsch, S.L., Arnold, J.G., Kiniry, J.R., Srinivasan, R., Williams, J.R., 2010. Soil and Water Assessment Tool: Input/Output File Documentation, Version 2009. Texas Water Resources Institute, Texas A&M University, College Station, Texas.
- Pebesma, E.J., 2004. Multivariable geostatistics in S: the gstat package. *Comput. Geosci.* 30, 683–691.
- R Development Core Team, 2011. R: A Language and Environment for Statistical Computing. Ver. 2.13.0. R Foundation for Statistical Computing, Vienna.
- Richter, D., 1995. Ergebnisse methodischer Untersuchungen zur Korrektur des systematischen Meßfehlers des Hellmann-Niederschlagsmessers. *Berichte des Deutschen Wetterdienstes* 194, Offenbach.
- Schiemann, R., Erdin, R., Willi, M., Frei, C., Berenguer, M., Sempere-Torres, D., 2011. Geostatistical radar-rain gauge combination with nonparametric correlograms: methodological considerations and application in Switzerland. *Hydrol. Earth Syst. Sci.* 15, 1515–1536.
- Schuermans, J.M., Bierkens, M.F.P., Pebesma, E.J., Uijlenhoet, R., 2007. Automatic prediction of high-resolution daily rainfall fields for multiple extents: the potential of operational radar. *J. Hydrometeorol.* 8 (6), 1204–1224.
- Searcy, J.K., Hardison, C.H., Langbein, W.B., 1960. Double mass curves. *Geological Survey Water Supply Paper 1541-B*. US Geological Survey, Washington DC.
- Shepard, D., 1968. A two-dimensional interpolation function for irregularly-spaced data. In: Blue, R.B., Sr., Rosenberg, A.M. (Eds.), *Proceedings of the 1968 23rd ACM National Conference*. August 27–29. ACM Press, New York, pp. 517–524.
- Srinivasan, R., Zhang, X., Arnold, J.G., 2010. SWAT ungauged: hydrological budget and crop yield predictions in the upper Mississippi river basin. *Trans. ASABE* 53 (5), 1533–1546.
- Stehr, A., Debel, P., Romero, F., Alcayaga, H., 2008. Hydrological modelling with SWAT under conditions of limited data availability: evaluation of results from a Chilean case study. *Hydrol. Sci. J.* 53, 588–601.
- Stein, M.L., 1999. *Interpolation of Spatial Data: Some Theory for Kriging*. Springer, New York.
- Strauch, M., Bernhofer, C., Koide, S., Volk, M., Lorz, C., Makeschin, F., 2012. Using precipitation data ensemble for uncertainty analysis in SWAT streamflow simulation. *J. Hydrol.* 414–415, 413–424.
- Tabios, G.Q., Salas, J.D., 1985. A comparative analysis of techniques for spatial interpolation of precipitation. *J. Am. Water Resour. Assoc.* 21, 365–380.
- Teegavarapu, R.S.V., Tufail, M., Ormsbee, L., 2009. Optimal functional forms for estimation of missing precipitation data. *J. Hydrol.* 374, 106–115.
- Thiessen, A.H., 1911. Precipitation averages for large areas. *Mon. Weather Rev.* 39 (7), 1082–1084.
- Velasco-Forero, C.A., Sempere-Torres, D., Cassiraga, E.F., Gómez-Hernández, J.J., 2009. A non-parametric automatic blending methodology to estimate rainfall fields from rain gauge and radar data. *Adv. Water Resour.* 32, 986–1002.
- Verworn, A., Haberlandt, U., 2011. Spatial interpolation of hourly rainfall – effect of additional information, variogram inference and storm properties. *Hydrol. Earth Syst. Sci.* 15, 569–584.
- Voltz, M., Webster, R., 1990. A comparison of kriging, cubic splines and classification for predicting soil properties from sample information. *J. Soil Sci.* 41, 473–490.
- Wackernagel, H., 2003. *Multivariate Geostatistics: An Introduction with Applications*, third ed. Springer, New York.
- Wagner, P.D., Kumar, S., Fiener, P., Schneider, K., 2011. Hydrological modeling with SWAT in a monsoon-driven environment: experience from the Western Ghats, India. *Trans. ASABE* 54 (5), 1783–1790.
- Webster, R., Oliver, M.A., 2007. *Geostatistics for Environmental Scientists*, second ed. John Wiley & Sons Ltd., Chichester.
- Weischet, W., 1995. *Einführung in Die Allgemeine Klimatologie*, sixth ed. Teubner, Stuttgart.
- Winchell, M., Srinivasan, R., Di Luzio, M., Arnold, J., 2010. *ArcSWAT Interface for SWAT2009. User's Guide*. Blackland Research Center, Texas Agricultural Experiment Station and Grassland, Soil and Water Research Laboratory, USDA Agricultural Research Service, Temple, Texas.
- Zhang, X., Srinivasan, R., 2009. GIS-based spatial precipitation estimation: a comparison of geostatistical approaches. *J. Am. Water Resour. Assoc.* 45 (4), 894–906.
- Zhang, X., Srinivasan, R., Debele, B., Hao, F., 2008. Runoff simulation of the headwaters of the Yellow River using the SWAT model with three snowmelt algorithms. *J. Am. Water Resour. Assoc.* 44 (1), 48–61.

## 4 Assessing climate change impacts on the water resources in Pune, India

Journal article (in review)

Authors: Wagner, P.D., Reichenau, T.G., Kumar, S., Schneider, K.

Journal: Regional Environmental Change

Date of submission: 4 October 2012

Citation style according to the standards of the journal Regional  
Environmental Change

## ASSESSING CLIMATE CHANGE IMPACTS ON THE WATER RESOURCES IN PUNE, INDIA

Paul D. Wagner<sup>1</sup>, Tim G. Reichenau<sup>1</sup>, Shamita Kumar<sup>2</sup> and Karl Schneider<sup>1</sup>

<sup>1</sup>Hydrogeography and Climatology Research Group, Institute of Geography, University of Cologne, D-50923 Köln, Germany

<sup>2</sup>Institute of Environment Education & Research, Bharati Vidyapeeth University, Pune 411043, India

### Abstract

*Climate change affects local and regional water resources. Especially in regions with water scarcity, high climate sensitivity, and dynamic socio-economic development, adaptation of water management and mitigation strategies are needed. Our study aims at (i) testing a new downscaling approach to utilize climate model results in a meso-scale hydrologic model, and at (ii) analyzing the impact of climate change on the water balance components in the Mula and Mutha Rivers catchment upstream of the city of Pune, India. The downscaling approach is based on representing a future climate scenario by rearranging historically measured data. We use regional climate model data, which are based on IPCC emission scenario A1B. For every week in the scenario run (2001-2100), the best matching week in terms of temperature and precipitation in a baseline period from 1988 to 2000 was identified. Hence, rearranged meteorological measurements from the baseline period were used as scenario input to the hydrologic model SWAT. We found a good agreement of the monthly statistics of the rearranged and the original measured data in the baseline period. However, the downscaling method is limited by the range of measured values provided in the baseline period. Thus towards the end of the scenario period, climate change impacts are likely to be underestimated. The scenario resulted in higher evapotranspiration, particularly in the first months of the dry season, and in repeated low water storages in the reservoirs at the end of rainy season.*

**KEYWORDS:** SWAT, Climate change, Downscaling, Water resources, Hydrologic modeling, India

## 1. Introduction

Climate change affects the entire natural hydrological system (Arnell 1996) including local and regional water resources. Climate change impacts on water resources are therefore of major concern in current hydrologic research. Especially in regions with scarce water resources, high climate sensitivity, and dynamic socio-economic development, research on developing suitable adaptation and mitigation strategies to balance water supply and demand is needed. While climate projections are typically available at large spatial scales with coarse spatial resolution, decisions on water management are usually made on significantly smaller spatial scales. Thus in order to assess management options, downscaling approaches must be employed to link climate change data with hydrologic models (Fowler et al. 2007).

The fourth assessment report of the Intergovernmental Panel on Climate Change (IPCC 2007) highlights climate change impacts on freshwater resources worldwide and their implications for sustainable development. In many parts of the world, climate change impacts on water resources have been investigated using different hydrologic models (e.g., Arnell and Reynard 1996; Fujihara et al. 2008; Mauser and Bach 2009). The Soil and Water Assessment Tool (SWAT, Arnold et al. 1998) is frequently used for this purpose (Gassman et al. 2007; Liu et al. 2011; Park et al. 2011). In India, Gosain et al. (2006) conducted a study on twelve major Indian river basins. They found a reduction of runoff in general, and in particular an increase of the severity of droughts and floods in different parts of India for a future climate scenario from 2041-60. Another study by Gosain et al. (2011) on the water resources of Indian river systems additionally includes impacts on blue and green water availability for a near term (2021-2050) and a long term scenario (2071-2098). Further studies on individual large scale catchments are available in northern (Akhtar et al. 2008; Singh and Bengtsson 2005) and eastern (Mujumdar and Ghosh 2008) parts of India. However, it is important to analyze climate change impacts on smaller spatial scales, as management decisions are particularly made at these scales. So far, studies on smaller catchments (i.e., meso- or small-scale studies, which are typically smaller than 10000 km<sup>2</sup>; Becker 1992) are very limited in India, e.g., recent studies conducted in West Bengal (Dhar and Mazumdar 2009) and Kerala (Raneesh and Santosh 2011) are available. Furthermore, it is of particular importance to assess water resources in the Western Ghats, as this area is the source of major east flowing river systems such as the Godavari and the Krishna Rivers.

Climate projections are typically provided by global climate models. These calculations serve as an input to regional climate models (RCMs) that produce projections with a finer

spatial resolution. Using outputs of RCMs directly as an input to hydrologic models is not recommended (Wilby et al. 2000) as the RCM data has systematic errors, which should be corrected by applying a bias correction (Fujihara et al. 2008; Teutschbein and Seibert 2010). However, the direct use of bias corrected RCM data is also often not favorable due to its coarse spatial scale ( $0.25^\circ$  grid), which is insufficient to represent spatial precipitation variability. This is particularly true for applications in mountainous catchments with heterogeneous precipitation patterns. In many applications it is therefore preferable to use only the trend of the RCM and apply it to the measured data. This transfer of a trend from a coarser spatial scale (here the RCM) to the smaller catchment scale is referred to as downscaling. Various downscaling approaches are available and their specific assumptions and shortcomings have been investigated by Diaz-Nieto and Wilby (2005) and Fowler et al. (2007). One way to include the RCM trend is to simulate mean temperature and precipitation sums for future weeks based on this trend and substitute the future weeks with historically measured weeks that have the same statistical characteristics (Mauser et al. 2008). A main advantage of this approach is that it provides a consistent weather input that preserves the interdependency of the climate variables, as historically measured data is used and rearranged according to a future scenario. However, a basic assumption of the approach described by Mauser et al. (2008) is a normal distribution of precipitation. This precondition was not met in our data set. Thus the concept was adapted and further developed for use in a monsoon climate region.

Our study aims at (i) evaluating this new downscaling approach and at (ii) assessing impacts of climate change on the water resources in a meso-scale catchment in the Western Ghats, India, by using the derived climate scenario and the hydrologic model SWAT.

## 2. Materials and Methods

### 2.1 Study area

The meso-scale catchment of the Mula and the Mutha Rivers (2036 km<sup>2</sup>) is located in the Western Ghats upstream of the city of Pune, India (18.53° N, 73.85° E; Fig. 1). It is a sub-basin and source area of the Krishna River, which drains towards the east and into the Bay of Bengal. Its elevation ranges from 550 m in Pune up to 1300 m a.s.l. on the top ridges in the Western Ghats. The catchment has a tropical wet and dry climate, which is characterized by seasonal rainfall from June to

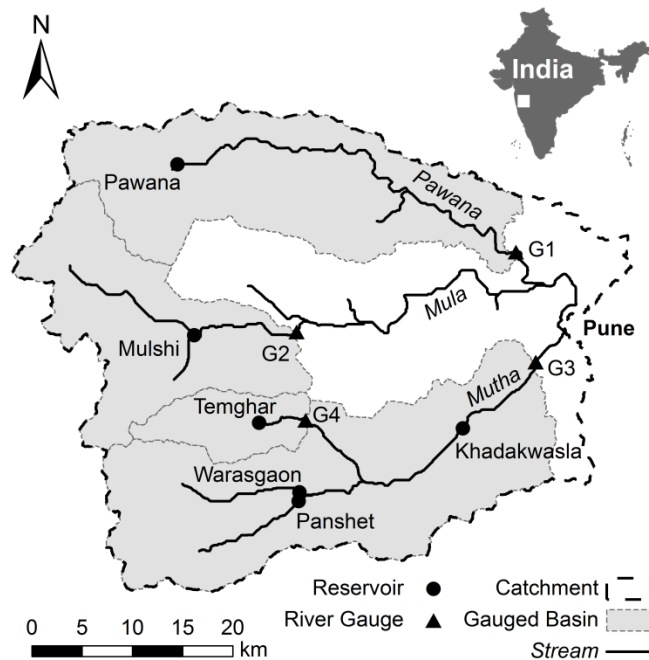


**Fig. 1** Mula-Mutha catchment with the locations of river gauges and reservoirs.

October and low annual temperature variations with an annual mean of 25°C at the catchment outlet in Pune. Annual precipitation amounts decrease from approximately 3500 mm in the western to 750 mm in the eastern part of the catchment (Gadgil 2002; Gunnell 1997). Land use is dominated by semi-natural vegetation, with forests (25%) mainly on the higher elevations in the west, whereas shrubland (26%) and grassland (19%) occupy lower elevations. Agriculturally used land (13%) is found mainly in proximity to rivers and dams (6% of the catchment area is covered by water). Agriculture is dominated by small fields (< 1 ha) with rain-fed agriculture during the monsoon season and irrigation during the dry season. Typically two crops per year are harvested. Urban area (10%) is mainly found in the eastern part of the catchment, where the city of Pune and its surrounding settlements are located (Wagner et al. 2012).

### 2.2 Climate data

#### 2.2.1 Climate change scenario

We used regional climate model data, which were provided by the Institute for Atmospheric and Environmental Sciences at the Goethe-University Frankfurt. The regional climate model COSMO-CLM (<http://www.clm-community.eu>; Rockel et al. 2008; Steppeler et al. 2003; e.g., Asharaf et al. 2012) was driven by the coupled global ocean-atmosphere

model ECHAM5/MPIOM (Jungclaus et al. 2006; Roeckner et al. 2003). Dobler and Ahrens (2010) have shown that ECHAM5/MPIOM driven COSMO-CLM simulations are suitable to represent the Indian summer monsoon as they provide improved spatial precipitation patterns. A baseline run for the 20<sup>th</sup> century control period from 1960 to 2000 and a projection run from 2001 to 2100 applying IPCC emission scenario A1B were available to this study. The A1B scenario assumes a future world of very rapid economic growth, a population growth that reaches its peak in 2050 and declines thereafter, as well as a rapid introduction of new and more efficient technologies. The development is based on a balanced mix of energy sources (Nakićenović et al. 2000). Temperature and precipitation data were provided at a spatial resolution of 0.25°. The six grid cells between 73.25° - 74.0° E and 18.25° - 18.75° N, which covered the whole Mula-Mutha catchment, were used as input data to our downscaling approach.

### **2.2.2 Measured climate data**

The full data set of measured maximum and minimum temperature, humidity, solar radiation, and wind speed data was only available at the IMD weather station in Pune (ID 430630, 18.53° N, 73.85° E, 559 m a.s.l.). Missing values were filled. To account for temperature differences in the catchment, temperature values were adjusted using adiabatic temperature gradients. The spatially distributed temperature records and the specific humidity measured at the weather station in Pune were employed to calculate spatially distributed relative humidity (Wagner et al. 2011). Precipitation data was available from 16 gauges within or near the study area. A thorough analysis of the data and of different interpolation schemes was carried out. Regression kriging using satellite data of the Tropical Rainfall Measuring Mission (TRMM) was found to be a suitable approach and hence used in this study to interpolate precipitation to a 1 km<sup>2</sup> grid (Wagner et al. 2012). Measured data was available from 1988 to 2008. Hence, RCM control run and measured data can be compared for a 13 year period from 1988 to 2000. In the following this period is referred to as the baseline period.

### **2.2.3 Downscaling approach**

The downscaling approach is based on the assumption that future climate can be represented by rearranging historically measured data. Rearranging historically measured data provides a consistent meteorological input, addresses the expected systematic future changes of temperature and precipitation, and avoids the errors arising from a direct use of RCM data. To yield a climate scenario based upon rearranging historical measurements, the following

approach is used: For each week of the scenario period (2020 to 2099), the most similar week is identified within the baseline period (1988 to 2000) using the RCM data for temperature and precipitation. Hence, the scenario is represented by rearranged baseline weeks. For these rearranged baseline weeks, the respective measured meteorological data are used, thus providing a consistent meteorological scenario input for the hydrologic model.

The approach is based upon the assumption, that (i) the RCM provides a consistent representation of temperature and precipitation in the baseline period and the scenario period, (ii) the future climate can be represented sufficiently well by rearranging historically measured data, (iii) by using the rearranged measured meteorological variables instead of RCM model results, the existing discrepancies between RCM data and measured meteorological variables can be accounted for appropriately.

Identification of the most similar week in the baseline period is achieved in two steps: (i) a bias correction is applied to the RCM data to account for systematic differences between the RCM data and the measured data, and (ii) a similarity index was developed that links scenario to baseline weeks.

- (i) Bias correction: Mean differences between RCM and measurements were assessed for all 52 weeks in the year for the baseline period from 1988 to 2000. For precipitation, the interpolated catchment average was compared to the mean value of the corresponding six grid cells. Temperature differences were assessed using the measured data for Pune and the corresponding grid cell of the RCM. The mean annual course of RCM temperature and precipitation differs significantly from the measured data (Fig. 2). To account for these systematic differences, the weekly differences were used to calculate a bias correction factor for precipitation ( $P_{Cor}$ ) and a temperature offset ( $T_{Cor}$ ) for each of the 52 weeks. The precipitation correction was only applied if mean daily precipitation for the week in the RCM was equal to or exceeded 1 mm per day. Thus, the precipitation correction factor is calculated as:

$$P_{Cor}(w_i) = \begin{cases} 1 & , \overline{P_{RCM}}(w_i) < 1 \text{ mm} \\ \frac{\overline{P_{Mes}}(w_i)}{\overline{P_{RCM}}(w_i)} & , \overline{P_{RCM}}(w_i) \geq 1 \text{ mm} \end{cases} , \quad (1)$$

where  $\overline{P_{Mes}}$  is the mean measured precipitation and  $\overline{P_{RCM}}$  is the mean precipitation for the respective week  $w_i$  in the RCM.

The temperature offset is defined as:

$$T_{Cor}(w_i) = \overline{T_{Mes}}(w_i) - \overline{T_{RCM}}(w_i), \quad (2)$$

where  $\overline{T_{Mes}}$  is the mean measured temperature and  $\overline{T_{RCM}}$  is the mean temperature for the respective week  $w_i$  in the RCM.

By applying this bias correction (also referred to as scaling approach; Teutschbein and Seibert 2010) to the entire RCM data, the mean annual course of temperature and precipitation in the RCM is adjusted to meet the mean annual course of the measured data in the baseline period. This approach is based on the assumption that the correction factors will not change in the scenario period.

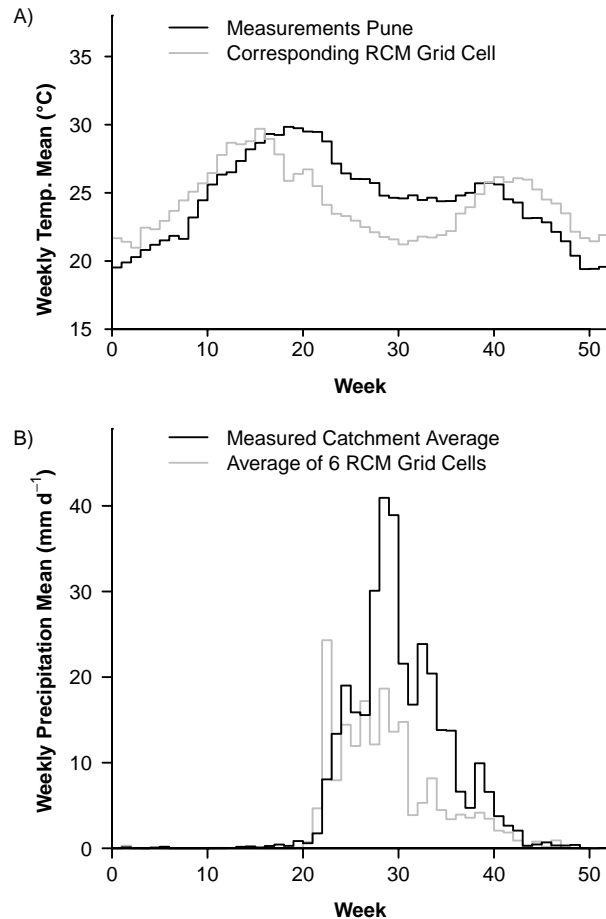


**Fig. 2** Comparison of A) temperature and B) precipitation in regional climate model (RCM) and measurements based on mean weekly average values for the period 1988-2000.

- (ii) Similarity index: For every week in the scenario period, the baseline period was searched for the best matching week in terms of temperature and precipitation. In this context, a week is simply defined as a period of seven consecutive days. Since the start day of the week is arbitrary, seven representations are possible. However, all start days yield statistically similar representations. Thus, we chose the first day of the respective period as the start day of the week.

Two criteria were used to identify the best match: (1) similarity of the precipitation amount, which was expressed by the rule that the precipitation sum of the baseline week should deviate less than 10% from the precipitation sum of the scenario

week, and (2) similarity of the temporal course of the daily temperature and precipitation values as well as similarity of the spatial distribution of the variables using the six grid cells. The similarity analysis was conducted for each week of the scenario period. The similarity index was calculated based on the RCM data comparing the scenario week to each week of the baseline period. Once the best matching week in the baseline period was identified, the measured data for this week was used as input to the hydrologic model.

Criterion (1) was chosen to preserve precipitation sums, which is important as the scenario data serves as an input for a hydrologic modeling study. In some cases, the first criterion cannot be met: In 99.6% of these cases, the absolute deviation is below 0.1 mm per week. In the other cases (0.4%), large precipitation amounts in the scenario period are not met by similar precipitation amounts in the baseline period. In these cases, the criterion is relaxed in steps of 10% to allow higher deviations of 20-50% until a suitable candidate is found.

For criterion (2), a similarity index was developed that takes temperature as well as precipitation similarity into account. To balance the contribution of both variables for the selection of the best matching week, we scaled the difference of the variables in the baseline and the scenario period to the variance of the respective variable as follows:

$$zx = \sqrt{\frac{1}{ij} \sum_{i=1}^7 \sum_{j=1}^6 \frac{(xb_{ij} - xs_{ij})^2}{\sigma_{xs}^2}} \quad (3)$$

With:  $xb_{ij}$  = meteorological variable  $x$  in the baseline week on day  $i$  at cell  $j$   
 $xs_{ij}$  = meteorological variable  $x$  in the scenario week on day  $i$  at cell  $j$   
 $\sigma_{xs}^2$  = variance of meteorological variable  $x$  based on values of all days  $i$  at each cell  $j$  in the respective week of the scenario period

This standardized  $zx$  value is calculated for every week in the baseline period, indicating the goodness-of-fit of each week in the baseline period to the week of interest in the scenario period. The minimum of the  $zx$  values indicates the best fit using only one variable. By squaring and adding these  $zx$  values for temperature ( $zT$ ) and precipitation ( $zP$ ), an indicator  $I_z$  is derived for each baseline week:

$$I_Z = (zT)^2 + (zP)^2. \quad (4)$$

The minimum value of  $I_Z$  indicates, which baseline week best fits the daily course and spatial distribution in both variables for the respective scenario week. In case of a dry week (defined as below 0.1 mm summed weekly precipitation for the six grid cells) the precipitation value  $zP$  was set to 0 and the selection of the best fitting baseline week was restricted to dry weeks and is therefore solely based on temperature, i.e., on  $zT$ .

Although, the mean courses of temperature and precipitation of the RCM were adjusted by applying a bias correction, weekly correlations between RCM and measurements were sometimes very weak. Thus, the selectable baseline weeks were filtered, applying the following consistency criteria:

- (i) Consistency of the season: We distinguished three seasons: (a) rainy season (June-September), (b) core dry season (November-May) and (c) transition season (October). A rainy season week (June-September) in the scenario period can only be represented by a rainy or transition season week in the baseline period. The same applies for dry season weeks, which are to be represented only by dry and transition season weeks. October is a special case because in some years, late monsoon rainfall still affects October weather. Thus, October is assumed to be a transition month and scenario weeks in the month of October may be represented by baseline season weeks of the dry season as well as June or September weeks. The method provides suitable flexibility to account for possible temporal shifts of the onset of the monsoon period (Lal et al. 2001).
- (ii) Consistency of RCM and measured data: A wet week in the scenario period can only be represented by a week in the baseline period that shows precipitation amounts in the RCM as well as in the measurements. The same applies for dry weeks respectively.

### 2.2.4 Validation of the downscaling approach

In order to validate the downscaling approach, we applied this approach to the baseline period. For each week in the baseline period, the baseline was searched for the most similar week, excluding weeks that overlapped with the week under consideration. Thus for validation of the method, the variables in equation 3 were adjusted to:

$$zx = \sqrt{\frac{1}{ij} \sum_{i=1}^7 \sum_{j=1}^6 \frac{(xb_{ij} - xv_{ij})^2}{\sigma_{xv}^2}} \quad (5)$$

With:  $xb_{ij}$  = meteorological variable  $x$  in the baseline week on day  $i$  at cell  $j$ , excluding weeks that overlapped with week  $v$   
 $xv_{ij}$  = meteorological variable  $x$  in the baseline period week  $v$  on day  $i$  at cell  $j$   
 $\sigma_{xv}^2$  = variance of meteorological variable  $x$  based on values of all days  $i$  at each cell  $j$  in respective week  $v$

Using the RCM model results for the baseline period for each week, the baseline period was searched for the best matching week by applying the previously defined rules (see 2.2.3). The validation of the method is successful, if this approach yields a statistically equivalent representation of the rearranged data set with respect to the original data set. The approach was evaluated in two steps: (i) by using RCM data only, and (ii) by using measured data. The first step provides evidence for the accuracy of the applied similarity indicator  $I_z$  (formula 4), whereas the second step provides a validation of the entire downscaling method.

### 2.3 Hydrologic model

In this study, the Soil and Water Assessment Tool (SWAT, Arnold et al. 1998) was used to assess the impact of climate change on water resources. In previous studies, we showed the suitability of SWAT to model the water fluxes in the Mula-Mutha catchment (Wagner et al. 2011; Wagner et al. 2012). Since details of the model setup and parameterization are available in the published previous studies, we will only present a brief summary of data inputs and model parameterization.

A digital elevation model (DEM) with a spatial resolution of 30 m was derived from ASTER satellite data. The spatial distribution of soils was taken from the digital Soil Map of the World (FAO 2003). Soil parameterization was partly adapted from a modeling study of the region by Immerzeel et al. (2008), and partly taken from the FAO (2003) database. The

land use map was derived from two satellite images taken in 2009 and 2010 by LISS-III on the Indian satellite IRS-P6. Applying a stratified knowledge-based approach, using a maximum likelihood classifier (Wagner et al. 2011), two land use classifications were produced and merged to derive a multitemporal land use classification. Crop rotations as well as irrigation schemes were set up for arable land (rice 7.5%, sugarcane 1.3%, mixed cropland 4.6% of the catchment area) to account for the two main cropping seasons in the region. For the six major dams in the catchment, a management scheme was developed, which is based on general management rules allowing for water storage in the rainy season and water release in the dry season (Wagner et al. 2011; Wagner et al. 2012).

The catchment model uses 25 sub-basins with 917 hydrological response units. SWAT model parameters were either a) estimated from readily available GIS databases, or b) were chosen from the literature for the given site condition, or c) default model parameters were used. A site specific calibration of the model parameters based upon minimizing the difference between measured and modeled runoff was not performed. Thus, the model is not tuned to the current climatic conditions (Kirchner 2006) in order to avoid a bias in performance under climate change conditions. Details of the model parameterization as well as the suitability of the model and its parameterization are given in Wagner et al. (2012). In the present study, the model showed good performance at the river gauges G1 and G4 (Fig. 1) judged by Nash-Sutcliffe efficiency (NSE, Nash and Sutcliffe 1970; G1: 0.68, G4: 0.67) and percentage bias (G1: +4%, G4: +24%), using the available daily discharge data during rainy seasons between 2001 and 2007. Model performance in the highly managed sub-catchments G2 and G3 depends strongly on dam management.

The model was run from 1988 to 2008 with measured data, and from 2009 to 2099 using the downscaled scenario data. Analysis of water resources was carried out using a 20-year baseline (1989-2008) and four 20-year scenario periods (2020-39, 2040-59, 2060-79, and 2080-99).

### 3. Results and Discussion

#### 3.1 Validation of the downscaling approach

In order to validate the downscaling approach, it was applied to the baseline period. By this means, a rearranged meteorological data set for the baseline period was derived. This data set was evaluated in two steps: a) by comparing original and rearranged RCM data, and b) by comparing original and rearranged measured data (see 2.4.4).

a) By comparing the statistical properties of original and rearranged RCM data, the quality of the derived similarity indicator  $I_Z$  was evaluated. Mean monthly values of the derived rearranged and the original baseline RCM data averaged over the six grid cells are shown in Figure 3. The statistical properties of temperature and precipitation are represented very accurately on a monthly basis. Deviations between the monthly mean of the rearranged temperatures and the monthly mean of the original data are smaller than  $0.5^\circ\text{C}$ . Similarly, the differences between the monthly standard deviation of the rearranged and the original RCM data are small ( $< 0.3^\circ\text{C}$ ). The monthly specific root mean square error (RMSE) that was calculated for each month by comparing the original to the rearranged mean values of this month in all 13 baseline years is below  $1^\circ\text{C}$  (Fig. 3A).

Figure 3B shows that differences in mean monthly precipitation are very small ( $< 0.2 \text{ mm d}^{-1}$ ). Standard deviations in August are underestimated by up to  $9.7 \text{ mm d}^{-1}$ . In all other months differences in standard deviation do not exceed  $3.5 \text{ mm d}^{-1}$ . The RMSE of

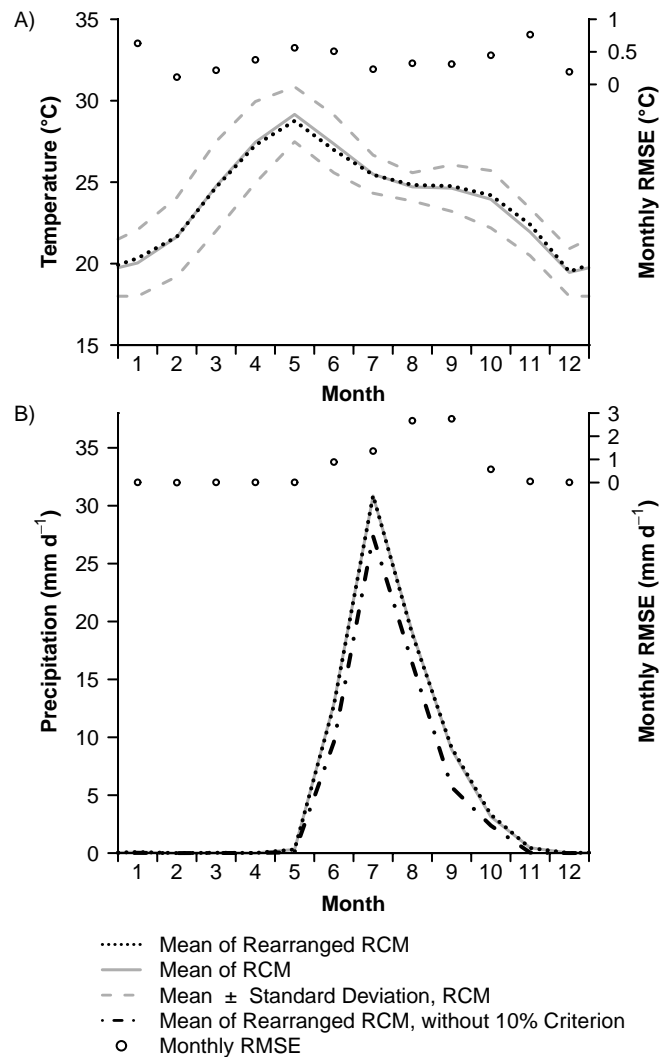


**Fig. 3** Comparison of statistical properties of original and rearranged bias corrected RCM data for A) temperature and B) precipitation in the baseline period 1988-2000. The root mean square error (RMSE) indicates the deviation of the mean monthly values in the baseline period for each month.

Figure 3B shows that differences in mean monthly precipitation are very small ( $< 0.2 \text{ mm d}^{-1}$ ). Standard deviations in August are underestimated by up to  $9.7 \text{ mm d}^{-1}$ . In all other months differences in standard deviation do not exceed  $3.5 \text{ mm d}^{-1}$ . The RMSE of

monthly precipitation means (Fig. 3B) indicates highest deviations from the original data set in August ( $2.7 \text{ mm d}^{-1}$ ) and September ( $2.8 \text{ mm d}^{-1}$ ). Additionally, Figure 3B shows that the 10% criterion, which requires that precipitation sums of similar weeks should not deviate by more than 10%, clearly leads to an improvement of the results. The good fit of rearranged and original monthly data indicates that the developed similarity indicator  $I_Z$  is suitable to identify the best matching weeks.

b) In the next step, we investigated, if the rearrangement of measured data yields a similar climatology when compared to the originally measured data in the baseline period. The measured mean annual course of minimum and maximum temperature in Pune is shown in Figure 4 along with the results of the rearranged measured data. The monthly temperature course matches very well. In May a slight underestimation is obvious. The deviations of the monthly means of rearranged and original measured data are smaller than one standard deviation in all months (maximum deviation  $1.2^\circ\text{C}$  in May). Similarly, the standard deviations are in agreement with the original data set (Fig. 4A).

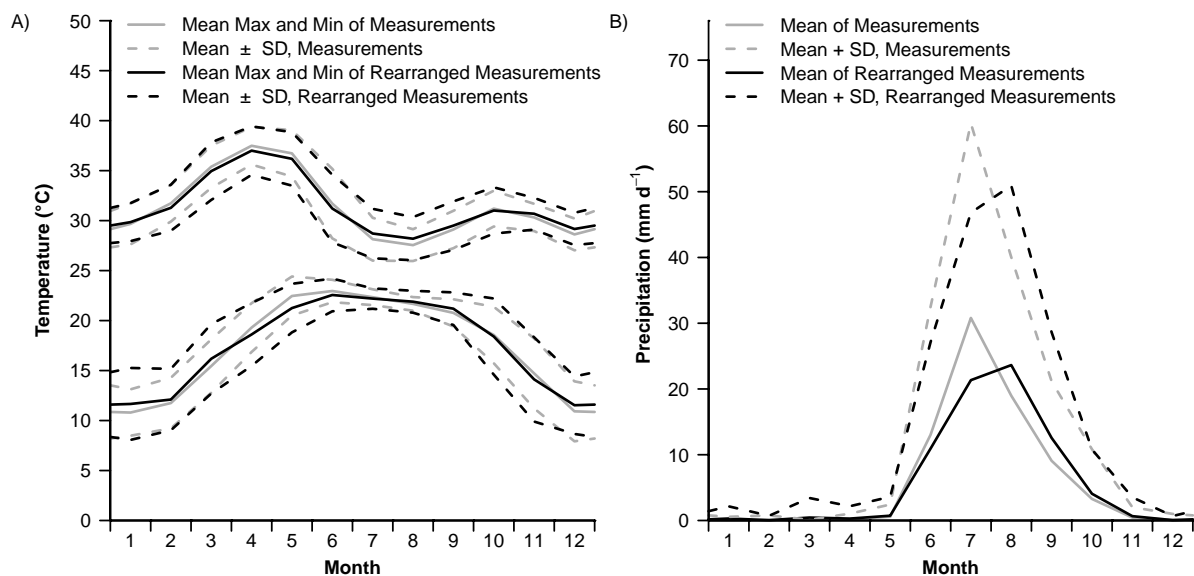


**Fig. 4** Comparison of original and rearranged measured data for A) maximum and minimum temperature and B) precipitation using mean monthly values and standard deviations (SD) of the baseline period 1988-2000.

A mean precipitation value for the catchment derived from interpolated measured data was used to evaluate the performance of the approach with regard to precipitation. As the interpolated data is used in the impact study, it is favorable to use the catchment average for evaluation. Evaluation based on single rain gauges might be misleading as they cannot represent the entire study area. As can be expected from the differences between RCM and measured data (see Fig. 2B), the mean monthly course of measured precipitation data cannot

be reproduced as accurately as temperature data. The rearranged data show a less pronounced annual course of the precipitation regime as compared to the measured regime. The peak precipitation amounts in July are underestimated, whereas slight under- (June) and overestimations (August, September) can be observed in the other rainy season months. Deviations from the measured data range from  $2.1 \text{ mm d}^{-1}$  to  $9.5 \text{ mm d}^{-1}$  during rainy season. However, with the exception of March (deviation  $0.4 \text{ mm d}^{-1}$ , standard deviation  $0.1 \text{ mm d}^{-1}$ ), the mean monthly course of the rearranged measured data is within one standard deviation of the originally measured precipitation. The standard deviation of the rearranged data shows a similar course as the measured standard deviation. Larger differences can be observed in June, July, August and September (Fig. 4).

In addition to the general agreement of the mean annual course of the climate variables, we evaluated the representation of the monthly course of temperature and precipitation for the baseline period. Mean monthly maximum and minimum temperatures in Pune are well reproduced (NSE of 0.83 and 0.87, respectively), whereas lower performance is achieved in reproducing the monthly precipitation course (NSE of 0.43). This is mainly due to (i) the differences between RCM and measurements (NSE of 0.34 for monthly precipitation) and (ii) the higher variation in precipitation. Furthermore, the number of wet weeks is significantly smaller than the number of dry weeks. Thus, it is less likely to achieve a good match in the rainy season.

### ***3.2 Evaluation of the downscaled scenario***

The climate scenario indicates a temperature increase of  $0.51^\circ\text{C}$  per decade between 2020 and 2099. For precipitation, no significant trend was found in the scenario. Thus we expect that the number of similar weeks in the baseline period with comparable temperatures decreases with increasing future temperatures. To analyze the expected increasing mismatch of the weather in the scenario and in the baseline period, temperature and precipitation values of the rearranged RCM scenario data were compared to the respective original values from the RCM.

Figure 5A illustrates that temperatures in the scenario period exceed the range of values found in the baseline period. Obviously, these high temperatures can particularly be found in the two last periods of 2060-79 and 2080-99. Looking at the match of mean weekly values of original and rearranged RCM temperatures in the four 20-year scenario periods, it becomes obvious, that a relatively good match is derived for the early 2020-39 period ( $R^2=0.94$ ). This correlation decreases in the later 20-year periods ( $R^2$  values: 2040-59: 0.91, 2060-79: 0.89,

2080-99: 0.82). Precipitation in the scenario period does not exceed the measured range. Thus, generally a good match between the rearranged bias corrected RCM precipitation data of the baseline period and the bias corrected RCM data of the scenario period is achieved (Fig. 5B).

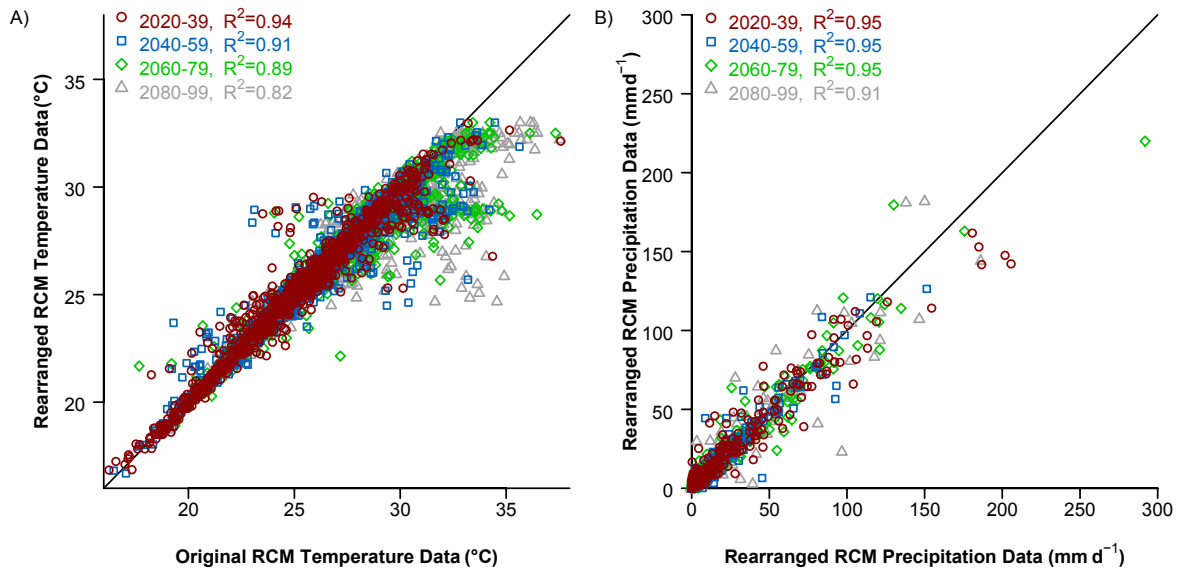


**Fig. 5** Comparison of the rearranged and the original data using mean weekly values of bias corrected RCM temperature (A) and precipitation (B) data for the scenario period.

The rearranged measured data provides the meteorological input for the hydrologic model for the scenario period. In addition to an agreeable representation of statistical characteristics, which was shown for the baseline period in section 3.1, the rearranged data for the scenario period should also reproduce the major trends of the RCM data. The rearranged data for the scenario period can be characterized by the mean monthly temperature course of the climate station in Pune (Fig. 6) and the mean monthly catchment precipitation (Fig. 7). Figure 6 shows that the mean monthly maximum and minimum temperatures increase by  $0.34^{\circ}\text{C}$  and  $0.25^{\circ}\text{C}$  per decade, respectively. As the mean monthly minimum temperatures do not exceed  $24^{\circ}\text{C}$ , the temperature range and the ability to represent the increasing scenario temperatures is limited. In order to evaluate whether the temperature trend of the RCM is adequately represented by the downscaled scenario, monthly values of the rearranged measured data were compared to the bias corrected RCM data (Fig. 8). In all 20-year periods, high RCM temperatures were underestimated by the rearranged measured data. However, coefficient of determination, offset, and slope of linear regressions for each 20-year period indicate a reasonable representation of the first three scenario periods. The quality of the representation decreases from the earlier scenario periods to the later scenario periods (Fig. 8). In the last period, a stronger underestimation of the RCM temperatures by the rearranged scenario

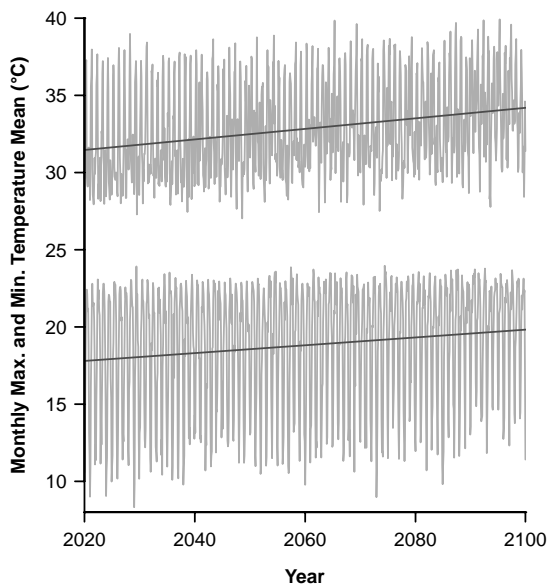


**Fig. 6** Development of maximum and minimum temperatures in the scenario period using rearranged measured data. Mean monthly values shown in grey; linear regression line shown in black.

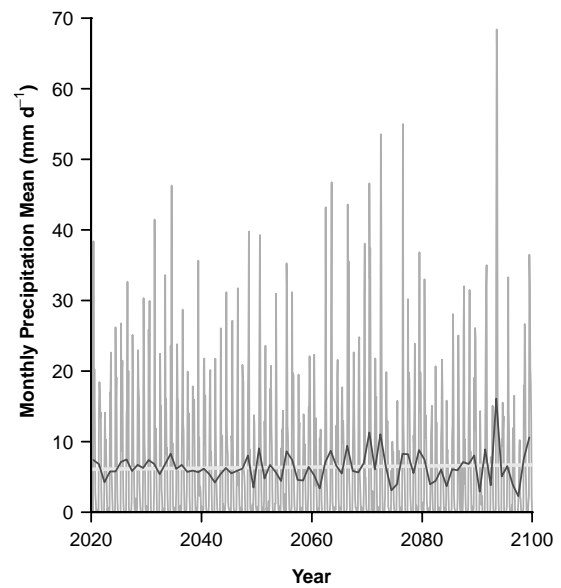


**Fig. 7** Mean monthly precipitation in the scenario period using rearranged measured data. Mean daily precipitation per month shown in grey; linear regression line shown in light grey; annual average shown in black.

representation is obvious. Hence, the temperature trend in the rearranged data set is reduced as compared to the trend in the RCM data. When discussing impacts of climate change on the water resources, this underestimation should be taken into account.

Similar to the RCM precipitation data, the precipitation data of the scenario representation does not show a trend (Fig. 7). The inter-annual variability of precipitation slightly increases towards the end of the scenario (black line in Fig. 7).

### 3.3 Climate change impacts

Analysis of the catchment's mean annual water balance components for the four scenario periods indicates similar precipitation amounts (2184-2520 mm) compared to the baseline period (2420 mm). Extremely dry years (< 1757 mm, 10% quantile of the baseline period) are

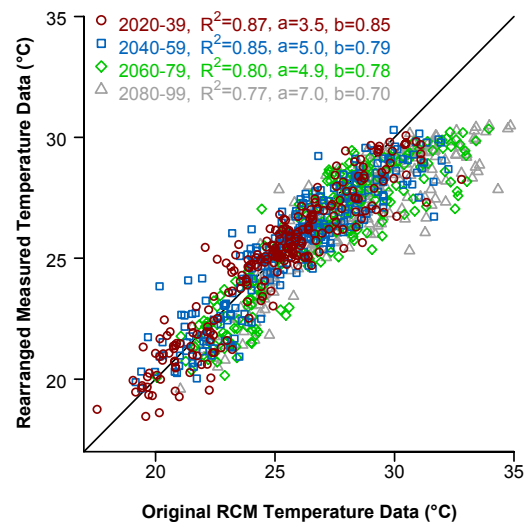


**Fig. 8** Comparison of rearranged measured temperature and bias corrected RCM data for the scenario period using mean monthly values.  $R^2$ , offset (a), and slope (b) shown for linear regressions for each 20-year period.

less common in 2020-39 ( $n=1$ ) and more common in 2060-79 ( $n=3$ ) as compared to the baseline period. Significantly more dry years occur in 2040-59 ( $n=5$ ) and 2080-89 ( $n=7$ ). It has to be noted that one third of the dry years between 2040 and 2099 are significantly drier (833-1292 mm) than the driest year in the baseline (1617 mm). Extremely wet years ( $> 3367$  mm, 90% quantile of the baseline period) are more common between 2060 and 2079 ( $n=3$ ). They occur as often as in the baseline in 2080-99, and do not occur in 2020-39 and 2040-59. The year with maximum precipitation in the last scenario period has also significantly more precipitation (5932 mm) as compared to the maximum annual precipitation of 3895 mm in the baseline period.

The combined impact of the scenario on the water resources in the catchment is illustrated by the storage of the four largest dams in the catchment at the end of monsoon season (Fig. 9). In the period from 1989 to 2008, mean annual precipitation usually allows the dams to be filled up to maximum storage capacity at the end of October. Dry years (e.g., 2000) lead to a reduced storage of 10-30%. Due to water abstraction for power generation, the storage of Mulshi dam is more variable as compared to the other dams. From 2040 onwards, the planned storage capacity of the dams is frequently not met. In the last 20 year period (2080-99), low dam storages between 20-60% occur regularly at the end of the monsoon period. A severely

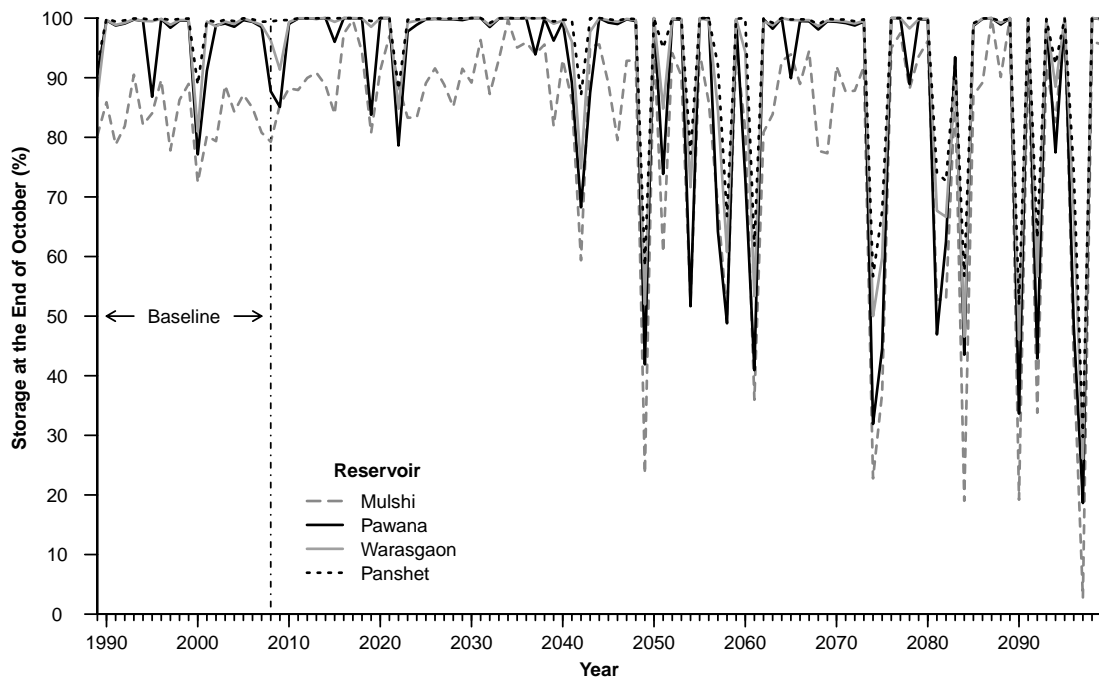


**Fig. 9** Storage of the four largest dams in the catchment at the end of monsoon season in baseline and scenario period.

dry year at the end of the scenario run could decrease the storage in Mulshi dam to almost zero, if the current water management is maintained. Taking into account that the dam storage in October defines water availability throughout the following dry season, the scenario results indicate increasing difficulties in meeting agricultural, industrial, and municipal water demands towards the end of the century.

Annual runoff amounts closely follow the precipitation amounts, because the catchment's response to precipitation is very fast. The runoff coefficient (runoff/precipitation) gives the fraction of precipitation that appears as runoff, and is thus a measure of the runoff that is independent of changes in precipitation. A slightly decreasing trend can be observed for the runoff coefficient (Fig. 10). This is in agreement with a slightly increasing annual evapotranspiration, which is also shown in Figure 10. Thus, increased temperatures lead to slightly more evapotranspiration and less runoff. However, the effect is not very pronounced on the catchment scale, as the main part of precipitation appears as direct runoff, thus reducing the amount of water that is available for evapotranspiration. As the applied downscaling approach underestimates high temperatures, the climate change effect on evapotranspiration might be underestimated, particularly in the last decades of the scenario period.

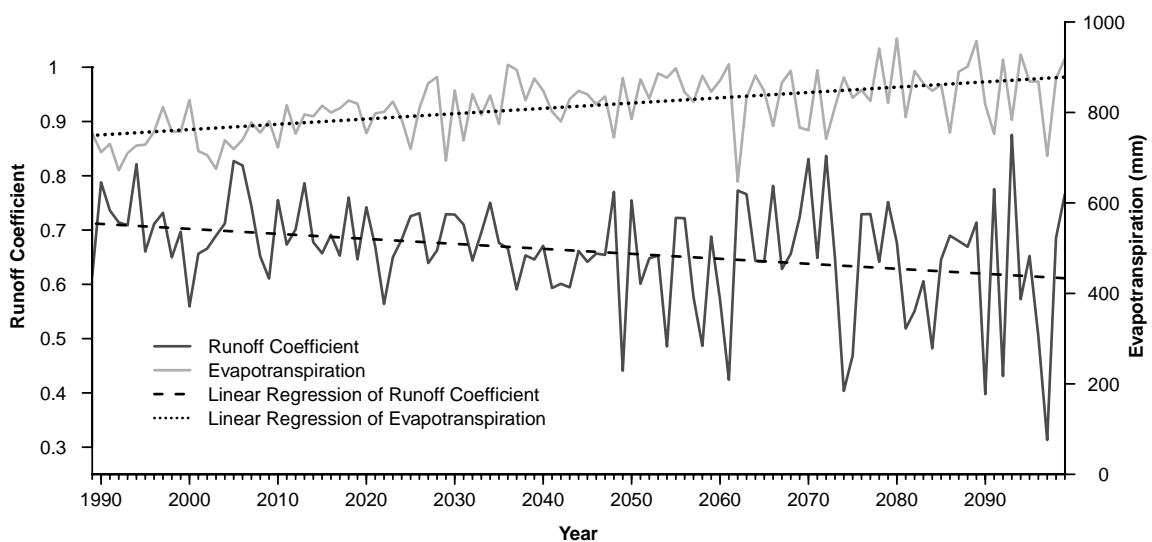


**Fig. 10** Annual runoff coefficient and evapotranspiration from 1989 to 2099.

Similar to the annual time scale, runoff closely follows the changes in precipitation on the monthly time scale, whereas evapotranspiration (ET) is driven by increasing temperatures and limited by water availability. From July to November, monthly ET in the scenario period is generally higher than in the baseline period (6-42%) and increases towards the end of the

century (Fig. 11). In January and February a different pattern can be observed: In the first scenario period (2020-39) ET is 31-71% higher than in the baseline period, but decreases in all future periods until ET is about the same level as in the baseline period in 2080-99 (absolute difference < 3 mm). The higher temperatures in the later scenario periods lead to an increased potential ET. As long as water availability is sufficient, the increased potential ET results in higher actual ET in the first dry season months. However, the water availability decreases more rapidly after the end of the rainy season. Consequently, the effect of increased temperatures on actual ET is limited in January and February, as the higher ET rates of the previous month result in decreased water availability. As there is no trend in precipitation, the total annual water availability remains the same and annual ET is only slightly increased. However, the intra-annual course of ET is changed. For the hottest period, 2080-99, this effect is very obvious, as ET is 14-42% higher between July and December compared to the baseline period, but no pronounced differences can be observed in the following month January-March. ET amounts in April, May, and June show a slight decrease for some scenario periods, but due to the rather small absolute changes (2-11 mm) this is only a slight indication.

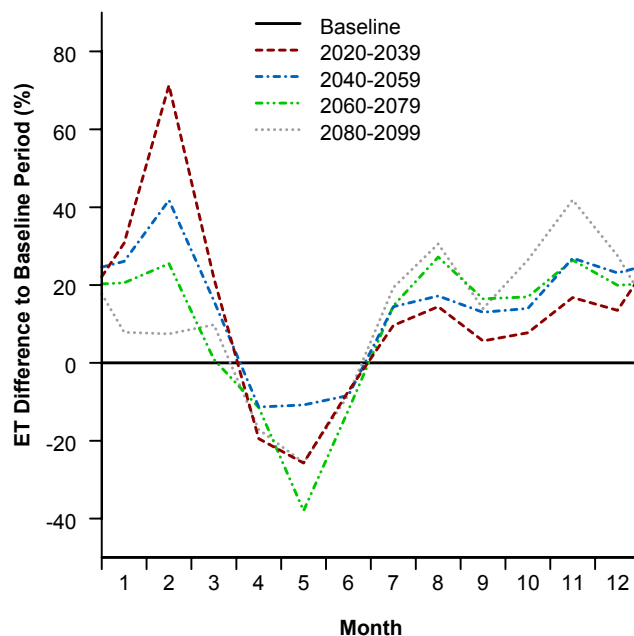


**Fig. 11** Average percentage change of monthly evapotranspiration (ET) sums for 20-year scenario periods in comparison to the 20-year baseline period.

## 4. Conclusions

The developed downscaling approach produced consistent future weather data suitable for hydrologic impact studies. The approach does not require that the meteorological variables meet any specific statistical preconditions (e.g., normal distribution). However, it is limited to the measured temperature and precipitation range of the baseline period, thus limiting its applicability to the near future, when temperature increases are moderate. In this study, we found that this limitation applies particularly to the last 20-year period of the scenario from 2080 to 2099. It is expected that the approach will yield a better performance, if measurements for a longer baseline period are available or if a closer match between RCM and measurements exists.

Dry years in the scenario period are more frequent and drier as compared to the years in the baseline period. Consequently the storage capacity of the large reservoirs in the catchment is frequently not achieved. Low water storage levels at the beginning of the dry season have severe consequences for different water users. First, the drinking water supply for the city of Pune is affected. As the city experiences rapid growth and development, it is expected that the water demand will increase, which will exacerbate the imbalance of demand and supply in the future. Second, implications on energy production can be expected, posing a problem to the megacity Mumbai, which obtains energy from the hydropower plant at the largest reservoir in the catchment (Mulshi). Third, agriculture is affected, as it heavily relies on irrigation during dry season. Although only 13% of the catchment is agricultural area, and only 1.3% are cultivated during summer season, large sugarcane cultivations downstream of Pune rely on the catchment's water resources. The year-round cultivation of sugarcane poses an additional challenge, as increased future temperatures will lead to an increase of irrigation water demand in April and May. Hence, if this cultivation is to be continued, more efficient irrigation techniques need to be employed.

The increasing future temperatures will result in higher actual evapotranspiration, even though this effect is not as pronounced as might be expected from the increase of potential evapotranspiration, since actual evapotranspiration is limited by water availability, which remains virtually unchanged as a clear trend in future precipitation is not discernible. However, the intra-annual course of actual evapotranspiration in the scenario periods indicates an earlier decrease of water availability in the dry season, which may affect rainfed agriculture as well as semi-natural vegetation.

### ***Acknowledgements***

We gratefully acknowledge support by a grant from the German National Academic Foundation. We would like to thank Bodo Ahrens and Shakeel Asharaf of the Institute for Atmospheric and Environmental Sciences at the Goethe-University Frankfurt for providing the regional climate model data. We are grateful to IMD Pune, Water Resources Department Nashik, Khadakwasla Irrigation Division Pune, Groundwater Department Pune, Department of Agriculture Pune, and NRSC Hyderabad for supplying environmental data, good cooperation and discussions. Moreover, we acknowledge supply of ASTER data by the USGS Land Processes Distributed Active Archive Center. Special thanks go to Karen Schneider for proofreading the manuscript and to the students from the Institute of Environment Education & Research at Bharati Vidyapeeth University Pune for assistance with the field measurements.

### **References**

- Akhtar M, Ahmad N, Booij MJ (2008) The impact of climate change on the water resources of Hindukush-Karakorum-Himalaya region under different glacier coverage scenarios. *J Hydrol* 355 (1-4):148-163
- Arnell NW (1996) *Global warming, river flows and water resources*. John Wiley & Sons, New York
- Arnell NW, Reynard NS (1996) The effects of climate change due to global warming on river flows in Great Britain. *J Hydrol* 183:397-424
- Arnold JG, Srinivasan R, Muttiah RS, Williams JR (1998) Large area hydrologic modeling and assessment - Part 1: Model development. *J Am Water Resour Assoc* 34:73-89
- Asharaf S, Dobler A, Ahrens B (2012) Soil moisture-precipitation feedback processes in the Indian summer monsoon season. *J Hydrometeorol*: in press
- Becker A (1992) Methodische Aspekte der Regionalisierung. In: Kleeberg H-B (ed) *Regionalisierung in der Hydrologie*. VCH, Deutsche Forschungsgemeinschaft, Weinheim, Germany, pp 16-32
- Dhar S, Mazumdar A (2009) Hydrological modelling of the Kangsabati river under changed climate scenario: case study in India. *Hydrol Process* 23:2394-2406

- Diaz-Nieto J, Wilby RL (2005) A comparison of statistical downscaling and climate change factor methods: impacts on low flows in the River Thames, United Kingdom. *Clim Change* 69 (2):245-268
- Dobler A, Ahrens B (2010) Analysis of the Indian summer monsoon system in the regional climate model COSMO-CLM. *J Geophys Res* 115 (D16101):1-12
- Food and Agriculture Organization of the United Nations (FAO) (2003) *Digital Soil Map of the World and Derived Soil Properties*, FAO, Rom
- Fowler HJ, Blenkinsop S, Tebaldi C (2007) Linking climate change modelling to impacts studies: recent advances in downscaling techniques for hydrological modelling. *Int J Climatol* 27:1547-1578
- Fujihara Y, Tanaka K, Watanabe T, Nagano T, Kojiri T (2008) Assessing the impacts of climate change on the water resources of the Seyhan River Basin in Turkey: Use of dynamically downscaled data for hydrologic simulations. *J Hydrol* 353 (1-2):33-48
- Gadgil A (2002) Rainfall characteristics of Maharashtra. In: Diddee J, Jog SR, Kale VS, Datye VS (eds) *Geography of Maharashtra*. Rawat Publications, Jaipur, India, pp 89-102
- Gassman PW, Reyes M, Green CH, Arnold JG (2007) The Soil and Water Assessment Tool: Historical development, applications, and future directions. *Trans ASABE* 50 (4):1211-1250
- Gosain AK, Rao S, Arora A (2011) Climate change impact assessment of water resources of India. *Curr Sci* 101 (3):356-371
- Gosain AK, Rao S, Basuray D (2006) Climate change impact assessment on hydrology of Indian river basins. *Curr Sci* 90 (3):346-353
- Gunnell Y (1997) Relief and climate in South Asia: The influence of the Western Ghats on the current climate pattern of peninsular India. *Int J Climatol* 17:1169-1182
- Immerzeel WW, Gaur A, Zwart SJ (2008) Integrating remote sensing and a process-based hydrological model to evaluate water use and productivity in a south Indian catchment. *Agric Water Manage* 95:11-24
- IPCC (2007) *Climate Change 2007: Impacts, Adaptation and Vulnerability*. Contribution of Working Group II to the Fourth Assessment Report of the Intergovernmental Panel on Climate Change. Parry ML, Canziani OF, Palutikof JP, van der Linden PJ, Hanson CE (eds) Cambridge University Press, Cambridge, UK

- Jungclauss JH, Keenlyside N, Botzet M, Haak H, Luo J-J, Latif M, Marotzke J, Mikolajewicz U, Roeckner E (2006) Ocean circulation and tropical variability in the coupled model ECHAM5/MPI-OM. *J Clim* 19 (16):3952-3972
- Kirchner JW (2006) Getting the right answers for the right reasons: Linking measurements, analyses, and models to advance the science of hydrology. *Water Resour Res* 42:W03S04
- Lal M, Nozawa T, Emori S, Harasawa H, Takahashi K, Kimoto M, Abe-Ouchi A, Nakajima T, Takemura T, Numaguti A (2001) Future climate change: Implications for Indian summer monsoon and its variability. *Curr Sci* 81 (9):1196-1207
- Liu L, Liu Z, Ren X, Fischer T, Xu Y (2011) Hydrological impacts of climate change in the Yellow River Basin for the 21st century using hydrological model and statistical downscaling model. *Quat Int* 244 (2):211-220
- Mausser W, Bach H (2009) PROMET – Large scale distributed hydrological modelling to study the impact of climate change on the water flows of mountain watersheds. *J Hydrol* 376 (3-4):362-377
- Mausser W, Marke T, Stoeber S (2008) Climate Change and Water Resources: Scenarios of Low-flow Conditions in the Upper Danube River Basin. *IOP Conf Ser: Earth Environ Sci* 4 (012027):1-11
- Mujumdar PP, Ghosh S (2008) Modeling GCM and scenario uncertainty using a possibilistic approach: Application to the Mahanadi River, India. *Water Resour Res* 44:W06407
- Nakićenović N, Alcamo J, Davis G, de Vries B, Fenhann J, Gaffin S, Gregory K, Grübler A, Jung TY, Kram T, La Rovere EL, Michaelis L, Mori S, Morita T, Pepper W, Pitcher H, Price L, Riahi K, Roehrl A, Rogner H-H, Sankovski A, Schlesinger M, Shukla P, Smith S, Swart R, van Rooijen S, Victor N, Dadi Z (2000) Special Report on Emissions Scenarios. A Special Report of Working Group III of the Intergovernmental Panel on Climate Change. Cambridge University Press, Cambridge, UK
- Nash JE, Sutcliffe JV (1970) River flow forecasting through conceptual models: Part I. A discussion of principles. *J Hydrol* 10 (3):282-290
- Park J-Y, Park M-J, Joh H-K, Shin H-J, Kwon H-J, Srinivasan R, Kim S-J (2011) Assessment of MIROC3.2 HiRes Climate and CLUE-s Land Use Change Impacts on Watershed Hydrology Using SWAT. *Trans ASABE* 54 (5):1713-1724
- Raneesh KY, Santosh GT (2011) A study on the impact of climate change on streamflow at the watershed scale in the humid tropics. *Hydrol Sci J*, 56 (6):946-965

- Rockel B, Will A, Hense A (2008) The regional climate model COSMO-CLM (CCLM). *Meteorol Z* 17 (4):347-348
- Roeckner E, Bäuml G, Bonaventura L, Brokopf R, Esch M, Giorgetta M, Hagemann S, Kirchner I, Kornbluh L, Manzini E, Rhodin A, Schlese U, Schulzweida U, Tompkins A (2003) The atmospheric general circulation model ECHAM 5. Part I: Model description. Rep. No. 349. Max Planck Institute for Meteorology, Hamburg, Germany
- Singh P, Bengtsson L (2005) Impact of warmer climate on melt and evaporation for the rainfed, snowfed and glacierfed basins in the Himalayan region. *J Hydrol* 300 (1-4):140-154
- Steppeler J, Dom G, Schattler U, Bitzer HW, Gassmann A, Damrath U, Gregoric G (2003) Meso-gamma scale forecasts using the non-hydrostatic model LM. *Meteorol Atmos Phys* 82:75-96
- Teutschbein C, Seibert J (2010) Regional Climate Models for Hydrological Impact Studies at the Catchment Scale: A Review of Recent Modeling Strategies. *Geogr Compass* 4:834-860
- Wagner PD, Fiener P, Wilken F, Kumar S, Schneider K (2012) Comparison and evaluation of spatial interpolation schemes for daily rainfall in data scarce regions. *J Hydrol* 464-465:388-400
- Wagner PD, Kumar S, Fiener P, Schneider K (2011) Hydrological modeling with SWAT in a monsoon-driven environment – experience from the Western Ghats, India. *Trans ASABE* 54 (5):1783-1790
- Wilby RL, Hay LE, Gutowski Jr. WJ, Arritt RW, Takle ES, Pan Z, Leavesley GH, Clark MP (2000) Hydrological responses to dynamically and statistically downscaled climate model output. *Geophys Res Lett* 27 (8):1199-1202



## 5 Assessing past land use change and its impacts on the water resources in Pune, India

Journal article (to be submitted)

Authors: Wagner, P.D., Kumar, S., Schneider, K.

## ASSESSING PAST LAND USE CHANGE AND ITS IMPACTS ON THE WATER RESOURCES IN PUNE, INDIA

Paul D. Wagner<sup>1</sup>, Shamita Kumar<sup>2</sup> and Karl Schneider<sup>1</sup>

<sup>1</sup>Hydrogeography and Climatology Research Group, Institute of Geography, University of Cologne, D-50923 Köln, Germany

<sup>2</sup>Institute of Environment Education & Research, Bharati Vidyapeeth University, Pune 411043, India

### Abstract

*Land use changes are altering the hydrologic system and have potentially large impacts on water resources. Rapid socio-economic development drives land use transition. This is particularly true in the case of the rapidly developing city of Pune, India. The present study aims at analyzing the past land use changes between 1989 and 2009 and their impacts on the water balance in the Mula and Mutha Rivers catchment upstream of Pune. Land use changes were identified by using three multitemporal land use classifications at the beginning (1989/90), in the middle (2000/01), and at the end (2009/10) of the period of interest. The hydrologic model SWAT (Soil and Water Assessment Tool) was used to assess impacts on runoff and evapotranspiration. Two model runs were performed and compared using the land use classifications of 1989/90 and 2009/10. The main land use changes were identified as an increase of urban area from 5.1% to 10.1% and an increase of cropland from 9.7% to 13.5% of the catchment area in the 20 year period of interest. Urbanization was mainly observed in the eastern part and conversion to cropland in the mid-northern part of the catchment. At the catchment scale we found that the impacts of these land use changes upon the water balance cancel each other. However, at the sub-basin scale urbanization led to an increase of the water yield by up to 7.6%, and a similar decrease of evapotranspiration, whereas the increase of cropland resulted in an increase of evapotranspiration by up to 5.9%.*

**KEYWORDS:** SWAT, Land use change, Water resources, India

## 1. Introduction

Land use changes are altering the hydrologic system and have potentially large impacts on water resources (Stonestrom et al., 2009). Rapid socio-economic development drives land use transition, which includes changes of land use classes, e.g., conversion of cropland to urban area due to urbanization, as well as changes within classes such as a change of crops or crop rotations. Particularly in regions where water availability is limited, land use changes could result in an increase of water scarcity and thus contribute to a deterioration of living conditions. DeFries and Eshleman (2004) underline the importance of understanding the impact of land use change on water resources, which they identify as a key research topic for the decades ahead.

To assess past land use changes satellite images provide valuable spatially-distributed information. Historic multispectral satellite images can be used to produce past land use classifications. However, in the absence of historic ground truth data different methods and data (e.g., historic topographic or land use maps) are employed to derive accurate past classifications (e.g., Miller et al., 2002; Seeber et al., 2010). These classifications are superior to commonly used freely available, global data sets (e.g., Hansen et al., 1998), as they provide a higher spatial resolution (30 m) and often have a higher level of detail with regard to the number of distinguished classes. Each land use classification is representative of the date of the satellite image and the phenology of the plants at this time in the year (Jensen, 2007). Particularly in regions with a high temporal variability in temperature (e.g., temperate and continental climates) or precipitation (e.g., tropical wet and dry climates), the date of the satellite imagery has a pronounced impact on the identifiable and distinguishable land use classes. In order to derive a classification, which is representative of the whole year, several land use classifications from different times in the year can be combined to produce one multitemporal land use classification (e.g., Villarreal et al., 2011; Yuan et al., 2005). By this means, the intra-annual differences are minimized. Thus, a series of such multitemporal land use classifications can be analyzed to identify the inter-annual or in the present case inter-decadal changes over a past period of time.

In order to assess impacts of land use change on water resources hydrologic models are typically employed, e.g., HBV (Bergström and Forsman, 1973; e.g., Ashagrie et al., 2006), MIKE-SHE (Refsgaard and Storm 1995; e.g., Im et al., 2009), SWAT, (Arnold et al., 1998; e.g., Fohrer et al., 2001), or WaSiM-ETH (Schulla, 1997; e.g., Niehoff et al., 2002). Models are particularly useful, as they can assess past as well as possible future impacts (using land

use scenarios). Huisman et al. (2009) employed an ensemble of ten hydrologic models (the four previously named and six other models) to assess the impact of land use change scenarios, which resulted in a range of predictions that were in general agreement with respect to the direction of the impact on discharge. The Soil and Water Assessment Tool (SWAT, Arnold et al., 1998) has proven its suitability for hydrologic impact studies (Gassman et al., 2007) and furthermore under conditions of limited data availability (Ndomba et al., 2008; Stehr et al., 2008). Hence, it is a suitable model to study the impact of land use changes on water resources in India.

Investigations of the effects of past land use changes on water availability have been carried out in many regional studies worldwide (e.g., Ghaffari et al., 2010: Iran; Im et al., 2009: Korea; Li et al., 2009: China; Miller et al., 2002: USA). Furthermore, impacts of land use scenarios on the water resources have been analyzed in many other regional studies e.g., in Germany (Klößing and Haberlandt, 2002; Barthel et al., 2012), Canada (Wijesekara et al., 2012), Ethiopia (Legesse et al., 2003), and Kenya (Mango et al., 2011).

Several investigations of land use changes and land use change impacts have been carried out in India. Chauhan and Nayak (2005) reported that industrial development and population pressure in Hazira, Gujarat, led to an increase of built-up area and a decrease in forest and agricultural areas between 1970 and 2002. Jayakumar and Arockiasamy (2003) have found an increase of cropland and a decrease of grassland and shrubland in a study on a part of the Eastern Ghats in South India. Deforestation between 1973 and 1995 was reported in a study on the southern part of the Western Ghats by Jha et al. (2000). Similarly, a study about Indian Himalayan catchments by Sharma et al. (2007) found a decrease of natural forest and an increase of agricultural land.

Impacts of land use change on the water resources in India were mainly assessed by using scenario analysis. Particularly, agricultural management practices are a focus of the research in India: Garg et al. (2012a; 2012b) found that agricultural water interventions had a pronounced impact on water resources, Sharma et al. (2001) employed land use and land management measures that decreased the water yield significantly, and Behera and Panda (2006) identified critical sub-watersheds and tested best management practices to minimize sediment and nutrient loads. Mishra et al. (2007) analyzed the effects of land use on runoff and sediment yield to prioritize the construction of structural water management measures. Wilk and Hughes (2002) conducted a study in South India employing several land use scenarios, and found that only the extreme and very unlikely scenarios had a pronounced

impact on runoff. The largest increases of runoff were found when converting forest and savanna to agriculture, whereas the largest decrease of runoff resulted from a conversion to forest in this study. Further Indian studies focus on the impact of land use change on groundwater (e.g., Khan et al., 2011; Ramesh, 2001; Singh, 2001).

A comprehensive assessment of land use change impacts on water resources in an area with seasonally limited water availability and which is subject to rapid socio-economic development and population growth will provide an exemplary view on the local impacts of major recent developments in India. The city of Pune has experienced such rapid socio-economic development and population growth in the recent decades. In Pune district, where Pune city is the largest urban and economic agglomeration, population has increased by more than 30% per decade between 1991 and 2011 (Government of India, 2011). It is the aim of this study to (i) assess the land use changes between 1989/90 and 2009/10, and (ii) analyze the impacts of these changes on the long-term water balance components in the Mula and Mutha Rivers catchment upstream of the city of Pune.

## 2. Materials and Methods

### 2.1 Study area

The meso-scale catchment of the Mula and the Mutha Rivers (2036 km<sup>2</sup>) is located in the Western Ghats upstream of the city of Pune, India (18.53° N, 73.85° E; Fig. 1). It is a sub-basin and source area of the Krishna River, which drains towards the east and into the Bay of Bengal. Its elevation ranges from 550 m in Pune up to 1300 m a.s.l. on the top ridges in the Western Ghats. The catchment has a tropical wet and dry climate, which is characterized by seasonal rainfall from June to October and low annual temperature

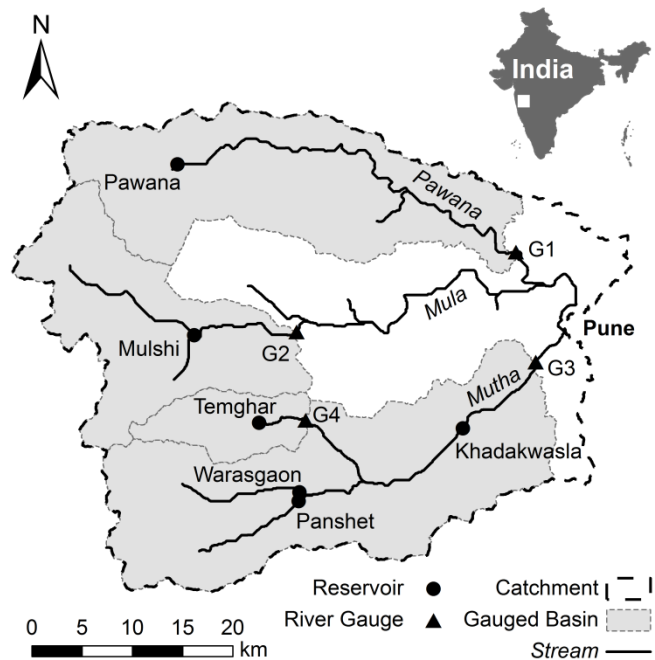


**Fig. 1** Mula-Mutha catchment with the locations of river gauges and reservoirs.

variations with an annual mean of 25°C at the catchment outlet in Pune. Annual rainfall amounts decrease from approximately 3500 mm in the western part of the catchment to 750 mm in the eastern part of the catchment (Gadgil, 2002; Gunnell, 1997). Land use is dominated by semi-natural vegetation, with forests mainly on the higher elevations in the west, whereas shrubland and grassland occupy lower elevations. Cropland is found mainly in proximity to rivers and dams, and is dominated by small fields (< 1 ha) with rain-fed agriculture during the monsoon season and irrigation during the dry season. Typically two crops per year are harvested, a Kharif (June-October) and a Rabi (November-March) crop. Urban area is mainly found in the eastern part of the catchment, where the city of Pune and its surrounding settlements are located (Wagner et al., 2012).

### 2.2 Assessment of land use changes

In order to analyze the land use changes in the study area between 1989/90 and 2009/10, we produced three multitemporal land use classifications for the cropping years 1989/90, 2000/01, and 2009/10. These classifications are based on multispectral satellite data. Different sensors were used to cover the 20 year timespan of this study. The classifications are based on Landsat 5 TM data for 1989/90, on Landsat 7 ETM+ data for 2000/01, and on IRS-P6

(Resourcesat-1) LISS-III data for 2009/10. All sensors have a similar spatial resolution of 30 m (TM/ETM+) or 23.5 m (LISS-III), and have bands in the visible, the near infrared, and the short wave infrared region (Landsat TM/ETM+: 6 bands; LISS-III: 4 bands). Furthermore, all of these satellite sensors are commonly used to produce land use classifications (e.g., LISS-III: Jayakumar and Arockiasamy, 2003; Saha et al., 2005; TM: Seeber et al., 2010; Villarreal et al., 2011; ETM+: Peiman, 2011; Yuan et al., 2005). Due to the absence of mapped ground truth data for the past, different methodologies were applied for the current and the two historic land use classifications.

### **2.2.1 Current land use classification**

For the current land use classification, ground truth data was mapped at three test sites in and near the study area. Field surveys were carried out during each of the two cropping seasons; one in September and October 2009 and another one in February and March 2010. Rice, wheat and sugarcane were the most important crops. Based on the field survey data, we confirmed the expected crop rotation of rice in rainy season and wheat in dry season. Sugarcane is a perennial plant. Due to their diversity and small scale patchiness, the other agricultural land use types were combined into a mixed cropland class. The next available cloud-free LISS-III satellite images corresponding to the two field surveys (30 November 2009, 6 March 2010) were used to produce two land use classification. The satellite images were geometrically corrected using ground truth points. A stratified knowledge-based approach, employing a maximum likelihood classifier was applied as follows: for agricultural land use thresholds in terms of elevation (< 800 m) and slope (< 10%) were set, as cropland is typically located in the valleys and in proximity to rivers. Pixels classified as cropland that exceeded these thresholds were labeled as grassland. A majority analysis on a moving 3 x 3 raster window was applied to remove misclassified, spatially singular pixels within homogenous areas (Wagner et al., 2011). Water bodies were defined using a threshold value for the near infrared band. The ground truth data were used to define the training areas for the classification and for validation of the classification results. Both classifications showed reasonable accuracies (Table 1).

In order to derive a single land use map that is representative for the whole cropping year, the two classifications were combined by using the rules shown in Table 2. For the combination of two semi-natural classes priority was given to the class with a higher percentage of trees (e.g., if a pixel was classified as forest in one of the classifications and as shrubland in the other one, the pixel was assigned as forest in the combined classification). As

bare soil is a temporary land use, a combination of cropland and bare soil, or grassland and bare soil was defined as cropland or grassland, respectively. In the cases of a contradictory combination of sugarcane, rice, and wheat, the 2009 land uses were given priority over the 2010 land uses, as higher user accuracies were achieved for these classes in the 2009 land use classification (Table 1). Areas were reclassified, where both classifications showed different uses and where none of the above described rules were applicable. For this reclassification both scenes and homogeneous ground truth information for 2009 and 2010 were used. Water areas were taken from the November classification corresponding to the maximum water level in the reservoirs. By this multitemporal assessment a classification was derived that is suitable to represent the whole cropping year.

**Table 1** Quality of the land use classifications in 2009/10 assessed by using mapped ground truth data.

Indicator	Classes	LISS-III Scene	
		30 Nov 2009	06 Mar 2010
Overall accuracy	Combined agricultural classes	79.1%	82.9%
	Distinguished agricultural classes	65.6%	58.8%
User's accuracy	Forest	78.6%	91.9%
	Shrubland	45.4%	70.8%
	Grassland	68.9%	52.7%
	Bare soil	41.0%	43.7%
	Mixed cropland	27.4%	41.8%
	Rice 2009/ Wheat 2010	86.4%	31.5%
	Sugarcane	92.4%	51.0%
	Urban	89.1%	91.1%

**Table 2** Applied rules to derive a multitemporal land use classification for the cropping year 2009/10.

Class Combinations	Multitemporal Result
Forest - Shrubland	Forest
Forest - Grassland	Shrubland
Shrubland - Grassland	Shrubland
Grassland - Bare soil	Grassland
Agricultural class - Bare soil	Agricultural class
Urban high density - Urban low density	Urban high density
Mixed cropland - Sugar or Rice	Sugar or Rice
Sugar or Rice of 2009 - Sugar or Wheat of 2010	Sugar or Rice of 2009
Mixed cropland 2009 - Wheat 2010	Mixed Cropland
Equal land use	Equal land use
No rules apply	New classification using both scenes

Reasonable accuracy of the classification was also indicated by a comparison with the most recent agricultural statistics (cropping year 2007-2008) available from the Department of Agriculture in Pune. Statistics are provided for each season (Kharif and Rabi) and for the perennial plant sugarcane. An administrative area (the subdistrict Mulshi) within the catchment that is about half of its size was used for this comparison. As compared to the statistics the classification showed less sugarcane area (-12%), and less total cropping area in Kharif season (-39%), and in Rabi season (-8%). Reasons for the pronounced difference in Kharif season might be: (i) the quality of the land use statistics, which are based on sampling methods, (ii) rice area in the 2009 classification might be underestimated, as the satellite image was taken in November, when some rice fields were already harvested, and (iii) the compared data is based on different years. However, the good overall accuracy (79.1%) of the land use classification in 2009 makes it seem unlikely that the total agricultural area is underestimated by 39% in Kharif season. The combination of the two land use classifications (2009 and 2010), which both showed reasonable accuracies in the validation with mapped ground truth (Table 1), gives further confidence in the quality of the derived multitemporal classification.

### **2.2.2 Historic land use classifications**

For the historic land use classifications mapped ground truth data was not available. Thus training areas for the forest, shrubland, grassland, and urban area classes were defined using topographic maps and satellite images. The topographic maps in this area date back to 1962-1980, so that a training area was only defined as forest, shrubland, grassland or urban area, if topographic map and satellite image showed consistent information. In addition, the regional knowledge of typical locations for forest (in the western part of the catchment), shrubland (on the foot of the hills), and grassland (in the valleys or on the plain mountain plateaus) in combination with Normalized Difference Vegetation Index (NDVI) values was used. Cropland was identified from the satellite image, where field structures were clearly observable. Current agricultural fields (high NDVI) were distinguished from harvested agricultural fields (low NDVI). A third, intermediate agricultural class was defined, which had an intermediate NDVI value. Clouds and cloud shadows were visually identified and masked.

Hence, the images were geometrically corrected using the previously corrected LISS-III satellite images. Subsequently, the same stratified knowledge-based approach (elevation and slope thresholds, majority analysis) with a maximum likelihood classifier was employed as in

the classification of the current land use classifications. The derived historic classifications were evaluated using the training areas which were defined above. Table 3 shows that all six classifications had a very good overall accuracy (92.4-98.6%) and good or better user accuracies (Story and Congalton, 1986) for each class (74.0-100.0%). This assessment indicates that the defined main land use classes were accurately distinguished.

**Table 3** Quality of the land use classifications in 1989/90 and 2000/01.

Indicator	Classes	Landsat 5 TM			Landsat 7 ETM+		
		25 Oct 1989	12 Dec 1989	2 Mar 1990	15 Oct 2000	19 Jan 2001	24 Mar 2001
Overall accuracy		95.9%	92.4%	93.0%	98.6%	96.7%	96.8%
User's accuracy	Forest	98.7%	97.7%	98.4%	98.7%	99.1%	99.3%
	Shrubland	82.2%	74.0%	74.0%	95.9%	81.9%	82.3%
	Grassland	98.1%	95.9%	94.8%	99.7%	97.7%	97.2%
	Cropland 1, current	97.6%	98.4%	98.6%	95.5%	96.3%	97.1%
	Cropland 2, harvested	99.5%	74.6%	94.1%	99.7%	97.9%	94.2%
	Cropland 3, intermediate	79.7%	97.9%	77.2%	96.3%	91.9%	99.0%
	Urban	99.5%	87.0%	99.5%	100.0%	99.2%	99.6%

Multitemporal classifications for the cropping years 1989/90, and 2000/01 were derived by using three classifications per cropping year (25 October 1989, 12 December 1989, 2 March 1990, and 15 October 2000, 19 January 2001, 24 March 2001). Water areas were taken from the October classifications, which correspond to the maximum water level in the reservoirs. In all other cases, the dominant land use was used for the multitemporal classification (majority approach). If all classifications showed a different land use, the pixel was reclassified using all bands of all three satellite scenes (Table 4). The three agricultural classes were combined to one general class.

**Table 4** Applied rules to derive multitemporal land use classifications for the cropping years 1989/90 and 2000/01.

Class Combinations	Multitemporal Result
Any two agricultural classes in at least two scenes	Agricultural class
Equal land use in two or three scenes	Dominant land use
No rules apply	New classification using all scenes

In order to distinguish the major crops (sugarcane, crop rotation rice-wheat), from the general agricultural class in the historic land use classification, we used (i) agricultural statistics to derive the percentage of total cropped area for these crops, and (ii) spectral signatures of rice and sugarcane to derive the spatial distribution of these percentages.

- (i) The agricultural statistics for the district of Pune indicate that both sugarcane and rice percentages of the total agricultural area increased between 1988/89 and 2007/08. A linear regression was used to derive the mean rate of this change. It was assumed that both sugarcane and rice percentages of the total agricultural area in the catchment have undergone the same linear change. Thus the change, as indicated by the regression, was applied to the percentages of both sugarcane and rice fields in the land use classification of 2009/10 (sugarcane: 9.8%, rice: 55.6%) to calculate the percentages for the classifications in 2000/01 (7.3%, 51.4%), and 1989/90 (4.3%, 46.2%).
- (ii) The spectral information divergence method (Du et al., 2004) was used to identify, which agricultural pixels are most similar to measured plant spectra. These spectra were taken during the field survey in September and October 2009. To apply the spectral information divergence method the satellite images taken in October 1989 and 2000 were atmospherically corrected using the MODTRAN4 based FLAASH module in ENVI Version 4.8 (Matthew et al., 2000). Hence, Landsat bands 1 to 4 in the visible and short wave infrared region were used to apply the method: A threshold value for each spectrum was set, which defines the minimum allowable variation between the pixel vector and the spectrum vector. If the threshold was exceeded, the pixel was not classified and thus remained mixed cropland. Threshold values used in the spectral information divergence method were set, so that the derived percentages of the total cropped area for sugarcane and rice fields in the final classification were equal to the percentages calculated from the agricultural statistics. The method provides a reasonable spatial distribution of rice fields in the mountainous, western part of the catchment, and of sugarcane fields in the lower regions, especially downstream of Pune. A majority analysis was applied to the newly distinguished crops to derive the final multitemporal land use classifications for the years 1989/90 and 2000/01.

### ***2.3 Assessment of land use change impacts on water resources***

In this study, the Soil and Water Assessment Tool (SWAT, Arnold et al., 1998) was used to assess the impact of land use change on water resources. In previous studies, we showed the suitability of SWAT to model the water fluxes in the Mula and Mutha Rivers catchment (Wagner et al., 2011; 2012). Since details of the model setup and parameterization are available in the published previous studies, we will only present a brief summary of data inputs and model parameterization.

A digital elevation model (DEM) with a spatial resolution of 30 m was derived from ASTER satellite data. The spatial distribution of soils was taken from the digital Soil Map of the World (FAO, 2003). Soil parameterization was partly adapted from a modeling study of the region by Immerzeel et al. (2008), and partly taken from the FAO (2003) database. Measured weather data for the period from 1988 to 2008 was used. The full data set of measured maximum and minimum temperature, humidity, solar radiation, and wind speed data was only available at the IMD weather station in Pune (ID 430630, 18.53° N, 73.85° E, 559 m a.s.l.). Missing values were filled. To account for temperature differences in the catchment, temperature values were adjusted using adiabatic temperature gradients. The spatially distributed temperature records and the specific humidity measured at the weather station in Pune were employed to calculate spatially distributed relative humidity (Wagner et al., 2011). Rainfall data was available from 16 gauges within or near the study area. A thorough analysis of the data and of different interpolation schemes was carried out. Regression kriging using satellite data of the Tropical Rainfall Measuring Mission (TRMM) was found to be a suitable approach and hence used in this study to interpolate rainfall to a 1 km<sup>2</sup> grid (Wagner et al., 2012). Two models were built for the land use classification of 1989/90 and 2009/10, respectively. In order to account for the two main cropping seasons in the region, crop rotations were set up as follows: For the rice fields, the typical crop rotation (as observed in the field survey) of growing rice in the Kharif season (June to October) and wheat in the Rabi season (November to March) was implemented. Sugarcane is cultivated year-round. Mixed cropland is simulated as a mixture of the general crop classes in SWAT (AGRL, AGRR; Neitsch et al., 2010). The bare soil class was modeled as mixed cropland (50%) and grassland (50%), as it is composed of harvested fields as well as non-agricultural bare soils. Irrigation schemes for all of these crops were set up (Wagner et al., 2011). For the six major dams in the catchment (Fig. 1), a management scheme was developed, which is based on general management rules allowing for water storage in the rainy season and water release in the dry season (Wagner et al., 2011; Wagner et al., 2012).

SWAT input parameters were either a) estimated from readily available GIS databases, or b) were chosen from the literature for the given site condition, or c) default model parameters were selected. A site specific calibration of model parameters was not applied, as the focus of this study is set on the impact of two different land use inputs on the water balance. This assessment could be biased, if a land use specific calibration was applied. Details of the model parameterization as well as the suitability of the model and its parameterization are given in Wagner et al. (2012). In the present study, the model was evaluated using the available daily

discharge data during rainy seasons between 2001 and 2007. With both land use classifications good performances at the river gauges G1 and G4 (Fig. 1) judged by Nash-Sutcliffe efficiency (NSE, Nash and Sutcliffe, 1970; G1: 0.68 to 0.69, G4: 0.67) and percentage bias (G1: +4% to +5%, G4: +24%) were achieved. Model performance in the highly managed sub-catchments G2 and G3 depends strongly on dam management.

For the analysis of land use change impacts on the water balance components, two model runs were performed with measured weather data from 1988 to 2008 using the land use classifications for 1989/90 and for 2009/10, respectively. This delta approach is frequently used to assess the impact of land use changes (e.g., Ghaffari et al., 2010; Im et al., 2009; Miller et al., 2002). Only model parameters that were defined by the land use map were different in the two model setups. Therefore, the number of hydrologic response units (HRUs), which are unique land use – soil – slope class combinations, differed in the two model setups. The 2009/10 model had more HRUs (917) than the 1989/90 model (640), because the 2009/10 land use classification had a higher level of detail (high density urban area and bare soil class). Furthermore, one of the major dams that became operational in the year 2000, was not included in the model run for the 1989/90 land use map and was included as being operational during the entire 21-year model run for the 2009/10 land use. The first year of the model runs was used as a model spin-up phase. Thus, analysis of water resources was carried out by comparing the 20-year average water balance components using the model results for the two different land use classifications.

### 3. Results

#### 3.1 Change Analysis

The major changes within the last 20 years as indicated by the three land use maps (see Fig. A1, A2, and A3 in the appendix) are changes from semi-natural vegetation to cropland and urban area. Thus the semi-natural vegetation classes of forest, shrubland and grassland are combined in Figure 2. The area of semi-natural vegetation decreased from 79.8% in 1989/90 to 74.7% in 2000/01 and 70.7% in 2009/10 (Fig. 2). Due to urbanization and industrial development the percentage of built-up land has increased in the region (5.1% in 1989/90, 8.1% in 2000/01, and 10.1% in 2009/10). Also the agricultural area has increased from 9.7% to 13.5% between 1989/90 and 2009/10. The district statistics do not show an increase in agricultural area, but in contrast show a decrease of total cropland by 11% between 1988/89 and 2007/08. This discrepancy may be due to the fact that the study area composes only 13% of the district so that different trends are possible and not contradictory. The percentage of catchment area covered by water increases slightly between 1989/90 (5.3%) and 2009/10 (5.7%).

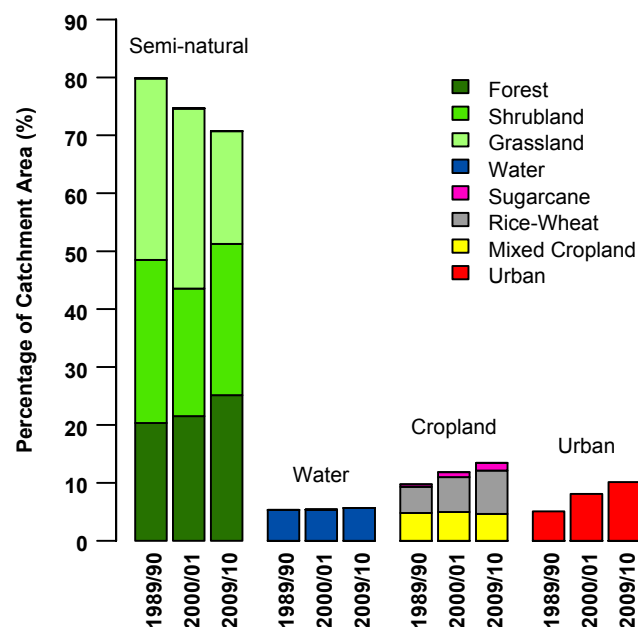


**Fig. 2** Percentage changes of land use classes between 1989/90 and 2009/10. Percentages are shown as bars for each land use classification. Forest, shrubland, and grassland are combined to one semi-natural land use bar. Sugar cane, the rice-wheat crop rotation, and the mixed cropland class are shown as one agricultural land use bar.

The land use classification of 1989/90 was compared to the land use classification of 2009/10 in order to identify the regions where the main changes between 1989 and 2009 occurred. Figure 3 shows the changed and unchanged areas (43.0% and 57.0% of the catchment area, respectively), in which the changed areas depict the land use of the 2009/10 classification. Only the major changes are shown, i.e., changes within the agricultural classes or within the urban land use classes were considered as unchanged areas. Major increases of urban area occurred on the fringes and to the northwest of the city of Pune. The growth towards the northwest follows the newly built National Highway 4 to Mumbai (clearly observable as a red line in sub-basin 2, Fig. 3) and covers the rapidly developing area of Pimpri Chinchwad. Mainly grassland (72.8%) and cropland (21.7%) are converted to urban area (Table 5). It should be noted that past growth of the city of Pune to the east and northeast is not reflected in this study, as these areas are not part of the catchment. The map indicates major changes to agricultural area in the valleys of the northern part of the catchment (sub-basins 2, 3, 4, 8, 9, 13). Mainly grassland (70.8%) and shrubland (17.1%) are converted to serve these purposes (Table 5). The slight increase of catchment area covered by water (Fig. 2) can be attributed to the construction of the Kasarsai reservoir in 1995 (sub-basin 3 in Fig. 3) and the expansion of the Temghar dam reservoir in the year 2000 (sub-basin 18).

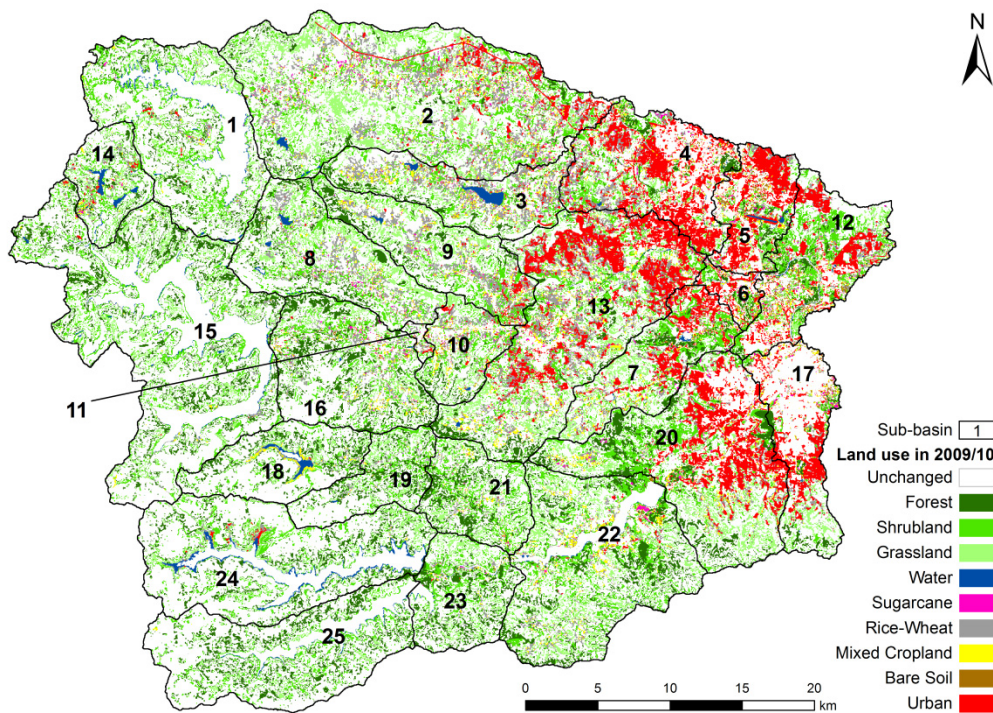


**Fig. 3** Current land use (2009/10) of the areas that have been changed between 1989/90 and 2009/10. Unchanged areas (57.0% of the catchment) are shown in white.

**Table 5** Information on the changed areas (43.0% of the catchment): i) Distribution of former land use (1989/90) of areas converted into the current land use (2009/10) for each class. ii) Area changed into the current land use class as percentage of the catchment area. iii) Net change per land use class between 1989/90 and 2009/10 as percentage of the catchment area (2009/10 bare soil class was split and added to cropland and grassland for this assessment).

		Land use in 2009/10						
		Forest	Shrubland	Grassland	Urban	Cropland	Water	Bare soil
Land use in 1989/90	i) Forest	0.0%	24.5%	4.0%	0.4%	2.1%	25.2%	2.0%
	Shrubland	75.7%	0.0%	79.5%	4.8%	17.1%	26.1%	37.9%
	Grassland	16.4%	59.8%	0.0%	72.8%	70.8%	37.2%	0.0%
	Urban	0.5%	1.8%	3.5%	0.0%	8.4%	3.0%	57.2%
	Cropland	6.5%	12.4%	12.8%	21.7%	0.0%	8.5%	0.0%
	Water	0.9%	1.4%	0.2%	0.3%	1.6%	0.0%	2.9%
ii) Changed area with 2009/10 land use as percentage of the catchment area		8.4%	11.9%	7.0%	6.5%	8.2%	0.8%	0.3%
iii) Net change per land use class between 1989/90 and 2009/10		+4.8%	-2.1%	-11.9%	+5.1%	+3.7%	+0.3%	–

Variations between the semi-natural classes (Fig. 2) should not be overinterpreted, as these classes overlap and are therefore hard to distinguish. The analysis of the changes by land use class between 1989/90 and 2009/10 shows that the land use changes of semi-natural classes are mainly intra-class changes (Table 5). The main percentage of the area that was changed to forest, shrubland, or grassland in 2009/10 was under semi-natural land use in 1989/90 (forest: 92.1%, shrubland: 84.3%, grassland: 83.5%; Table 5). Thus, even though the changes to semi-natural classes in 2009/10 account for 27.3% of the catchment area, they should not be interpreted as major changes. As indicated before (Fig. 2) the main changes are an increase of urban area and cropland. This is also reflected in the percentage of the catchment area that was changed to cropland (8.2%) and to urban area (6.5%) between 1989/90 and 2009/10 (Table 5). On the sub-basin level these changes are more pronounced, with up to 22.3% of the area changed to cropland in some sub-basins and up to 32.4% of the area changed to urban area in other sub-basins. For this reason, a focus will be set on the sub-basin level in the following analysis of the impacts of these land use changes on the water resources in the study area.

### 3.2 Land use change impacts

Two 21-year model runs were performed using the multitemporal land use classifications of 1989/90 and 2009/10, respectively. This delta approach does not necessarily provide results that reflect the hydrologic observations of the past 20 years, but illustrates the impacts of the main changes on the hydrologic components (Miller et al., 2002). On the catchment scale the positive and negative impacts cancel each other, so that differences in the long-term water

balance components are smaller than 3 mm. However, more pronounced changes are discernible on the sub-basin level. Figures 4 and 5 show the percentage change of evapotranspiration (ET) and water yield per sub-basin. A major decrease of ET is obvious in the eastern part of the catchment (-0.8% to -8.1%). Main increases (> 4.5%) can be observed in the mid-northern part (sub-basins 2 and 3) and in one small sub-basin (14) in the Western Ghats. In order to relate these changes in ET to the changes in land use, the changes in each land use class for each sub-basin are assessed as the difference between the area under this land use in 2009/10 and 1989/90 expressed as percentage of the sub-basin area. The percentages of changed cropland and urban area, which were previously identified as the major land use changes in the catchment, are shown for each sub-basin in Figures 4 and 5. As indicated by significant correlations ( $p$ -value < 0.001) and linear regression analysis (Fig. 6), the changes in ET can be attributed to changes of cropland ( $R^2=0.46$ ) and urban land ( $R^2=0.48$ ). Figure 6 shows that cropland and ET are positively correlated, whereas urban land and ET have a negative correlation. It is clearly shown that the change of urban land can explain the decrease of ET but not its increase (Fig. 6B). The other land uses do not show a correlation at the 0.1% significance level.

Figure 5 shows the impact of land use changes on runoff as a percentage change of the water yield within each sub-basin. The most pronounced increase in water yield (> 3.5%) was found in the eastern sub-basins (4, 5, 6, 12, and 17). The increase in water yield was less pronounced in the adjacent sub-basins towards the west. No increase or only slight increases were detected in the western part of the catchment. The major driver of the increase in water yield is the change of urban area ( $R^2=0.63$ ). The positive correlation (Fig. 7A) of change in urban land and in water yield is highly significant ( $p$ -value < 0.001). Correlations with other land use changes did not yield a relationship at this significance level. However, since mainly grassland is converted to urban land, the change in grassland shows a negative correlation with the change in water yield, which is significant at the 0.5% significance level. The sub-basin size does not yield a significant relationship with the increase in water yield (Fig. 7B). Obviously, land use changes are more important than sub-basin size with regard to the impact on the water yield. However Fig. 7B indicates that the potential response to land use changes is larger in smaller sub-basins, as the range of the impacts on water yield is larger for the sub-basins smaller than 100 km<sup>2</sup>, and decreases with an increase of the size of the sub-basin.

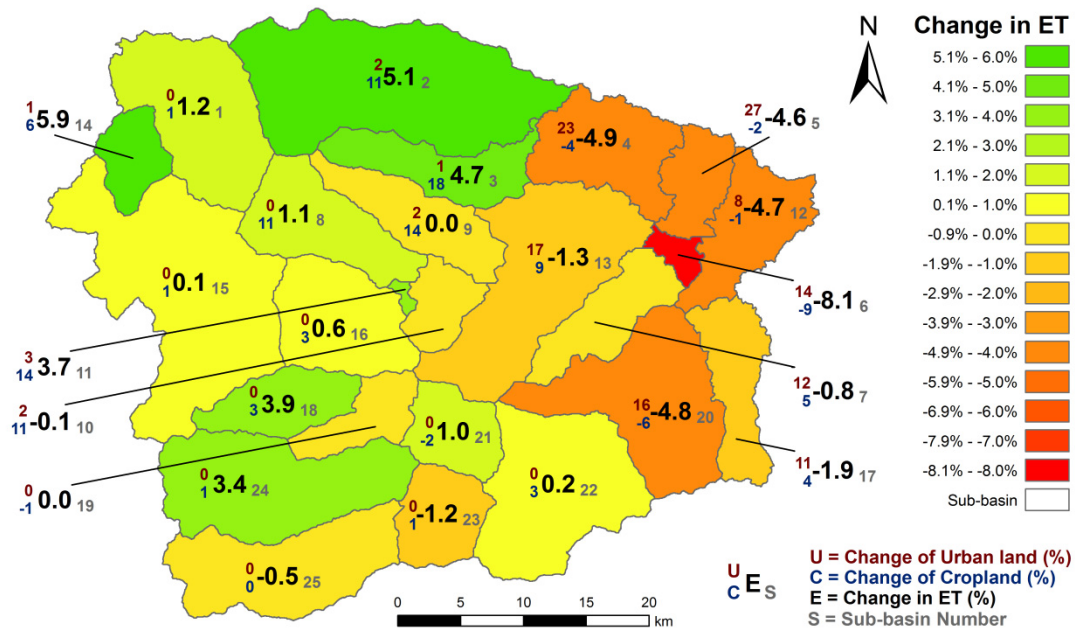


Fig. 4 Change in evapotranspiration (ET) per sub-basin and changed cropland and urban area as percentage of sub-basin area between 1989/90 and 2009/10.

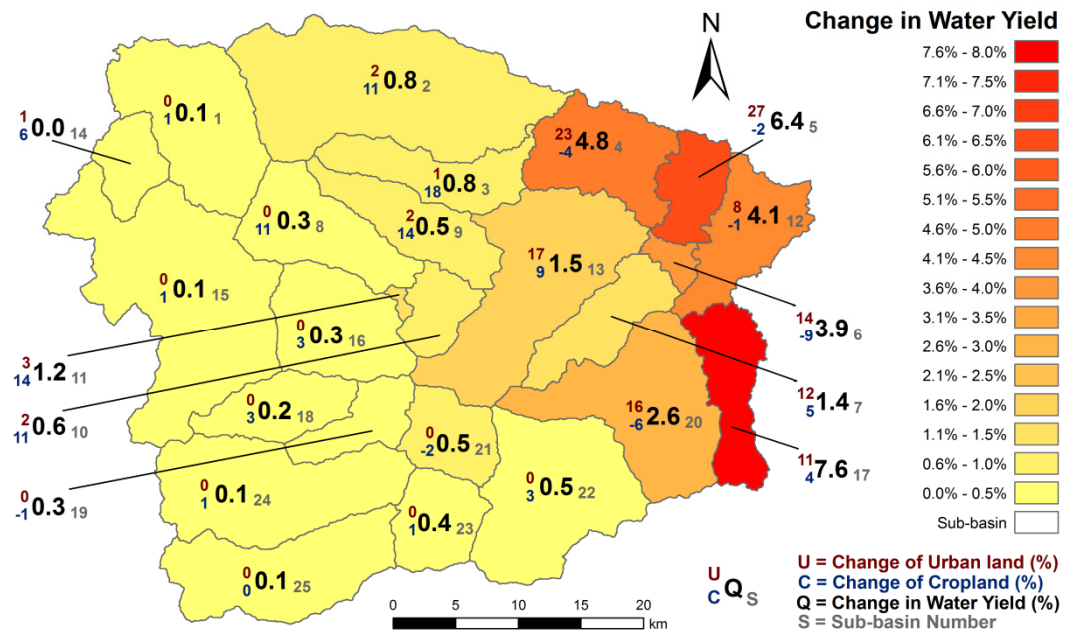
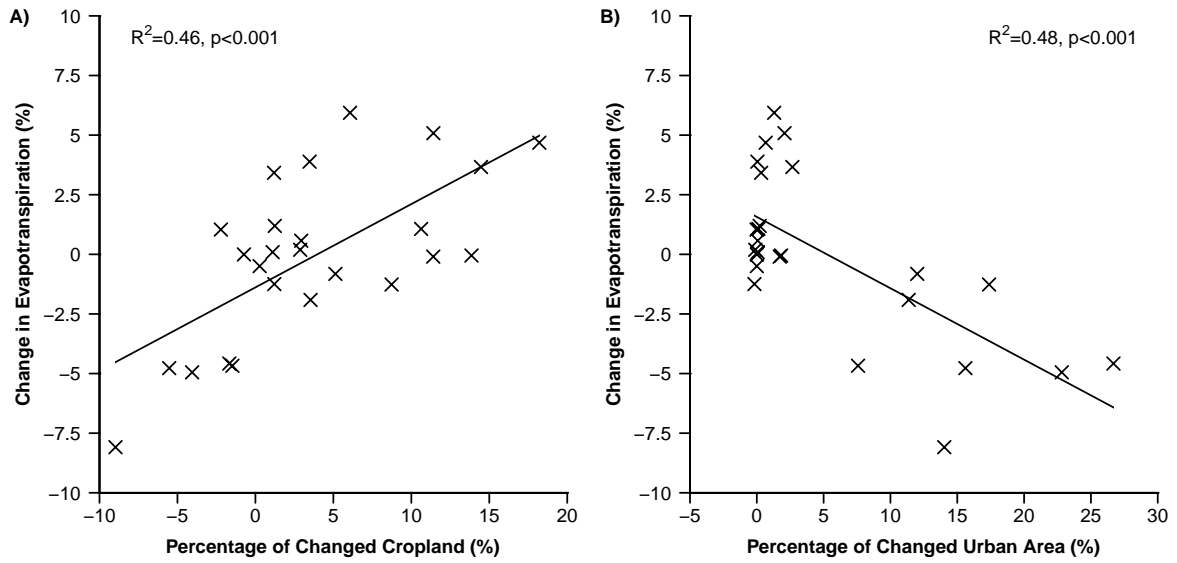


Fig. 5 Change in water yield per sub-basin and changed cropland and urban area as percentage of sub-basin area between 1989/90 and 2009/10.

The shown relationships are reflected in the spatial patterns of the changes in ET (Fig. 4) and water yield (Fig. 5). In the eastern part of the catchment an increase of urban area can be observed, whereas cropland decreases or increases only slightly (Fig. 3, Fig. 4). In these eastern sub-basins water yield increases (Fig. 5) whereas ET decreases (Fig. 4). Larger increases of cropland (9% to 18% of the sub-basin area) are apparent in the mid-northern part of the catchment, which often result in increased ET in these sub-basins. Water yield increases slightly in these sub-basins. The increase of ET can be attributed to the irrigation of crops in dry season. Between December and May increased irrigation water use and water withdrawal from the rivers can be observed in sub-basins with an increase of irrigated cropland (e.g., sub-basin 2). Thus ET increases in these sub-basins. However, as river water is used, this does not necessarily have a negative impact on the water yield within the sub-basin itself. On the contrary, irrigation water that is taken from the river contributes to a slight increase of the water yield within the sub-basin. For sub-basins that are downstream of other sub-basins and experience an increase in cropland this explains why ET and runoff increase at the same time (e.g., sub-basins 2, 11, 16). However, some sub-basins that do not have inflow from upstream sub-basins also show an increase in ET and water yield (e.g., sub-basins 1, 18, 24). This is because of a decrease of the storage in these sub-basins between 1989/90 and 2009/10.

In some sub-basins the opposing effects of an increase in water yield due to an increase of urban area and an increase in ET due to an increase in cropland cancel each other out (e.g., sub-basins 7, 13). However in sub-basin 6, where the percentage of changed urban area is positive and the percentage of changed cropland is negative, both land use changes lead to a decrease of ET, and result in the largest decrease of ET on the sub-basin level.



**Fig. 6** Change in evapotranspiration explained by the percentage of changed cropland (A) and changed urban area (B) in each sub-basin.

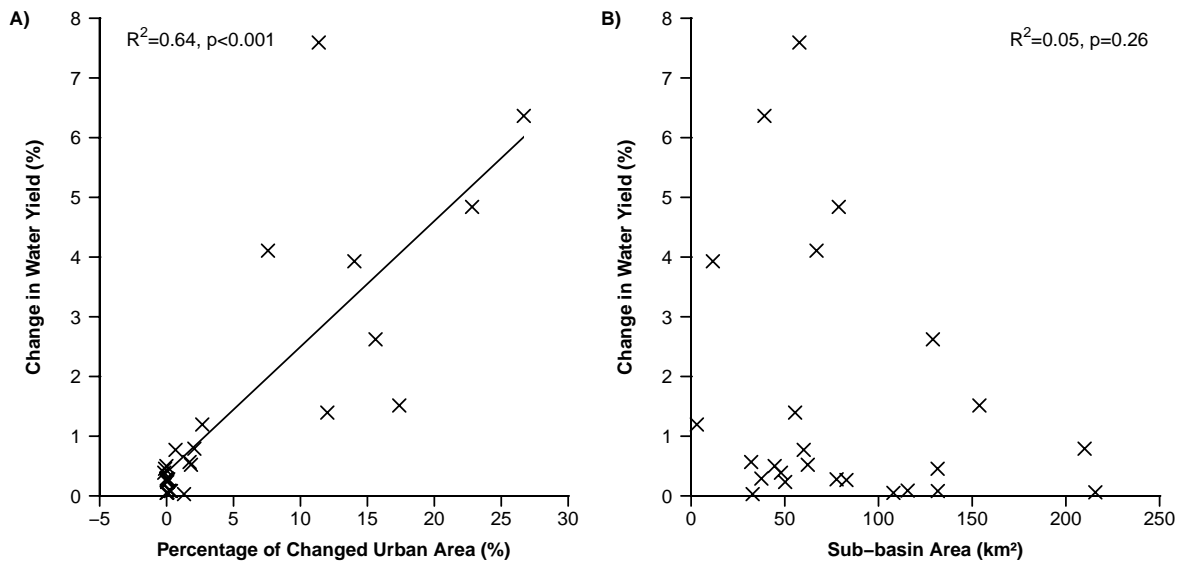


**Fig. 7** Change in water yield and its relation to the percentage of changed urban area in each sub-basin (A) and to the size of the sub-basins (B).

## 4. Discussion

The produced land use classifications have an agreeable accuracy and hence the major land use changes in the study area were accurately identified. However, unlikely changes from urban area to cropland have been observed in the present study (Table 5). These may result from a) a misclassification of cropland in the 2009/10 classification or b) misclassified urban area in the 1989/90. However, these comprise only 8.4% of the catchment area that was changed to cropland (8.2% of the catchment, Table 5) and indicate therefore a small, acceptable uncertainty of the method.

Similarly, the changes within the semi-natural class between forest, shrubland, and grassland may be attributed to the applied methodology. The three satellite images for the historic land use classifications 1989/90 and 2000/01 were not taken at the same time of the year (Table 3), due to the availability of cloud-free scenes. Classification differences can be attributed to different phenological states of the plants. Although multitemporal approaches generally help to minimize these problems (e.g., Oetter et al., 2000; Wolter et al., 1995; Yuan et al., 2005), it is obvious that the different dates of the satellite had an impact on the classification. This is particularly true for the semi-natural classes which depend on the natural water availability that constantly declines during dry season. As the month of the second scene in the 1989/90 and 2000/01 classification differ (December 1989, January 2001), the time gap probably had an impact on the classification of the shrubland class, which was 28% of the catchment area in 1989/90 and only 22% in 2000/01.

For the 2009/10 classification a different methodology was applied to produce a multitemporal classification as the majority approach is not applicable when combining two land use classifications. Therefore, different rules were applied to derive the multitemporal land use classes. With regard to the semi-natural classes these rules gave priority to the class with a higher percentage of trees. This might have led to a higher percentage of forest and a smaller percentage of grassland in the 2009/10 classification as compared to the historic land use classifications. The semi-natural classes are a continuum and therefore generally hard to distinguish. With the data that was available to this study, it seems unlikely to derive very accurate estimates of intra-class changes. However, the general decrease of semi-natural land is a reliable result of this study.

The location of the main land use changes (increase of urban area and increase of cropland) in the catchment suggests that urbanization causes a relocation of cropland from the former city fringes to the nearest possible location. An expansion of urban area was mainly

found at the fringes and in the northwest of the city of Pune (Fig. 3). In these areas cropland either decreased or increased only slightly (Fig. 4). The pronounced increase of cropland in the mid-northern part of the catchment (Fig. 3, Fig. 4), might be in part, a result of the urbanization process. As cropland is converted to urban area on the city fringes, arable grassland in the valleys of the Western Ghats is converted to cropland. It is reasonable that this relocation of cropland can be observed towards the west, as water availability increases there. The fact that cropland mainly increases in the northern part of the catchment may be due to better accessibility (e.g., highway) and a higher potential of arable land. The valleys in the southern part of the catchment are either covered with reservoirs or are very small and therefore not suitable for a major conversion to cropland.

The increase of the water yield and decrease in evapotranspiration due to an increase of built-up area (Fig. 6B, Fig. 7A) was also found in other studies (e.g., Im et al., 2009; Wijesekara et al., 2012). However, these impacts on water yield and evapotranspiration appear to be not very pronounced ( $< 8.1\%$ ) as compared to the rate of urbanization. This is possibly due to the monsoon dominated rainfall in the catchment. Heavy rains rapidly exceed the infiltration capacity of the soil and thus lead to Hortonian surface runoff. Therefore runoff on non-paved surfaces differs only slightly from runoff on paved surfaces, which is indicated by our results. Moreover, Du et al. (2012) found that the impact of urbanization on annual runoff is smaller as compared to its impact on floods. In particular, smaller floods are more affected than larger floods by an increase of impervious area (Du et al., 2012).

It has to be noted that a part of the increase of the water yield caused by urbanization results from conversion to high density urban area. High and medium urban density were not distinguished in the 1989/90 classification, as the total built-up land was significantly smaller as in 2009/10. Hence, the observed change in water yield is in part a consequence of the higher level of detail of the 2009/10 land use classification. In order to assess the impact of the distinguished high density area, the model was run for the land use of 2009/10 combining the two urban land use classes to one medium density class. A comparison with the previous results indicates that the higher urban density setup had a pronounced impact in sub-basin 17, which includes the inner city of Pune, and where half of the percentage change in water yield (3.9%) can be attributed to the high urban density setup. However, in the majority of the sub-basins (20) no effect or only a small effect on the water yield (accounting for less than 0.15%), and only a slight effect in the sub-basins 4, 5, 6, and 20 (accounting for 1.0%, 0.9%, 0.3% and 0.5%, respectively) can be observed. It should be taken into consideration that

urbanization can include an increased sealing of surfaces, which is possibly overestimated in case of sub-basin 17, but seems reasonable for the other sub-basins. The current assessment provides evidence that this process leads to an increase of the water yield.

It is well known that impacts on the annual water balance of a catchment are relatively small due to compensating effects in a catchment (e.g., Fohrer et al., 2001). In a large scale study on the Meuse River basin, Ashagrie et al. (2006) conclude that the overall impact of land use changes was too small to be detected. Wilk and Hughes (2002) argue that the complexity of large river basins could mask many of the impacts of land use changes that have been identified on smaller scales. Similarly, the FAO (2002) suggests that impacts of land use on hydrology can be studied best in small basins (< 1000 km<sup>2</sup>). In this study, this effect is underlined by the fact that impacts on the water balance cancel out on the catchment scale, whereas they are observable on the sub-basin scale, and are more pronounced in the smaller sub-basins (e.g., impact on ET in sub-basins 6, 11, 14, Fig 4; higher impacts on the water yield in smaller sub-basins, Fig. 7B).

## 5. Conclusions

Multitemporal land use classifications derived from multispectral satellite data provide suitable data to assess past land use changes. In the present study, urbanization was identified as the main driver of change in the study area. Urbanization has resulted in a shift of cropland towards the west, specifically into the valleys of the Western Ghats. As the rapid growth of the city of Pune is expected to progress, it can be expected that further urbanization will probably reduce the cropland in the study area, as a further shift towards the west is not possible (deforestation of the biodiversity-rich Western Ghats is unlikely). Thus, an increased demand for food due to population growth and a decreased supply of food due to decreased cropland will be a negative consequence of this development.

Our results regarding the water balance indicate that ongoing urbanization will result in less evapotranspiration and more runoff. In the mean annual water balance, this effect was balanced by an increase of cropland in some areas of the catchment. However, the annual course of runoff was changed, as urbanization resulted in more runoff in rainy season, whereas increased irrigation water withdrawal from the rivers led to less runoff in dry season. This change in runoff affects the downstream population, irrigation agriculture, and industries, all of whom rely heavily on the water supplied from the Mula and Mutha Rivers catchment. The loss of these resources for downstream water users could be prevented by storing the increased runoff in downstream reservoirs (e.g., in the Ujani dam). However, water users between Pune and the Ujani dam (about 100 km distance) would be affected by a decrease of runoff from the catchment in dry season. Beyond these implications for water quantity, further urbanization will obviously have negative effects on water quality (e.g., due to increased sewage water and industrial waste water).

The increase of the water yield was relatively moderate on the sub-basin level. On the one hand further urbanization towards the west may lead to more pronounced impacts (e.g., higher peak discharges, flooding) as the western part of the catchment receives significantly more precipitation than the eastern part. On the other hand, these impacts might be less pronounced as heavy rains rapidly exceed the infiltration capacity of the soil and thus seal the surface, resulting in the same effect on runoff as paved areas. Possibly, as indicated by Du et al. (2012), smaller floods may be affected by these changes. An analysis of future land use scenarios and their impacts on the water resources would shed light on the impacts of further urbanization in the Western Ghats.

## Acknowledgements

We gratefully acknowledge support by a grant from the German National Academic Foundation. We are grateful to IMD Pune, Water Resources Department Nashik, Khadakwasla Irrigation Division Pune, Groundwater Department Pune, Department of Agriculture Pune, and NRSC Hyderabad for supplying environmental data, cooperation and enlightened discussions. Moreover, we acknowledge the supply of ASTER data by the USGS Land Processes Distributed Active Archive Center. Special thanks go to the students from the Institute of Environment Education & Research at Bharati Vidyapeeth University Pune for assistance with the field measurements.

## Appendix A

Multitemporal land use classifications of 1989/90, 2000/01, and 2009/10. See Figures A1, A2, and A3, respectively.

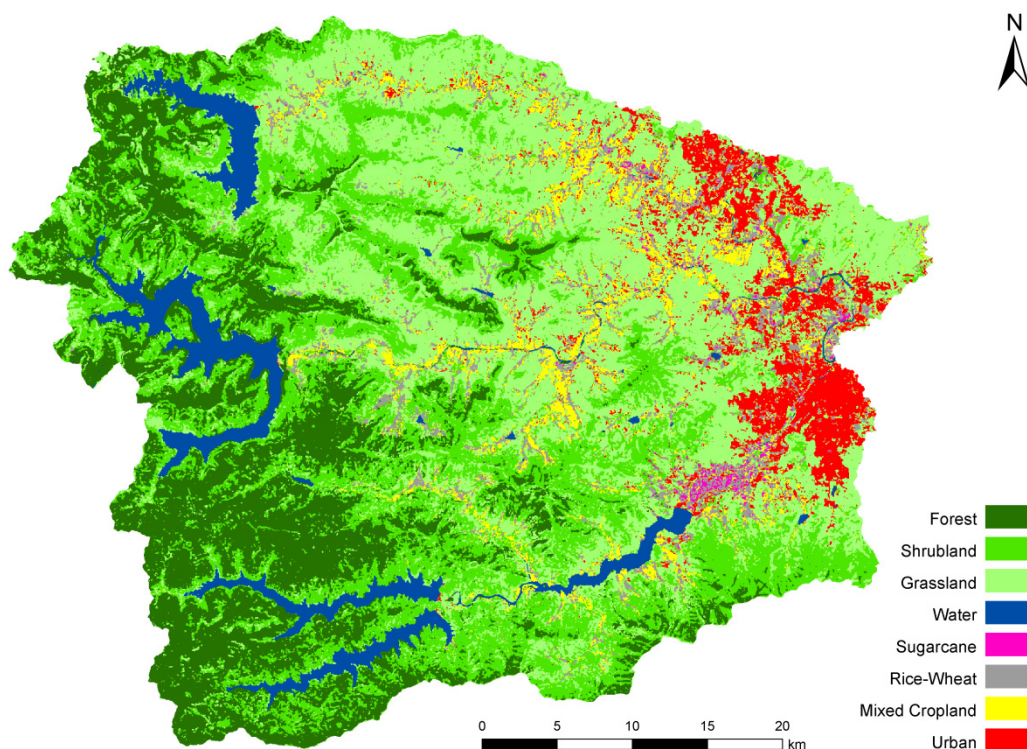


**Fig. A1** Multitemporal land use classification 1989/90.

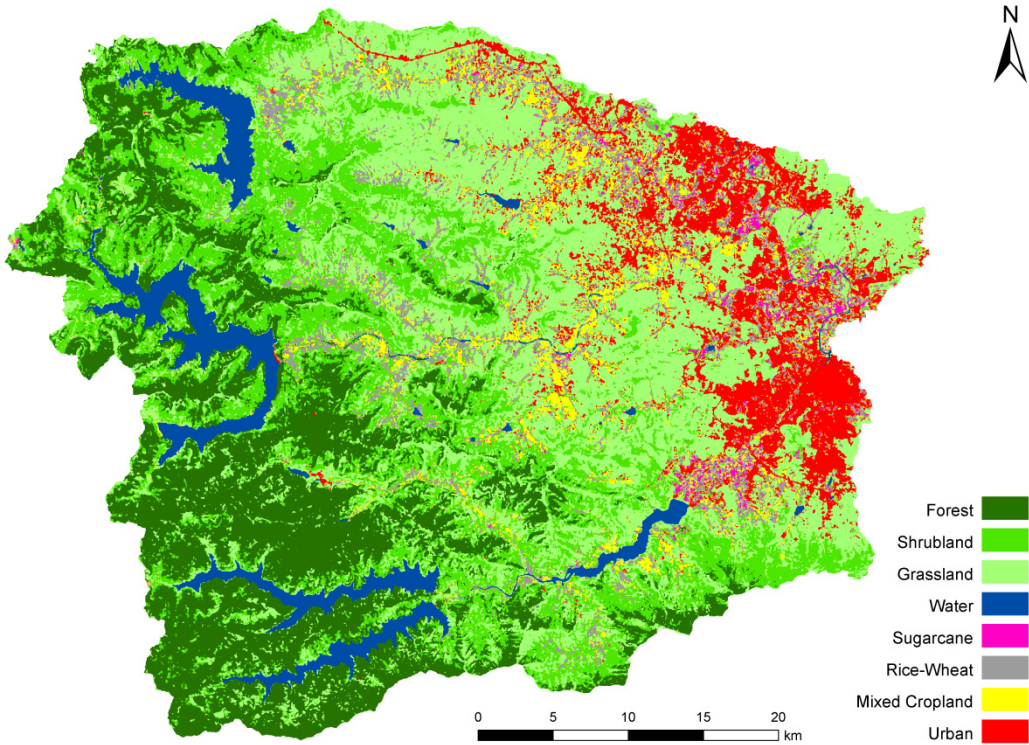


Fig. A2 Multitemporal land use classification 2000/01.

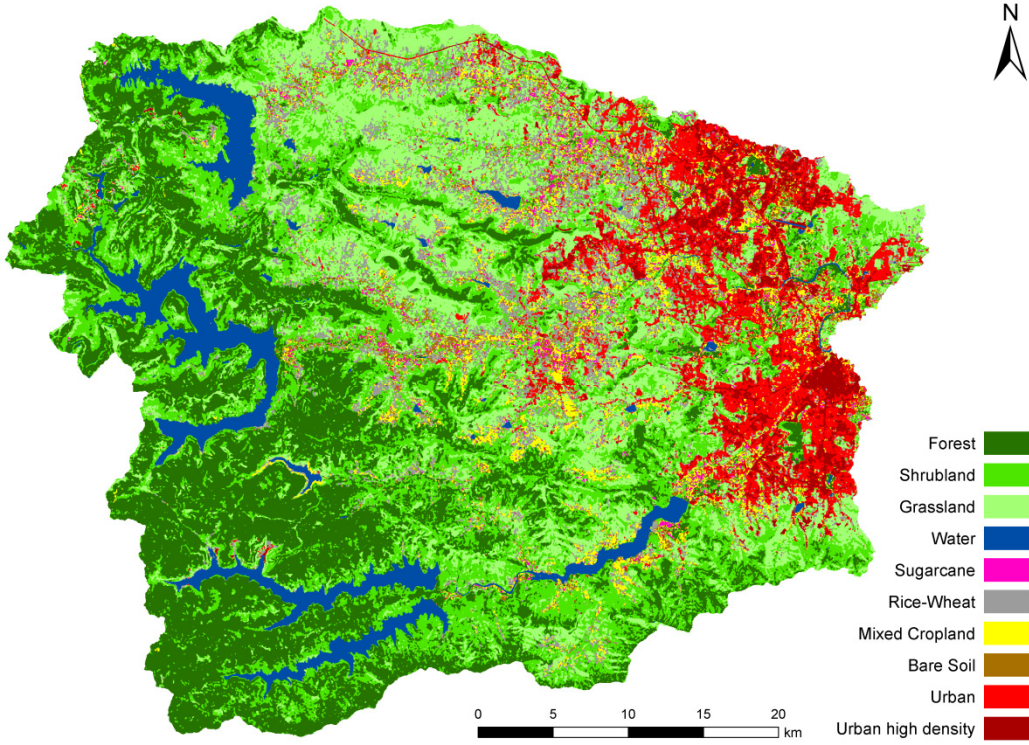


Fig. A3 Multitemporal land use classification 2009/10.

## References

- Arnold, J.G., Srinivasan, R., Muttiah, R.S., Williams, J.R., 1998. Large area hydrologic modeling and assessment - Part 1: Model development. *J. Am. Water Resour. Assoc.* 34, 73-89.
- Ashagrie, A.G., de Laat, P.J., de Wit, M.J., Tu, M., Uhlenbrook, S., 2006. Detecting the influence of land use changes on discharges and floods in the Meuse River Basin - the predictive power of a ninety-year rainfall-runoff relation? *Hydrol. Earth Syst. Sci.* 10, 691-701.
- Barthel, R., Reichenau, T.G., Krimly, T., Dabbert, S., Schneider, K., Hennicker, R., Mauser, W., 2012. Integrated modeling of global change impacts on agriculture and groundwater resources. *Water Resour. Manag.* 26(7), 1929-1951.
- Behera, S., Panda, R.K., 2006. Evaluation of management alternatives for an agricultural watershed in a sub-humid subtropical region using a physical process based model. *Agric. Ecosyst. Environ.* 113, 62-72.
- Bergström, S., Forsman, A., 1973. Development of a conceptual deterministic rainfall-runoff model. *Nord. Hydrol.* 4, 147-170.
- Chauhan, H.B., Nayak, S., 2005. Land use/land cover changes near Hazira Region, Gujarat using remote sensing satellite data. *J. Indian Soc. Remote Sens.* 33(3), 413-420.
- DeFries, R., Eshleman, K.N., 2004. Land-use change and hydrologic processes: a major focus for the future. *Hydrol. Process.* 18, 2183-2186.
- Du, Y., Chang, C.-I., Ren, H., Chang, C.-C., Jensen, J.O., D'Amico, F.M., 2004. New hyperspectral discrimination measure for spectral characterization. *Opt. Eng.* 43(8), 1777-1786.
- Du, J., Qian, L., Rui, H., Zuo, T., Zheng, D., Xu, Y., Xu, C.-Y., 2012. Assessing the effects of urbanization on annual runoff and flood events using an integrated hydrological modeling system for Qinhuai River basin, China. *J. Hydrol.* 464-465, 127-139.
- Fohrer, N., Haverkamp, S., Eckhardt, K., Frede, H.-G., 2001. Hydrologic Response to land use changes on the catchment scale. *Phys. Chem. Earth (B)* 26(7-8), 577-582.
- Food and Agriculture Organization of the United Nations (FAO), 2002. Land-water linkages in rural catchments. Land and water bulletin 9, FAO, Rome.
- Food and Agriculture Organization of the United Nations (FAO), 2003. Digital Soil Map of the World and Derived Soil Properties, FAO, Rome.

- Gadgil, A., 2002. Rainfall characteristics of Maharashtra. In: Diddee, J., Jog, S.R., Kale, V.S., Datye, V.S. (Eds.), *Geography of Maharashtra*. Rawat Publications, Jaipur, pp. 89-102.
- Garg, K.K., Karlberg, L., Barron, J., Wani, S.P., Rockstrom, J., 2012a. Assessing impacts of agricultural water interventions in the Kothapally watershed, Southern India. *Hydrol. Process.* 26, 387-404.
- Garg, K.K., Wani, S.P., Barron, J., Karlberg, L., Rockstrom, J., 2012b. Up-scaling potential impacts on water flows from agricultural water interventions: opportunities and trade-offs in the Osman Sagar catchment, Musi sub-basin, India. *Hydrol. Process.* in press, doi: 10.1002/hyp.9516.
- Gassman, P.W., Reyes, M., Green, C.H., Arnold, J.G., 2007. The Soil and Water Assessment Tool: Historical development, applications, and future directions. *Trans. ASABE* 50(4), 1211-1250.
- Ghaffari, G., Keesstra, S., Ghodousi, J., Ahmadi, H., 2010. SWAT-simulated hydrological impact of land-use change in the Zanjanrood basin, Northwest Iran. *Hydrol. Process.* 24, 892-903.
- Government of India, 2011. Population Growth - Levels and Trends. In: *Census of India 2011, Provisional Population Totals, Paper 1 of 2011: Maharashtra*. Available at: [http://www.censusindia.gov.in/2011-prov-results/data\\_files/maharashtra/7-%20Chapter%20-%204.pdf](http://www.censusindia.gov.in/2011-prov-results/data_files/maharashtra/7-%20Chapter%20-%204.pdf). Accessed 11 October 2012.
- Gunnell, Y., 1997. Relief and climate in South Asia: The influence of the Western Ghats on the current climate pattern of peninsular India. *Int. J. Climatol.* 17, 1169-1182.
- Hansen, M., DeFries, R., Townshend, J.R.G., Sohlberg, R., 1998. *UMD Global Land Cover Classification*. Department of Geography, University of Maryland, College Park, Maryland.
- Huisman, J.A., Breuer, L., Bormann, H., Bronstert, A., Croke, B.F.W., Frede, H.-G., Gräff, T., Hubrechts, L., Jakeman, A.J., Kite, G., Lanini, J., Leavesley, G., Lettenmaier, D.P., Lindström, G., Seibert, J., Sivapalan, M., Viney, N.R., Willems, P., 2009. Assessing the impact of land use change on hydrology by ensemble modeling (LUCHEM) III: Scenario analysis. *Adv. Water Resour.* 32(2), 159-170.
- Im, S., Kim, H., Kim, C., Jang, C., 2009. Assessing the impacts of land use changes on watershed hydrology using MIKE SHE. *Environ. Geol.* 57, 231-239.

- Immerzeel, W.W., Gaur, A., Zwart, S.J., 2008. Integrating remote sensing and a process-based hydrological model to evaluate water use and productivity in a south Indian catchment. *Agric. Water Manage.* 95, 11-24.
- Jayakumar, S., Arockiasamy, D., 2003. Land use/land cover mapping and change detection in part of Eastern Ghats of Tamil Nadu using remote sensing and GIS. *J. Indian Soc. Remote Sens.* 31, 251-260.
- Jensen, J.R., 2007. *Remote Sensing of the Environment: An Earth Resource Perspective*, second ed. Pearson Prentice Hall, Upper Saddle River, New Jersey.
- Jha, C.S., Dutt, C.B.S., Bawa, K.S., 2000. Deforestation and land use changes in Western Ghats, India. *Curr. Sci.* 79(2), 231-238.
- Khan, H.H., Khan, A., Ahmed, S., Perrin, J., 2011. GIS-based impact assessment of land-use changes on groundwater quality: Study from a rapidly urbanizing region of South India. *Environ. Earth Sci.* 63(6), 1289-1302.
- Klöcking, B., Haberlandt, U., 2002. Impact of land use changes on water dynamics - a case study in temperate meso and macroscale river basins. *Phys. Chem. Earth* 27, 619-629.
- Legesse, D., Vallet-Coulomb, C., Gasse, F., 2003. Hydrological response of a catchment to climate and land use changes in Tropical Africa: case study South Central Ethiopia. *J. Hydrol.* 275(1-2), 67-85.
- Li, Z., Liu, W., Zhang, X., Zheng, F., 2009. Impacts of land use change and climate variability on hydrology in an agricultural catchment on the Loess Plateau of China. *J. Hydrol.* 377(1-2), 35-42.
- Mango, L.M., Melesse, A.M., McClain, M.E., Gann, D., Setegn, S.G., 2011. Land use and climate change impacts on the hydrology of the upper Mara River Basin, Kenya: results of a modeling study to support better resource management. *Hydrol. Earth Syst. Sci.* 15, 2245-2258.
- Matthew, M.W., Adler-Golden, S.M., Berk, A., Richtsmeier, S.C., Levine, R.Y., Bernstein, L.S., Acharya, P.K., Anderson, G.P., Felde, G.W., Hoke, M.P., Ratkowski, A., Burke, H.-H., Kaiser, R.D., Miller, D.P., 2000. Status of atmospheric correction using a MODTRAN4-based algorithm. *SPIE Proceedings 4049, Algorithms for Multispectral, Hyperspectral, and Ultraspectral Imagery VI.*, April 24, 2000, Orlando, Florida, 199-207.

- Miller, S.N., Kepner, W.G., Mehaffey, M.H., Hernandez, M., Miller, R.C., Goodrich, D.C., Devonald K.K., Heggem, D.T., Miller, W.P., 2002. Integrating landscape assessment and hydrologic modeling for land cover change analysis. *J. Am. Water Resour. Assoc.* 38(4), 915-929.
- Mishra, A., Kar, S., Singh, V.P., 2007. Prioritizing structural management by quantifying the effect of land use and land cover on watershed runoff and sediment yield. *Water Resour. Manag.* 21, 1899-1913.
- Nash, J.E., Sutcliffe, J.V., 1970. River flow forecasting through conceptual models: Part I. A discussion of principles. *J. Hydrol.* 10(3), 282-290.
- Ndomba, P., Mtalo, F., Killingtveit, A., 2008. SWAT model application in a data scarce tropical complex catchment in Tanzania. *Phys. Chem. Earth* 33, 626-632.
- Neitsch, S.L., Arnold, J.G., Kiniry, J.R., Srinivasan, R., Williams, J.R., 2010. Soil and Water Assessment Tool: Input/Output File Documentation, Version 2009. Texas Water Resources Institute, Texas A&M University, College Station, Texas.
- Niehoff, D., Fritsch, U., Bronstert, A., 2002. Land-use impacts on storm-runoff generation: scenarios of land-use change and simulation of hydrological response in a meso-scale catchment in SW-Germany. *J. Hydrol.* 267(1-2), 80-93.
- Oetter, D.R., Cohen, W.B., Berterretche, M., Maersperger, T.K., Kennedy, R.E., 2000. Land cover mapping in an agricultural setting using multiseasonal Thematic Mapper data. *Remote Sens. Environ.* 76, 139-155.
- Peiman, R., 2011. Pre-classification and post-classification change-detection techniques to monitor land-cover and land-use change using multi-temporal Landsat imagery: a case study on Pisa Province in Italy. *Int. J. Remote Sens.* 32, 4365-4381.
- Ramesh, R., 2001. Effects of land-use change on groundwater quality in a coastal habitat of South India. *IAHS-AISH Publication* 269, 161-166.
- Refsgaard, J.C., Storm, B., 1995. MIKE SHE. In: Singh, V.P. (Ed.). *Computer Models of Watershed Hydrology*. Highlands Ranch, Colorado, pp. 809-846.
- Saha, A.K., Arora, M.K., Csaplovics, E., Gupta, R.P., 2005. Land Cover Classification Using IRS LISS III Image and DEM in a Rugged Terrain: A Case Study in Himalayas. *Geocarto Int.* 20(2), 33-40.

- Schulla, J., 1997. Hydrologische Modellierung von Flussgebieten zur Abschätzung der Folgen von Klimaänderungen. Zürcher Geographische Schriften 69, Geographisches Institut ETH, Zürich.
- Seeber, C., Hartmann, H., Xiang, W., King, L., 2010. Land use change and causes in the Xiangxi catchment, Three Gorges Area derived from multispectral data. *J. Earth Sci.* 21(6), 846-855.
- Sharma, E., Bhuchar, S., Xing, M., Kothiyari, B.P., 2007. Land use change and its impact on hydro-ecological linkages in Himalayan watersheds. *Trop. Ecol.* 48(2), 151-161.
- Sharma, T., Satya Kiran, P.V., Singh, T.P., Trivedi, A.V., Navalgund, R.R., 2001. Hydrologic response of a watershed to land use changes: A remote sensing and GIS approach. *Int. J. Remote Sens.* 22(11), 2095-2108.
- Singh, R.B., 2001. Impact of land-use change on groundwater in the Punjab-Haryana plains, India. IAHS-AISH Publication 269, 117-122.
- Stehr, A., Debels, P., Romero, F., Alcayaga, H., 2008. Hydrological modelling with SWAT under conditions of limited data availability: evaluation of results from a Chilean case study. *Hydrol. Sci. J.* 53, 588-601.
- Stonestrom, D.A., Scanlon, B.R., Zhang, L., 2009. Introduction to special section on Impacts of Land Use Change on Water Resources. *Water Resour. Res.* 45, W00A00.
- Story, M., Congalton, R.G., 1986. Accuracy assessment: A user's perspective. *Photogramm. Eng. Remote Sens.* 52(3), 397-399.
- Villarreal, M.L., Norman, L.M., Wallace, C.S.A., van Riper III, C., 2011. A multitemporal (1979-2009) land-use/land-cover dataset of the binational Santa Cruz Watershed. Open-File Report 2011-1131. U.S. Geological Survey, Reston, Virginia.
- Wagner, P.D., Fiener, P., Wilken, F., Kumar, S., Schneider, K., 2012. Comparison and evaluation of spatial interpolation schemes for daily rainfall in data scarce regions. *J. Hydrol.* 464-465, 388-400.
- Wagner, P.D., Kumar, S., Fiener, P., Schneider, K., 2011. Hydrological modeling with SWAT in a monsoon-driven environment - experience from the Western Ghats, India. *Trans. ASABE* 54(5), 1783-1790.
- Wijesekara, G.N., Gupta, A., Valeo, C., Hasbani, J.-G., Qiao, Y., Delaney, P., Marceau, D.J., 2012. Assessing the impact of future land-use changes on hydrological processes in the Elbow River watershed in southern Alberta, Canada. *J. Hydrol.* 412-413, 220-232.

- Wilk, J., Hughes, D.A., 2002. Simulating the impacts of land-use and climate change on water resource availability for a large south Indian catchment. *Hydrol. Sci. J.* 47(1), 19-30.
- Wolter, P.T., Mladenoff, D.J., Host, G.E., Crow, T.R., 1995. Improved forest classification in the Northern Lake States using multi-temporal Landsat imagery. *Photogramm. Eng. Remote Sens.* 61, 1129-1143.
- Yuan, F., Sawaya, K.E., Loeffelholz, B.C., Bauer, M.E., 2005. Land cover classification and change analysis of the Twin Cities (Minnesota) Metropolitan Area by multitemporal Landsat remote sensing. *Remote Sens. Environ.* 98, 317-328.

## 6 Summary of Results and Conclusions

The impacts of climate change and land use change on the water resources of the Mula and Mutha Rivers catchment (2036 km<sup>2</sup>) upstream of Pune, India, were analyzed in this thesis. The study area experiences seasonally limited water availability, rapid socio-economic development, and population growth. Thus, it represents characteristics of many regions in India, including the increasing pressure on the water resources. By using generally available data, local data, field measurements (field surveys, spectral measurements), and expert knowledge in a hydrologic modeling approach, impacts of climate change and past land use change on the water resources were analyzed. The developed methodology is transferable to other data scarce regions. Furthermore, the results indicate the major consequences of global change impacts in a monsoon-driven environment and thus allow for the development of water management adaptation and mitigation strategies.

### ***6.1 Use of generally available data for hydrologic modeling***

It was found that the Soil and Water Assessment Tool (SWAT) is suitable to simulate water fluxes in the studied monsoon-driven environment. A good representation of the catchment was achieved by using model parameters that were either estimated from GIS databases, were chosen from the literature, or else default model parameters were selected. However, necessary adaptations had to be made with regard to forest growth, setup of regional specific crop rotations, and water management schemes of major dams in the catchment. Regional knowledge and generally applicable principles (e.g., elevation dependence of temperature) are of particular value in data scarce regions as they can be used to preprocess and increase the quality and spatial representation of the input data. Satellite data was used to produce land use classifications, improve the forest parameterization, and to determine the spatial extension of the reservoirs for dam parameterization. Expert knowledge was employed to improve land use classifications by using thresholds for cropland, which is typically found below an elevation of 800 m and is unlikely on slopes greater than 10%. Based on only one point measurement, temperature and humidity values were calculated for

each sub-basin using the elevation dependence of temperature. Furthermore, a dam management scheme based on storage of water in rainy season and release of water in dry season was developed, which led to a pronounced increase in model performance. However, a multiple-site validation of the model with measured runoff indicated that the model performance varied in the different parts of the catchment. These shortcomings were primarily attributed to an insufficient representation of rainfall by the model. The use of only four rain gauges was not sufficient to achieve an accurate spatial representation of rainfall in all parts of the catchment. Particularly in the mountainous headwater sub-catchments, more rainfall measurements and suitable interpolation methods were needed to provide an accurate representation of the spatially variable rainfall input.

### ***6.2 Suitable interpolation methods for rainfall in data scarce regions***

Consequently, rainfall measurements from 16 gauges within or close to the catchment were employed and seven interpolation methods that differed in complexity and use of secondary information were tested. Spatial interpolation methods can significantly improve the spatial representation of input data for a hydrologic model. In the study area, the interpolation of rainfall had a pronounced impact on the accuracy of the catchment model. Particularly, the methods that used additional information from covariates were successful. Due to the catchments location in the downwind area of the Western Ghats, it was found that the frequently used covariate elevation was not suitable for rainfall interpolation in this study. The rain shadow of the main orographic barrier in the region, the Western Ghats escarpment, caused a general decrease of rainfall in the catchment from west to east. This decrease depends upon the distance from the escarpment rather than upon the difference in elevation. By correlating rainfall amounts to the distance in wind direction from the escarpment this relationship was empirically proven. Although the main prevalent climatic conditions are represented by this relationship, smaller scale variability cannot be addressed by this method. Satellite data such as a mean annual rainfall pattern derived from observations of the Tropical Rainfall Measuring Mission (TRMM) can provide such detail. Using the TRMM pattern as a covariate provided superior results as compared to the empiric relationship of distance in wind direction from the escarpment. Furthermore, the TRMM based interpolation methods are transferable to other regions within the range of the TRMM observations (38° S to 38° N). The applied geostatistical interpolation methods were modified to make them applicable with sparse input data. To this end, a monthly pooling approach was employed. Moreover, geostatistical methods have the advantage that they provide additional information, e.g.,

semivariograms show the spatial autocorrelation of rainfall. However, our results indicate that less computational intensive methods that make use of covariates (Regression-inverse distance weighting) yield good results as well.

It was found that the commonly used cross-validation of interpolation methods is not sufficient to identify the most suitable interpolation method in data scarce regions. Additional evidence that provides a measure of the spatial accuracy of the derived rainfall distribution is needed. Hydrologic models can be used to produce such evidence. Modeled runoff temporally and spatially integrates rainfall and can thus be used for a comparison with measured runoff. This provides a spatially integrative evaluation of the accuracy of the spatial rainfall distribution.

The most suitable interpolation method (regression kriging) indicated a good model performance on a daily time step using the available discharge data during rainy season. In the two sub-catchments that were less influenced by dam management the Nash-Sutcliffe efficiency was 0.68 and 0.67 and percentage bias was +4% and +24%, respectively. It has to be noted that this performance was achieved without accounting for an uncertainty range in runoff measurements, which would possibly have led to an even better evaluation of the model. Also, the model parameters were estimated based on measurements and generally available data. While a calibration of model parameters based on the comparison of modeled and measured runoff would possibly yield better model performance, it would also lead to a bias of the impact analysis. Thus a calibration of model parameters was not performed. Hence, a transferable methodology for hydrologic modeling in data scarce regions was developed that yields good model results.

### ***6.3 Climate change impacts on water resources***

A new downscaling approach was developed to link coarse data from a regional climate model to the catchment scale. This approach rearranges meteorological measurements from the baseline period according to the regional climate model data. By this means the interdependence of different climate variables is preserved, a consistent weather input is provided to the model, and the development of the climate variables in the regional climate model is reflected in the downscaled scenario data. The approach substitutes each scenario week by a best matching baseline week. The best match is determined in terms of temperature and rainfall similarity. The method is limited by the range of the values of the climate variables in the baseline period. If scenario temperatures exceed the temperature range of the baseline period it is more difficult to find a good match. The method is therefore more

suitable for the near future, whereas the later and hotter periods are underestimated. Hence, the impacts on the water resources were also underestimated at the end of the scenario period. However, it is expected that this approach will yield a better performance if measurements for a longer baseline period (with a larger range of temperature values) are available or if a closer match between regional climate model and measurements exists. This closer match can be realized in the future if the spatial resolution of regional climate models is increased.

Regional climate model data based on IPCC emission scenario A1B was used as an input to the developed downscaling technique. The hydrologic model was run with the rearranged weather data for the scenario period from 2020 to 2099. The climate change scenario indicated a temperature increase that led to higher annual evapotranspiration in the study area. However, the increase of actual evapotranspiration was not as pronounced as might be expected from the increase of potential evapotranspiration. This was due to the virtually unchanged water availability (no clear trend in future rainfall was discernible) that limited actual evapotranspiration. However, the intra-annual course of actual evapotranspiration indicated an earlier decrease of water availability in the dry season. Obviously, this temporal shift in water availability will affect agriculture as well as semi-natural vegetation.

It was also found that the more frequent and more extreme dry years had a pronounced impact on the storage capacity of the dams, which was frequently not met in the scenario period. The water storages at the end of the rainy season define water availability throughout the dry season. Thus, low water storages have severe consequences for different water users. First, the drinking water supply of the city of Pune is affected. Second, implications on energy production can be expected, posing a problem to the megacity Mumbai, which obtains energy from the hydropower plant at the largest reservoir in the catchment. Third, irrigation agriculture depends on the water storage in the reservoirs. It is likely that even more irrigation water is needed due to the increased temperatures and earlier decrease of water availability in dry season. This will make it more difficult to meet the irrigation water demand in dry years. Thus, an adaptation of water management including prioritizing water supply from reservoirs to different water users and more efficient irrigation techniques are needed to mitigate these impacts.

The analysis of climate change impacts was based on a single regional climate model. The developed downscaling technique is feasible for an application with other climate models. Using an ensemble of climate models or model realizations would increase the confidence in the probability and magnitude of the observed impacts. However, the reactions to the climate

change scenario were illustrated by the presented exemplary assessment. The vulnerability of the catchment to more frequent and more severe dry years and the earlier decrease of water availability in dry seasons as a result of increasing temperature are generally valid findings.

#### ***6.4 Land use change impacts on water resources***

The analysis of land use changes within the last 20 years in the study area indicated an increase of cropland from 9.7% to 13.5% and an increase of urban area from 5.1% to 10.1% of the catchment area. Semi-natural vegetation (forest, shrubland, and grassland) decreased from 79.8% to 70.7%. The applied methodology using multitemporal multispectral satellite data on a decadal basis in combination with ground truth measurements (field surveys and spectral measurements) was suitable to derive the temporal course and spatial distribution of the land use change within the past two decades. The locations of these changes suggest that a relocation of cropland has taken place, caused by ongoing urbanization and conversion of arable land to built-up area in the eastern part of the catchment. Cropland was relocated to more remote places in the western part of the catchment. It is likely that urbanization will continue, due to ongoing socio-economic development and population growth. However, a further increase of agricultural land seems unlikely because of a lack of suitable land.

With regard to the impacts of these changes on the water balance it was found that the negative and positive impacts cancel each other out in a long term average on the catchment level. An analysis on the sub-basin level revealed that urbanization led to an increase in runoff whereas an increase in cropland resulted in more evapotranspiration due to the increased use of irrigation water. Particularly in the dry season, irrigation agriculture resulted in increased water use and withdrawal from the rivers. These impacts lead to more runoff in rainy season (due to urbanization) and to less runoff in dry season (due to irrigation water use). Hence, downstream water users have more water when water availability is sufficient and less water when water is scarce. Future urbanization will exacerbate this effect. Thus while the annual water availability does not change significantly, the seasonal differences will increase. Downstream reservoirs such as the Ujani dam (about 100 km downstream of Pune) could be used to mitigate the impacts of the land use changes. Water users between Pune and the Ujani dam would be affected, unless additional small scale water storage solutions are implemented (e.g., small reservoirs, ponds, tanks). While these measures could help to mitigate the impacts on water quantity, additional measures need to be taken to mitigate the impact of urbanization (e.g., increased sewage water and industrial waste water) on water quality. The impact of urbanization on annual runoff is relatively small as compared to its effect on flooding.

Particularly smaller floods are affected by urbanization. However in the study area, these impacts might not be as pronounced as expected from the literature, as heavy monsoon rains rapidly exceed the infiltration capacity of the soil and thus seal the surface, resulting in the same effect on runoff as paved areas. An analysis of future land use scenarios and their impacts on the water resources would shed light on the impact of further urbanization in the high rainfall areas of the Western Ghats.

The analysis of land use changes revealed some uncertainty with regard to changes within the semi-natural land use class. But the general increase of cropland and urban area as well as the respective impacts on the water resources were very clear. As urbanization is likely to continue, the derived knowledge from the analysis of past changes can be used to mitigate likely future impacts.

### **6.5 General conclusions**

In this thesis a detailed knowledge on hydrologic modeling in data scarce regions and impacts of global change on water resources was acquired. In order to adapt a semi-distributed hydrologic model to the study area, suitable data preprocessing methods were developed, and model modifications were implemented. Hence, the model was used to analyze major impacts of climate change and past land use changes on the water resources in the study area.

It was found that generally available datasets (e.g., DEM, soil map, and satellite images) provide useful information. However, these data have to be combined with locally available data and knowledge (e.g., rainfall data, runoff data, topographic maps, field measurements, local expert knowledge) in order to derive a suitable representation of the study area. A thorough data analysis, including quality checks and gap filling has to be applied. This is important to make sure that the “garbage in, garbage out” principle (Beven, 2001) does not apply, particularly if sparse input data are used. The spatial representation of rainfall was important because it had a major impact on the model performance. A methodology was developed that combines generally available data with locally available data. In this context, the use of remote sensing data (DEM, land use classifications, covariate for rainfall interpolation, derivation of model parameters) for hydrologic modeling was very clear in this thesis. Particularly, the TRMM based rainfall pattern that was used as a covariate for rainfall interpolation will be useful in future studies. The methodology is transferable to other data scarce tropical and sub-tropical regions. It may be adopted for predictions in ungauged basins

and therefore contributes to the research aims of the decadal initiative (2003-2012) of the International Association of Hydrological Sciences on this topic.

The knowledge of the study area was enhanced, by building a hydrologic model for the studied catchment. Rainfall characteristics were identified, past land use changes - which are likely to continue in the future - were assessed, and a possible future climate for the 21<sup>st</sup> century was calculated by downscaling a climate scenario to the catchment scale. It was thus analyzed how the catchment's hydrology reacts to global change impacts. More frequent dry years will limit water availability in the dry season and temperature increases will result in an earlier decrease of water availability in the dry season. The major land use changes in the catchment were urbanization and an increase of cropland. While urbanization led to an increase in runoff in rainy season, the increase of cropland resulted in a decrease of runoff and an increase of evapotranspiration in dry season. Thus, the combined impact of climate change and land use change would particularly affect water availability in dry season, so that water scarcity would become more severe in a time of the year when water availability is already limited.

The catchment experiences socio-economic development, population growth and seasonally limited water availability like many other regions in India. However, the area is relatively water rich, which is a major difference when compared to other regions. Additionally, the large reservoirs in the catchment allow for the ability to manage water supply in the catchment. Thus, if suitable mitigation strategies are developed and water management is adapted, it is likely that major impacts on the water resources can be mitigated. Many other Indian regions which have less water resources and which are dependent on upstream regions have fewer opportunities to mitigate the impacts of global change.

As the catchment is relatively water rich it supplies water to water users outside the catchment. These are mainly downstream water users, since the river drains towards the east, crosses the dry Deccan Plateau (and thus the entire Indian subcontinent) until it drains into the Bay of Bengal. Furthermore, the largest reservoir in the catchment serves for power generation for the megacity Mumbai. As the hydropower plant uses the elevation difference at the Western Ghats escarpment, the water drains towards the west and is therefore lost for further use in the catchment or by water users downstream of Pune. Thus, these water users are also affected by the impacts on the catchment's water resources. In the assessment of past land use change impacts, the impacts on the annual water balance cancel out on the catchment

level. However, the changes result in more runoff in rainy season (due to urbanization) and less runoff in dry season (due to irrigation water use) so that water is supplied to downstream water users at different, less favorable times. This effect can be balanced by storing the water downstream of the catchment. Either existing large reservoirs (Ujani dam) or the construction of smaller reservoirs, ponds, or water tanks can be used for this purpose. Additional measures need to be taken to mitigate the impact of further urbanization on water quality. Climate change effects such as the higher frequency of dry years similarly affect water users outside the catchment. Particularly the impacts on the water storage in the Mulshi dam will affect electricity supply to Mumbai. Therefore, future mitigation strategies will have to balance and prioritize the supply of water to different water users inside and outside of the catchment. This is obviously a challenging future research question.

With regard to future research, it would be beneficial to couple hydrologic and socio-economic models so that an integrative assessment of water availability and demand is possible. Such integrative modeling approaches could be used to develop and test water management strategies, which are suitable to mitigate the effects of global change on the water resources. Since the developed methodology is transferable to other regions, it would be worthwhile to apply it to other regions, e.g., regions with even less data. This transfer would indicate if additional preprocessing measures or local measurements are necessary to cover up for missing data. Generally, additional data is useful to improve models. Regarding the hydrologic model for the Mula and Mutha Rivers catchment, the most promising improvements may be expected from i) additional measurements of runoff in an unmanaged sub-catchment and of rainfall on the top ridges of the Western Ghats, and ii) more detailed information on reservoir discharge. The developed downscaling method can be used with other regional climate models to assess the probability of future climate changes in the study area. This would increase the confidence in the probability and in the magnitude of the expected climate change impacts. Furthermore, the development of future land use scenarios based on the analyzed past land use changes would allow for a spatially distributed analysis of future land use change impacts. A scenario assessment that includes the combined effects of climate change and land use change on the water resources would be of particular interest for the local water managers.

# References\*

- Arnold, C.L., Gibbons, C.J., 1996. Impervious surface coverage: the emergence of a key environmental indicator. *J. Am. Plan. Assoc.* 62(2), 243-258.
- Arnold, J.G., Moriasi, D.N., Gassman, P.W., Abbaspour, K.C., White, M.J., Srinivasan, R., Santhi, C., Harmel, R.D., van Griensven, A., Van Liew, M.W., Kannan, N., Jha, M.K., 2012. SWAT: Model use, calibration, and validation. *Trans. ASABE* 55(4), 1491-1508.
- Arnold, J.G., Srinivasan, R., Muttiah, R.S., Williams, J.R., 1998. Large area hydrologic modeling and assessment - Part 1: Model development. *J. Am. Water Resour. Assoc.* 34, 73-89.
- Behera, S., Panda, R.K., 2006. Evaluation of management alternatives for an agricultural watershed in a sub-humid subtropical region using a physical process based model. *Agric. Ecosyst. Environ.* 113, 62-72.
- Beven, K.J., 2001. *Rainfall-runoff Modelling: The Primer*. John Wiley & Sons Ltd., Chichester.
- Beven, K.J., Kirkby, M.J., 1979. A physically based, variable contributing area model of basin hydrology. *Hydrol. Sci. Bull.* 24(1), 43-69.
- Bouraoui, F., Benabdallah, S., Jrad, A., Bidoglio, G., 2005. Application of the SWAT model on the Medjerda River basin (Tunisia). *Phys. Chem. Earth. (A/B/C)* 30(8-10), 497-507.
- Cao, W., Bowden, W.B., Davie, T., Fenemor, A., 2006. Multi-variable and multi-site calibration and validation of SWAT in a large mountainous catchment with high spatial variability. *Hydrol. Process.* 20, 1057-1073.
- Chaponnière, A., Boulet, G., Chehbouni, A., Aresmouk, M., 2008. Understanding hydrological processes with scarce data in a mountain environment. *Hydrol. Process.* 22, 1908-1921.
- Chauhan, H.B., Nayak, S., 2005. Land use/land cover changes near Hazira Region, Gujarat using remote sensing satellite data. *J. Indian Soc. Remote Sens.* 33(3), 413-420.
- CIA World Factbook, 2012. India: Economy. Available at: <https://www.cia.gov/library/publications/the-world-factbook/geos/in.html#Econ>. Accessed 8 November 2012.

---

\* References for chapter 1 and chapter 6

- Conan, C., de Marsily, G., Bouraoui, F., Bidoglio, G., 2003. A long-term hydrological modelling of the Upper Guadiana River basin (Spain). *Phys. Chem. Earth (A/B/C)* 28(4-5), 193-200.
- Costa, M.H., Botta, A., Cardille, J.A., 2003. Effects of large-scale changes in land cover on the discharge of the Tocantins River, Southeastern Amazonia. *J. Hydrol.* 283(1-4), 206-217.
- DeFries, R., Eshleman, K.N., 2004. Land-use change and hydrologic processes: a major focus for the future. *Hydrol. Process.* 18, 2183-2186.
- Dhar, S., Mazumdar, A., 2009. Hydrological modelling of the Kangsabati River under changed climate scenario: case study in India. *Hydrol. Process.* 23, 2394-2406.
- Diaz-Nieto J., Wilby R.L., 2005. A comparison of statistical downscaling and climate change factor methods: impacts on low flows in the River Thames, United Kingdom. *Clim. Change* 69(2), 245-268.
- Foley, J.A., DeFries, R., Asner, G.P., Barford, C., Bonan, G., Carpenter, S.R., Chapin, F.S., Coe, M.T., Daily, G.C., Gibbs, H.K., Helkowski, J.H., Holloway, T., Howard, E.A., Kucharik, C.J., Monfreda, C., Patz, J.A., Prentice, I.C., Ramankutty, N., Snyder, P.K., 2005. Global Consequences of Land Use. *Science* 309(5734), 570-574.
- Fowler, H.J., Blenkinsop, S., Tebaldi, C., 2007. Linking climate change modelling to impacts studies: recent advances in downscaling techniques for hydrological modelling. *Int. J. Climatol.* 27, 1547-1578.
- Gadgil, S., 2003. The Indian monsoon and its variability. *Annu. Rev. Earth Planet. Sci.* 31, 429-467.
- Garg, K.K., Wani, S.P., Barron, J., Karlberg, L., Rockstrom, J., 2012. Up-scaling potential impacts on water flows from agricultural water interventions: opportunities and trade-offs in the Osman Sagar catchment, Musi sub-basin, India. *Hydrol. Process.* in press, doi: 10.1002/hyp.9516.
- Gassman, P.W., Reyes, M., Green, C.H., Arnold, J.G., 2007. The Soil and Water Assessment Tool: Historical development, applications, and future directions. *Trans. ASABE* 50(4), 1211-1250.
- Ghaffari, G., Keesstra, S., Ghodousi, J., Ahmadi, H., 2010. SWAT-simulated hydrological impact of land-use change in the Zanjanrood basin, Northwest Iran. *Hydrol. Process.* 24, 892-903.

- Gleick, P.H., 2003. Water Use. *Annu. Rev. Environ. Resour.* 28, 275-314.
- Gosain, A.K., Rao, S., Arora, A., 2011. Climate change impact assessment of water resources of India. *Curr. Sci.* 101(3), 356-371.
- Gosain, A.K., Rao, S., Basuray, D., 2006. Climate change impact assessment on hydrology of Indian river basins. *Curr. Sci.* 90(3), 346-353.
- Houser, P., Shuttleworth, W., Famiglietti, J., Gupta, H., Syed, K., Goodrich, D., 1998. Integration of soil moisture remote sensing and hydrologic modeling using data assimilation. *Water Resour. Res.* 34(12), 3405-3420.
- Im, S., Kim, H., Kim, C., Jang, C., 2009. Assessing the impacts of land use changes on watershed hydrology using MIKE SHE. *Environ. Geol.* 57, 231-239.
- Immerzeel, W.W., Droogers, P., 2008. Calibration of a distributed hydrological model based on satellite evapotranspiration. *J. Hydrol.* 349(3-4), 411-424.
- Immerzeel, W.W., Gaur, A., Zwart, S.J., 2008. Integrating remote sensing and a process-based hydrological model to evaluate water use and productivity in a south Indian catchment. *Agric. Water Manage.* 95, 11-24.
- IPCC, 2007a. *Climate Change 2007: Impacts, Adaptation and Vulnerability. Contribution of Working Group II to the Fourth Assessment Report of the Intergovernmental Panel on Climate Change.* Cambridge University Press, Cambridge.
- IPCC, 2007b. *Climate Change 2007: The Physical Science Basis. Contribution of Working Group I to the Fourth Assessment Report of the Intergovernmental Panel on Climate Change.* Cambridge University Press, Cambridge.
- Jayakumar, S., Arockiasamy, D., 2003. Land use/land cover mapping and change detection in part of Eastern Ghats of Tamil Nadu using remote sensing and GIS. *J. Indian Soc. Remote Sens.* 31, 251-260.
- Jha, M., Arnold, J.G., Gassman, P.W., Giorgi, F., Gu, R.R., 2006. Climate change sensitivity assessment on upper Mississippi river basin streamflows using SWAT. *J. Am. Water Resour. Assoc.* 42(4), 997-1015.
- Jha, C.S., Dutt, C.B.S., Bawa, K.S., 2000. Deforestation and land use changes in Western Ghats, India. *Curr. Sci.* 79(2), 231-238.
- Kelkar, U., Narula, K.K., Sharma, V.P., Chandna, U., 2008. Vulnerability and adaptation to climate variability and water stress in Uttarakhand State, India. *Glob. Environ. Change* 18(4), 564-574.

- Kim, N.W., Chung, I.M., Won, Y.S., Arnold, J.G., 2008. Development and application of the integrated SWAT-MODFLOW model. *J. Hydrol.* 356(1-2), 1-16.
- Kirchner, J.W., 2006. Getting the right answers for the right reasons: Linking measurements, analyses, and models to advance the science of hydrology. *Water Resour. Res.* 42, W03S04.
- Kripalani, R.H., Kulkarni, A., Sabade, S.S., Khandekar, M.L., 2003. Indian monsoon variability in a global warming scenario. *Nat. Hazards* 29, 189-206.
- Kusre, B.C., Baruah, D.C., Bordoloi, P.K., Patra, S.C., 2010. Assessment of hydropower potential using GIS and hydrological modeling technique in Kopili River basin in Assam (India). *Appl. Energy* 87(1), 298-309.
- Liu, L., Liu, Z., Ren, X., Fischer, T., Xu, Y., 2011. Hydrological impacts of climate change in the Yellow River Basin for the 21st century using hydrological model and statistical downscaling model. *Quat. Int.* 244(2), 211-220.
- Mango, L.M., Melesse, A.M., McClain, M.E., Gann, D., Setegn, S.G., 2011. Land use and climate change impacts on the hydrology of the upper Mara River Basin, Kenya: results of a modeling study to support better resource management. *Hydrol. Earth Syst. Sci.* 15, 2245-2258.
- Miller, S.N., Kepner, W.G., Mehaffey, M.H., Hernandez, M., Miller, R.C., Goodrich, D.C., Devonald K.K., Heggem, D.T., Miller, W.P., 2002. Integrating landscape assessment and hydrologic modeling for land cover change analysis. *J. Am. Water Resour. Assoc.* 38(4), 915-929.
- Mishra, A., Kar, S., Singh, V.P., 2007. Prioritizing structural management by quantifying the effect of land use and land cover on watershed runoff and sediment yield. *Water Resour. Manag.* 21, 1899-1913.
- Moriasi, D.N., Wilson, B.N., Douglas-Mankin, K.R., Arnold, J.G., Gowda, P.H., 2012. Hydrologic and water quality models: Use, calibration, and validation. *Trans. ASABE* 55(4), 1491-1508.
- Mulligan, M., 2004. Modelling Catchment Hydrology. In: *Environmental Modelling. Finding Simplicity in Complexity.* Wainwright, J., Mulligan, M. (Eds.), John Wiley & Sons Ltd., Chichester.

- Nakićenović, N., Alcamo, J., Davis, G., de Vries, B., Fenhann, J., Gaffin, S., Gregory, K., Grübler, A., Jung, T.Y., Kram, T., La Rovere, E.L., Michaelis, L., Mori, S., Morita, T., Pepper, W., Pitcher, H., Price, L., Riahi, K., Roehrl, A., Rogner, H.-H., Sankovski, A., Schlesinger, M., Shukla, P., Smith, S., Swart, R., van Rooijen, S., Victor, N., Dadi, Z., 2000. Special Report on Emissions Scenarios. A Special Report of Working Group III of the Intergovernmental Panel on Climate Change. Cambridge University Press, Cambridge.
- Ndomba, P., Mtalo, F., Killingtveit, A., 2008. SWAT model application in a data scarce tropical complex catchment in Tanzania. *Phys. Chem. Earth* 33, 626-632.
- Notter, B., Hurni, H., Wiesmann, U., Abbaspour, K.C., 2012. Modelling water provision as an ecosystem service in a large East African river basin. *Hydrol. Earth Syst. Sci.* 16, 69-86.
- Oreskes, N., 2004. Beyond the Ivory Tower. The scientific consensus on climate change. *Science* 306(5702), 1686.
- Pandey, V.K., Panda, S.N., Pandey, A., Sudhakar, S., 2009. Evaluation of effective management plan for an agricultural watershed using AVSWAT model, remote sensing and GIS. *Environ. Geol.* 56(5), 993-1008.
- Park, J.-Y., Park, M.-J., Joh, H.-K., Shin, H.-J., Kwon, H.-J., Srinivasan, R., Kim, S.-J., 2011. Assessment of MIROC3.2 HiRes climate and CLUE-s land use change impacts on watershed hydrology using SWAT. *Trans. ASABE* 54(5), 1713-1724.
- Pohlert, T., Huisman, J.A., Breuer, L., Frede, H.-G., 2007. Integration of a detailed biogeochemical model into SWAT for improved nitrogen predictions - Model development, sensitivity, and GLUE analysis. *Ecol. Model.* 203(3-4), 215-228.
- Ramankutty, N., Graumlich, L., Achard, F., Alves, D., Chhabra, A., DeFries, R.S., Foley, J.A., Geist, H., Houghton, R.A., Klein Goldewijk, K., Lambin, E.F., Millington, A., Rasmussen, K., Reid, R.S., Turner II, B.L., 2006. Global land-cover change: recent progress, remaining challenges. In: Lambin, E.F., Geist, H. (Eds.). *Land-use and land-cover change: local processes and global impacts*. Springer, Berlin, pp. 9-39.
- Refsgaard, J.C., Storm, B., 1995. MIKE SHE. In: Singh, V.P. (Ed.). *Computer Models of Watershed Hydrology*. Highlands Ranch, Colorado, pp. 809-846.
- Sahin, V., Hall, M.J., 1996. The effects of afforestation and deforestation on water yields. *J. Hydrol.* 178(1-4), 293-309.

- Schneider, K., 2003. Assimilating remote sensing data into a land surface process model. *Int. J. Remote Sens.* 24(14), 2959-2980.
- Seeber, C., Hartmann, H., Xiang, W., King, L., 2010. Land use change and causes in the Xiangxi catchment, Three Gorges Area derived from multispectral data. *J. Earth Sci.* 21(6), 846-855.
- Sharma, E., Bhuchar, S., Xing, M., Kothiyari, B.P., 2007. Land use change and its impact on hydro-ecological linkages in Himalayan watersheds. *Trop. Ecol.* 48(2), 151-161.
- Simonovic, S.P., 2002. World water dynamics: global modeling of water resources. *J. Environ. Manage.* 66, 249-267.
- Singh, V.P. 1995. Watershed modeling. In: Singh, V.P. (Ed.), *Computer models of watershed hydrology*. Water Resources Publications, Highlands Ranch, Colorado, pp. 1-22.
- Sivapalan, M., Takeuchi, K., Franks, S.W., Gupta, V.K., Karambiri, H., Lakshmi, V., Liang, X., McDonnell, J.J., Mendiondo, E.M., O'Connell, P.E., Oki, T., Pomeroy, J.W., Schertzer, D., Uhlenbrook, S., Zehe, E., 2003. IAHS decade on predictions in ungauged basins (PUB), 2003-2012: shaping an exciting future for the hydrological sciences. *Hydrol. Sci. J.* 48(6), 857-880.
- Sophocleous, M.A., Koelliker, J.K., Govindaraju, R.S., Birdie, T., Ramireddygari, S.R., Perkins, S.P., 1999. Integrated numerical modeling for basin-wide water management: The case of the Rattlesnake Creek basin in south-central Kansas. *J. Hydrol.* 214(1-4), 179-196.
- Stehr, A., Debels, P., Romero, F., Alcayaga, H., 2008. Hydrological modelling with SWAT under conditions of limited data availability: evaluation of results from a Chilean case study. *Hydrol. Sci. J.* 53(3), 588-601.
- Stonestrom, D.A., Scanlon, B.R., Zhang, L., 2009. Introduction to special section on Impacts of Land Use Change on Water Resources. *Water Resour. Res.* 45, W00A00.
- SWAT Literature Database, 2012. SWAT Literature Database for Peer-Reviewed Journal Articles. Available at: [https://www.card.iastate.edu/swat\\_articles](https://www.card.iastate.edu/swat_articles). Accessed 29 October 2012.
- Teutschbein, C., Seibert, J., 2010. Regional Climate Models for Hydrological Impact Studies at the Catchment Scale: A Review of Recent Modeling Strategies. *Geogr. Compass* 4, 834-860.

- Timmermann, A., Oberhuber, J., Bacher, A., Esch, M., Latif, M., Roeckner, E., 1999. Increased El Niño frequency in a climate model forced by future greenhouse warming. *Nature* 398, 694-697.
- Tripathi, M.P., Panda, R.K., Raghuwanshi, N.S., 2005. Development of effective management plan for critical subwatersheds using SWAT model. *Hydrol. Process.* 19, 809-826.
- United Nations, 2012. *World Urbanization Prospects: The 2011 Revision, CD-ROM Edition.* Department of Economic and Social Affairs, Population Division, New York.
- Vincendon, B., Ducrocq, V., Saulnier, G.-M., Bouilloud, L., Chancibault, K., Habets, F., Noilhan, J., 2010. Benefit of coupling the ISBA land surface model with a TOPMODEL hydrological model version dedicated to Mediterranean flash-floods. *J. Hydrol.* 394(1-2), 256-266.
- Vörösmarty, C.J., Green, P., Salisbury, J., Lammers, R.B., 2000. Global water resources: Vulnerability from climate change and population growth. *Science* 289, 284-288.
- Vörösmarty, C.J., McIntyre, P.B., Gessner, M.O., Dudgeon, D., Prusevich, A., Green, P., Glidden, S., Bunn, S.E., Sullivan, C.A., Reidy Liermann, C., Davies, P.M., 2010. Global threats to human water security and river biodiversity. *Nature* 467, 555-561.
- Watson, B.M., McKeown, R.A., Putz, G., MacDonald, J.D., 2008. Modification of SWAT for modelling streamflow from forested watersheds on the Canadian Boreal Plain. *J. Environ. Eng. Sci.* 7(S1), 145-159.
- Wijesekara, G.N., Gupta, A., Valeo, C., Hasbani, J.-G., Qiao, Y., Delaney, P., Marceau, D.J., 2012. Assessing the impact of future land-use changes on hydrological processes in the Elbow River watershed in southern Alberta, Canada. *J. Hydrol.* 412-413, 220-232.
- World Bank, 2012. *India: World Development Indicators.* Available at: <http://data.worldbank.org/country/india>. Accessed 8 November 2012.

# Eigenbeteiligung an den Veröffentlichungen

An den in dieser Arbeit verwendeten Fachartikeln und den ihnen zugrunde liegenden wissenschaftlichen Arbeiten (Feldmessungen, Methodenentwicklung, Modellierung, Analyse der Ergebnisse, Konzeption und Ausarbeitung der Artikel) habe ich maßgeblichen Anteil. Dies wird durch meine Erstautorenschaft in allen verwendeten Teilpublikationen belegt.

# Erklärung

Ich versichere, dass ich die von mir vorgelegte Dissertation selbständig angefertigt, die benutzten Quellen und Hilfsmittel vollständig angegeben und die Stellen der Arbeit - einschließlich Tabellen, Karten und Abbildungen -, die anderen Werken im Wortlaut oder dem Sinn nach entnommen sind, in jedem Einzelfall als Entlehnung kenntlich gemacht habe; dass diese Dissertation noch keiner anderen Fakultät oder Universität zur Prüfung vorgelegen hat; dass sie - abgesehen von unten angegebenen Teilpublikationen - noch nicht veröffentlicht worden ist sowie, dass ich eine solche Veröffentlichung vor Abschluss des Promotionsverfahrens nicht vornehmen werde. Die Bestimmungen der Promotionsordnung sind mir bekannt. Die von mir vorgelegte Dissertation ist von Prof. Dr. Karl Schneider betreut worden.

Nachfolgend genannte Teilpublikationen liegen vor:

- Wagner, P.D., Kumar, S., Fiener, P., Schneider, K., 2010. Analyzing water resources in a monsoon-driven environment – an example from the Indian Western Ghats. In: *Conference Proceedings of the 2010 International SWAT Conference*, August 4-6, 2010, Seoul, South Korea: 182-191.
- Wagner, P.D., Kumar, S., Fiener, P., Schneider, K., 2011. Hydrological Modeling with SWAT in a Monsoon-Driven Environment: Experience from the Western Ghats, India. *Transactions of the ASABE* 54(5): 1783-1790.
- Wagner, P.D., Kumar, S., Wilken, F., Fiener, P., Schneider, K., 2011. Impacts of precipitation interpolation on hydrologic modeling in data scarce regions. In: *Conference Proceedings of the 2011 International SWAT Conference*, June 15-17, 2011, Toledo, Spain: 447-457.
- Wagner, P.D., Fiener, P., Wilken, F., Kumar, S., Schneider, K., 2012. Comparison and evaluation of spatial interpolation schemes for daily rainfall in data scarce regions. *Journal of Hydrology* 464-465: 388-400.
- Wagner, P.D., Reichenau, T.G., Kumar, S., Schneider, K., 2012. Assessing climate change impacts on the water resources in Pune, India. *Regional Environmental Change*: In Review.